

**STUDY ON REINFORCED SOFT ACTUATOR FOR EXOSKELETON
ACTUATORS**

by

Mohammad Shuqir

A Thesis Submitted to the Faculty of

The College of Engineering and Computer Science

In Partial Fulfillment of the Requirements for the Degree of

Master of Science

Florida Atlantic University

Boca Raton, FL

August 2018

Copyright 2018 by Mohammad Shuqir

**STUDY ON REINFORCED SOFT ACTUATOR FOR EXOSKELETON
ACTUATORS**

by

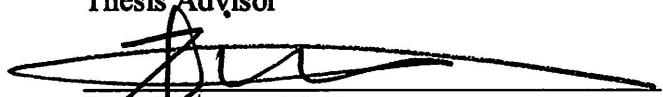
Mohammad Shuqir

This thesis was prepared under the direction of the candidate's thesis advisor, Dr. Erik Engeberg, Department of Ocean and Mechanical Engineering, and has been approved by all members of the supervisory committee. It was submitted to the faculty of the College of Engineering and Computer Science and was accepted in partial fulfillment of the requirements for the degree of Master of Science.

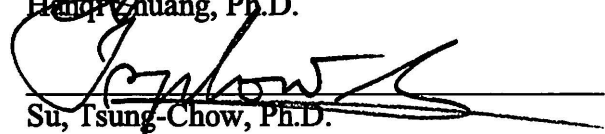
SUPERVISORY COMMITTEE:



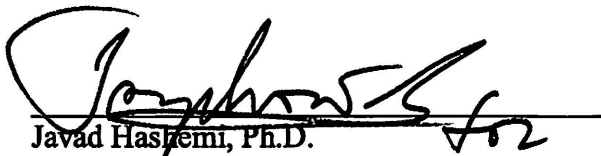
Erik Engeberg, Ph.D.
Thesis Advisor



Hanqi Zhuang, Ph.D.



Su, Tsung-Chow, Ph.D.



Javad Hasfemi, Ph.D.
Chair, Department of Ocean and
Mechanical Engineering



Stella N. Batalama, Ph.D.
Dean, College of Engineering and
Computer Science



Khaled Sobhan, Ph.D.
Interim Dean, Graduate College

08/02/2018
Date

ACKNOWLEDGEMENTS

I would like to express my thanks and gratitude to everyone who supported me throughout the journey, my wife, family and friends; and Dr. Engeberg for his mentorship and passion for research have provided continuous guidance and inspiration, and funding; and my fellow graduate students in the BioRobotics lab for their advice throughout the process, especially, Moaed Abd, Mostafa Al-Saidi, Joseph Ingicco and Craig Ades.

This work was supported by the Department of Energy Minority Serving Institution Partnership Program (MSIPP) managed by the Savannah River National Laboratory under SRNS contract TOA#0000332969 in collaboration with Florida International University's Applied Research Center and Idaho National laboratory. This research was also supported by the NIH: NIBIB award # 1R01EB025819 and I-SENSE at FAU.

ABSTRACT

Author: Mohammad Shuqir
Title: Study on Reinforced Soft Actuator for Exoskeleton Actuators
Institution: Florida Atlantic University
Thesis Advisor: Dr. Erik Engeberg
Degree: Master of Science
Year: 2018

This thesis concerns the design, construction, control, and testing of soft robotic actuators to be used in a soft robotic exoskeleton; the Boa Exoskeleton could be used for joint rehabilitation including: wrist, elbow and possibly shoulder or any joint that requires a soft body actuator to aid with bending movement. We detail the design, modeling and fabrication of two types of actuators: Fiber-reinforced Actuator and PneuNet Actuator. Fiber-Reinforced actuator was chosen for the exoskeleton due to its higher force. The Fiber-Reinforced actuator molds were 3D printed, four models were made. Two materials were used to fabricate the models: Dragon Skin 30A and Sort-A-Clear 40A. Two number of windings: (n=40) and (n=25), actuators wrapped with carbon fiber. An air tank was used to supply pressure. The actuators were studied at different pressures. Pressure-force relation was studied, and a close to linear relationship was found. Boa Exoskeleton was made for wrist. Electromyography (EMG) was used; Four EMG receptors were put around the arm. EMG was utilized to actuate the Boa Exoskeleton and record the muscle movement. Five tests were done on six human subjects to validate the Boa Exoskeleton.

**STUDY ON REINFORCED SOFT ACTUATOR FOR EXOSKELETON
ACTUATORS**

List of Tables.....	x
List of Figures.....	xi
List of Equations.....	xii
1 INTRODUCTION	1
1.1 Goals and Objectives.....	2
1.2 Literature Review	2
1.2.1 Soft Robotics, PneuNet and Reinforced Actuators	3
1.2.2 Human Exoskeleton Characteristics	5
1.2.3 Existing Soft Robotic Exoskeleton	6
2 ACTUATORS DESIGN.....	8
2.1 PneuNet Actuator	8
2.2 Fiber-Reinforced Actuator	11
3 ACTUATOR FABRICATION.....	17
3.1 Ordering	17
3.2 3D Printing	17
3.3 Actuator Fabrication.....	18
3.3.1 PneuNet Actuator Fabrication.....	19

3.3.2	Fiber-Reinforced Actuator Fabrication	21
3.4	Boa exoskeleton arranging	28
4	CONTROL AND TESTING	30
4.1	PneuNet Actuator	30
4.2	Boa Actuator	33
4.3	Boa Exoskeleton.....	36
5	RESULTS	42
5.1	PneuNet Actuator	42
5.2	Fiber-Reinforced Actuator	47
5.3	Boa Exoskeleton.....	61
6	DISCUSSION.....	77
7	CONCLUSIONS	79
9	APPENDIX	80
10	REFERENCES	105

LIST OF TABLES

Table 1: Itemized Boa Exoskeleton parts list.	17
Table 2: 3D printed PneuNet mold actuator components.....	18
Table 3: 3D printed Fiber-Reinforced mold actuator components.	18
Table 4: Human subject tests order combinations.	41
Table 5: ANOVA 1 for PneuNet Actuators.....	47
Table 6: Force as a linear relation of pressure coefficients for Boa actuator (30-8).	57
Table 7: Force as a linear relation of pressure coefficients for Boa actuator (30-5).	57
Table 8: Force as a linear relation of pressure coefficients for Boa actuator (40-8).	58
Table 9: Force as a linear relation of pressure coefficients for Boa actuator (40-5).	58
Table 10: One-way ANOVA for Boa Actuator.	60
Table 11: Two-way ANOVA for Boa Actuator.	61
Table 12: Area under the curve of EMG flexion signal E_{F1}	73
Table 13: Root Mean Square of EMG flexion signal E_{F1}	74

LIST OF FIGURES

Figure 1. The Boa Exoskeleton during testing in the BioRobotics Lab, FAU.	1
Figure 2. PneuNet actuator SoftRobotics toolkit design.....	9
Figure 3. SolidWorks Design mold for $\theta = 3^{\circ}$	10
Figure 4. Soft Actuator Dimensions for $\theta = 3^{\circ}$	11
Figure 5. Fiber-Reinforced actuator SoftRobotics toolkit design.	12
Figure 6. (a)Fiber-Reinforced with $n=25$ windings inner mold design and parts.	
(b)Reinforced actuator inner mold parts assembled on SolidWorks.	13
Figure 7. 5-mm winding spacing Fiber-Reinforced actuator inner mold design and	
dimensions.	14
Figure 8. (a)Fiber-Reinforced with 5 mm winding spacing outer mold design and	
parts. (b)Fiber-Reinforced actuator outer mold parts assembled on	
SolidWorks.	15
Figure 9. Fiber-Reinforced actuator outer mold design and dimensions.....	16
Figure 10. Shore hardness scale based on [28].	19
Figure 11. Fabrication steps for molding the PneuNet soft actuator.	20
Figure 12. Fabricated PneuNet soft actuators with taper angle 0° and 3°	21
Figure 13. Classification of the four Fiber-Reinforced actuators.	22
Figure 14. Components of the first stage, the inner mold for Fiber-Reinforced	
actuator.....	23
Figure 15. Mixing elastomer materials during fabrication.	24

Figure 16. First stage of fabricating Fiber-Reinforced actuator winding spacing	
5-mm.	25
Figure 17. Adding fabric layer to the bottom of the Fiber-Reinforced actuator.	25
Figure 18. First stage of fabricating fiber-Reinforced actuator.	26
Figure 19. Components of the second stage, the outer mold for Reinforced actuator.	26
Figure 20. Fiber-Reinforced actuator during process of fabrication.	27
Figure 21. Fabricated Fiber-Reinforced soft actuators.	28
Figure 22. Boa Exoskeleton.	29
Figure 23. Testing station for PneuNet Actuator.	30
Figure 24. Matlab Simulink controller for PneuNet Actuator.	32
Figure 25. KINOVEA Photo Sequences for PneuNet actuator.	33
Figure 26. Testing station for Boa Actuator.	34
Figure 27. Matlab Simulink controller for Boa Actuator.	35
Figure 28. Boa Exoskeleton during testing.	36
Figure 29. Boa Exoskeleton testing diagram.	37
Figure 30. Boa Exoskeleton testing station.	38
Figure 31. Matlab/Simulink control diagram for Boa Exoskeleton.	39
Figure 32. Force for SPA with taper angle 3° . For frequencies 0.5-6 rad/s from top to bottom respectively.	43
Figure 33. Hysteresis of the soft actuator with taper angle 3° for all frequencies. For frequencies 0.5-6 rad/s from top to bottom respectively	44
Figure 34. Standard deviation and mean of maximum forces for SPA with taper angle 3° for frequencies 0.5 to 6 rad/s respectively.	45

Figure 35. Standard deviation and mean of maximum forces for SPA with taper angle 0° for frequencies 0.5 to 6 rad/s respectively.	46
Figure 36. Displacement of the tip of the soft actuators.	47
Figure 37. Force (N), Pressure (MPa) with time for Boa (30-5) actuator.	48
Figure 38. Force (N), Pressure (MPa) with time for Boa (30-8) actuator.	49
Figure 39. Force (N), Pressure (MPa) with time for Boa (40-8) actuator.	50
Figure 40. Force (N), Pressure (MPa) with time for Boa (40-5) actuator.	51
Figure 41. Force vs Pressure for Boa actuator (30-8).	52
Figure 42. Force vs Pressure for Boa actuator (30-5).	53
Figure 43. Force vs Pressure for Boa actuator (40-8).	54
Figure 44. Force vs Pressure for Boa actuator (40-5).	55
Figure 45. Force vs Pressure at inflation and deflation for Boa Actuator (40-5).	56
Figure 46. Mean of maximum forces for all Boa actuators with STD.	59
Figure 47. Boa Exoskeleton during testing in BioRobotics Lab, FAU.	61
Figure 48. Boa Exoskeleton “EMG Actuated” tests on subject 1.	63
Figure 49. Boa Exoskeleton test "Non-Assistive" on subject 1.	64
Figure 50. Boa Exoskeleton test "Full Assistive" on subject 1.	65
Figure 51. Boa Exoskeleton test "No Exoskeleton" on subject 1.	66
Figure 52. Boa Exoskeleton test "No Exoskeleton/ No Weight" on subject 1.	67
Figure 53. EMG comparison for human subject 1.	68
Figure 54. EMG comparison for human subject 2.	69
Figure 55. EMG comparison for human subject 3.	70
Figure 56. EMG comparison for human subject 4.	71

Figure 57. Ratio of combined EMG signals to the Flexion Angle ϕ for all human subjects.....	72
Figure 58. Area under the curve of EMG flexion signal E_{F1}	74
Figure 59. Root Mean Square of EMG flexion signal E_{F1}	75
Figure 60. Area under the curve of all EMG signals for all tests, for all human subjects.....	76
Figure 61. Boa Exoskeleton “EMG Actuated” tests on subject 2.....	80
Figure 62. Boa Exoskeleton “Full Assistive” tests on subject 2.....	81
Figure 63. Boa Exoskeleton “Non-Assistive” tests on subject 2.....	82
Figure 64. Boa Exoskeleton “No Exoskeleton” tests on subject 2.	83
Figure 65. Boa Exoskeleton “No Exoskeleton/ No Weight” tests on subject 2.	84
Figure 66. Boa Exoskeleton “EMG Actuated” tests on subject 3.....	85
Figure 67. Boa Exoskeleton “Full Assistive” tests on subject 3.....	86
Figure 68. Boa Exoskeleton “Non-Assistive” tests on subject 3.....	87
Figure 69. Boa Exoskeleton “No Exoskeleton” tests on subject 3.	88
Figure 70. Boa Exoskeleton “No Exoskeleton/ No Weight” tests on subject 3.	89
Figure 71.Boa Exoskeleton “EMG Actuated” tests on subject 4.....	90
Figure 72. Boa Exoskeleton “Full Assistive” tests on subject 4.....	91
Figure 73. Boa Exoskeleton “Non-Assistive” tests on subject 4.....	92
Figure 74. Boa Exoskeleton “No Exoskeleton” tests on subject 4.	93
Figure 75. Boa Exoskeleton “No Exoskeleton/ No Weight” tests on subject 4.	94
Figure 76. Boa Exoskeleton “EMG Actuated” tests on subject 5.....	95
Figure 77. Boa Exoskeleton “Full Assistive” tests on subject 5.....	96

Figure 78. Boa Exoskeleton “Non-Assistive” tests on subject 5.	97
Figure 79. Boa Exoskeleton “No Exoskeleton” tests on subject 5.	98
Figure 80. Boa Exoskeleton “No Exoskeleton/ No Weight” tests on subject 5.	99
Figure 81. Boa Exoskeleton “EMG Actuated” tests on subject 6.....	100
Figure 82. Boa Exoskeleton “Full Assistive” tests on subject 6.....	101
Figure 83. Boa Exoskeleton “Non-Assistive” tests on subject 6.	102
Figure 84. Boa Exoskeleton “No Exoskeleton” tests on subject 6.	103
Figure 85. Boa Exoskeleton “No Exoskeleton/ No Weight” tests on subject 6.	104

1 INTRODUCTION

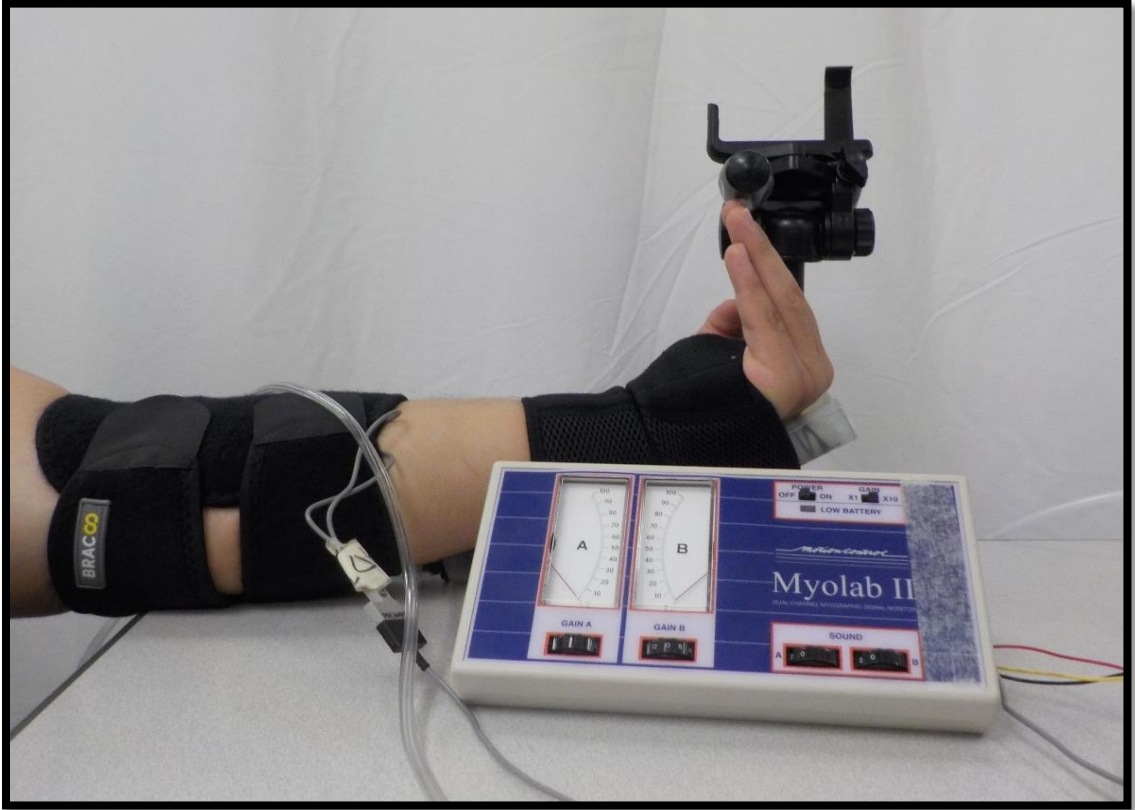


Figure 1. The Boa Exoskeleton during testing in the BioRobotics Lab, FAU.

This thesis work was started during the spring 2017 semester and pertains to the design, fabrication, control, and testing of a soft robotic exoskeleton (Figure 1). The Boa Exoskeleton, the name comes from the looks of actuator, a Boa snake looks.

First it started with a PneuNet-type actuator, a comprehensive study was done during spring and summer of 2017 on changing the pitch angle of the inner chamber of the actuator, during the study, the goal in mind was to use these actuators for human aid, more

specifically, a human exoskeleton that would be useful in rehabilitation, damaged nerves or muscles and anywhere it requires a non-rigid soft bending movement. Later to find the PneuNet-type actuator does not exert sufficient force, the next step was the move to the Boa actuator, reinforced with carbon fiber windings, and a higher shore hardness material to produce a sufficient amount force that has the potential.

Current studies on soft actuators are still underway, few attempts on human soft robotic prosthetics and exoskeletons were done. The Boa Exoskeleton could be a small, cost-effective addition to current studies, with a big potential to have practical use in physical therapy and rehabilitation one day. Most importantly, as soft robotics is a relatively new immature research field, the full potential of soft robotic is still being discovered. Hopefully, this thesis work will help contribute to the development of other novel soft robotic platforms.

1.1 Goals and Objectives

The purpose of this thesis project was to create a novel soft robotics platform. The goal was to design, build, and test a self-contained proof of concept robot. Its two main objectives were: (1) to implement a modified form of soft actuation to mimic and support the bending movement of joints (2) then to test its capabilities, including the output force and input pressure.

1.2 Literature Review

A literature review was conducted to facilitate actuator design, construction, and testing. It focused largely on how to (1) utilize current soft robotics knowledge, especially prior research into reinforced actuator geometry and design, (2) make the necessary adjustments and redesign some parts to achieve our goal, and (3) employ prior research

done regarding the material used, process of fabricating and usage of reinforced soft actuators.

1.2.1 Soft Robotics, PneuNet and Reinforced Actuators

Biology has been a source of inspiration for designing future revolutionary machines. Softness and acquiescence are salient features used by biological beings, which they often display simplicity in interacting with their surrounding [1]. For the last decade, the slant in the world of robots was the use of heavy, rigid actuators coupled with also rigid transmission mechanisms, these robots are very precise and repeatable; hence appropriate for heavy and non-heavy industrial applications [2]. Actuators in these systems are composed of rigid electromagnetic components and in some applications steel and aluminum alloys, in biology on the contrary soft materials are dominant, even animals with stiff exoskeleton possess soft tissues, and some of them have lived life stages wherein they are completely soft such as caterpillars [3]. Soft robotics can gently interact with the surrounding environment which makes it more reliable to deal with any delicate objects [4].

There has been a growing interest in studying soft robotics, in which researchers have been investigating unconventional materials for robotic systems, these soft materials such as polymer based materials are examined for novel sensory devices and actuators [5]. The soft material gives flexibility or elastomeric structural elements, the robots in return have low weight to force ratio, therefore they can be designed to have low center of gravity, also can be designed to distribute pressure on the objects they interact with [6].

Actuators in the robotic systems transfer energy from any form into motion that controls the interaction of the robotic system and the object or environment, the move to

soft actuators emphasize the need for a safer human-robot interaction [7]. Pneumatic soft actuators offer an underestimated entry into soft robotics, “for pneumatic actuation to be most useful, it must satisfy three conditions: i) it should be flexibly controllable in direction and force; ii) it should take advantage of its non-linearities to simplify the accomplishment of functions that are difficult with linear actuators; and iii) it must be easily incorporated into designs that are practical to fabricate, inexpensive, and functional” [6].

Several kinds of pneumatic rubber actuators have been developed and reported [8]. Examples of them are MacKibben artificial muscle developed in 1950s Romac actuator, Rubber gas actuator driven by hydrogen storage alloy, Flexible microactuator Bubbler actuator, Pneumatic wobble motor, Pneumatic planar soft actuator, Pneumatic soft actuator, and colonoscope insertion actuator[8].

PneuNet actuator uses a series of parallel chambers embedded in elastomers, distribution, configuration and size of the PneuNets determines the resulting movement [9]. The chambers upon pressurization, the portion that has the thinnest wall will expand first, as it requires the least pressure to deform, with higher pressure the chambers continues to expand and consequently bends the top surface, and forms a concave shape [9]. through their research in[9] when using composite materials they concluded that the stiffer material will bend the chambers, and the more flexible material will expand them [9]. PneuNets have proven to be very versatile and propitious. Developed and publicized by Harvard University’s Whitesides Research Group, two designs were studied; slow and fast PneuNet actuators, the study instigated the angular speed of bending the PneuNet actuator using compressed air taking advantage of air’s low viscosity thus provides rapid inflation rate, light weight, ease of control and it can be discarded after use to the atmosphere [10]. The

actuators were fabricated using silicone-based elastomers, each actuator consists of an extensible top layer which houses the chambers of the internal network for fluid distribution , and an inextensible bottom layer reinforced with embedded paper to restrain linear movement from the bottom [10].

Fiber reinforced actuators in turn, are like PneuNet actuators in the principle of operation, they both operate on pressurized air, only they differ in design, thus they differ in outcome. Fiber reinforced actuators are simple in design with a tubular geometry that is easy to fabricate, the fiber reinforcements are arranged helically along the tube to restrict the deformation in ways that can be design to enable desired deformation patterns [11]. In addition to that a strain limiting layer on the bottom to restrict the deformation enabling the actuator to bend [11]. In a study done in 2016 [12] to design actuator that replicates the index of finger and thumb motion, the approach was to design actuator that consists of multiple segments, where each segment can produce different trajectory [12]. All the segments share the same cylindrical body, but the fiber reinforcement arranged in a helical pattern at different angle, therefore the actuator mimics the links and joints of the biological digit [12].

1.2.2 Human Exoskeleton Characteristics

Integrating human and robot into a single system proposes a promising new generation of assistive technology for people with disabilities and people who needs assist while doing heavy duty kind of work [13]. Humans naturally uses advanced algorithms like to control their multi-degree of freedom systems, only limited to the muscle strength, which varies between humans, assistive Exoskeleton can be a great addition to the muscle strength [13]. In human-machine interaction field, wearable devices for rehabilitation and

assisting should be as user friendly as possible for a reliable human-robot relation [14]. Some wearable devices used for human wrist rehabilitation, such as a wrist glove, has proved that soft actuators can effectively assist the joint movement [10]. Another notable soft robotic exoskeleton property, is it's light weight, where the exoskeleton can have only the actuators and the air tubes, the rest of the system components can be distributed around the waist, the back or in a stationary unit [15].

Chronic stroke survivor experience either partial or total absence of hand motor ability [16]. A robot-based therapy improves hand motor functioning after chronic stroke [16]. A study on stroke rehabilitation [17] have concluded that repetitive training of upper limb results in significant functional improvement in strength and velocity [17]. Which that makes robotic rehabilitation devices more desirable since they can offer steadiness over periods of time, they also utilize onboard sensors to control and provide digital outcomes for analysis [18].

1.2.3 Existing Soft Robotic Exoskeleton

Many robotic rehabilitation systems have been developed for the multi-degree-of-freedom human hand. The rigid designs provide robust high force applications, however they are typically heavy, expensive and require time and precision for joint alignment [19].

Soft robotic glove was done by a group a researchers referenced [20], designed to assist hand grasping in performing activities of daily life. Using PneuNet actuators to support fingers and thumb motions to assist in hand closing and grasping [20]. EMG was proposed to control the glove, with different control strategies to achieve palmar and pincer grasps [20]. EMG signals of human muscles are important signals to understand how the human decides to move The skin surface EMG signals, are mainly used as controller input

signals [21]. Cable actuated soft exoskeleton is half way between rigid and soft alternative to soft actuator exoskeleton, actuates through pulling cables which are connected to the fabric arm exoskeleton, assisting hand movement in palmar and dorsal side [22]. The Cable actuated exoskeleton can provide high assistive force, whereas the soft actuator exoskeleton is a much lighter and more portable solution. Another group of researchers [23] designed a soft wearable glove exoskeleton embedded with soft PneuNet actuators that could achieve hand grasping and pinching with a force ranges from 0.25 N to a maximum of 3.59 N [23]. Reinforced soft actuators can withstand higher pressure than PneuNet actuator naturally due to the fiber enforcement, therefore can produce higher force, our approach is to study these actuators to implement them in the Boa Exoskeleton.

2 ACTUATORS DESIGN

After completing a literature review, the design was inspired from “soft robotics toolkit” [24]. The designs were modified using SolidWorks 2015. Two actuators were designed, first we started with a PneuNet actuator, then Fiber-Reinforced actuator. Afterwards, the SolidWorks Mold Tools Toolbox was used to generate a three-part mold for the PneuNet and two three-part molds for the Fiber-Reinforced. The molds were 3D printed and used to make an initial actuator body for design modification. Following initial testing, improvements were made to the actuator’s design and modifications were made to maximize the output force and bending. The following sections provide more details regarding each of two actuators design.

2.1 PneuNet Actuator

A pneumatic soft actuator with one degree of freedom of motion is designed in this thesis. The work was done in 2017 [25]. The design conceptualized in [24] shown in Figure 2, was modified on SolidWorks 2015, a nozzle was added to allow ease of connect to a tube, other modifications were made to ensure consistency when changing variables.

The angular speed of bending of a PneuNet actuator depends on: i) the rate of inflation i.e. the input pressure, ii) the geometry of the internal channels and exterior walls, and [10]. In this paper, we will be studying one variable parameter while the other parameters are constants since the outcome of the actuator depends on the internal geometry. The most common parameters that are believed to make a difference in the outcome are: i) PneuNet actuator taper angle, θ ; ii) Common, inflating channel taper angle,

β ; iii) Inter-chamber spacing interval. We investigated the impact of changing the taper angle θ , on the outcome of the soft actuator as our only variable.

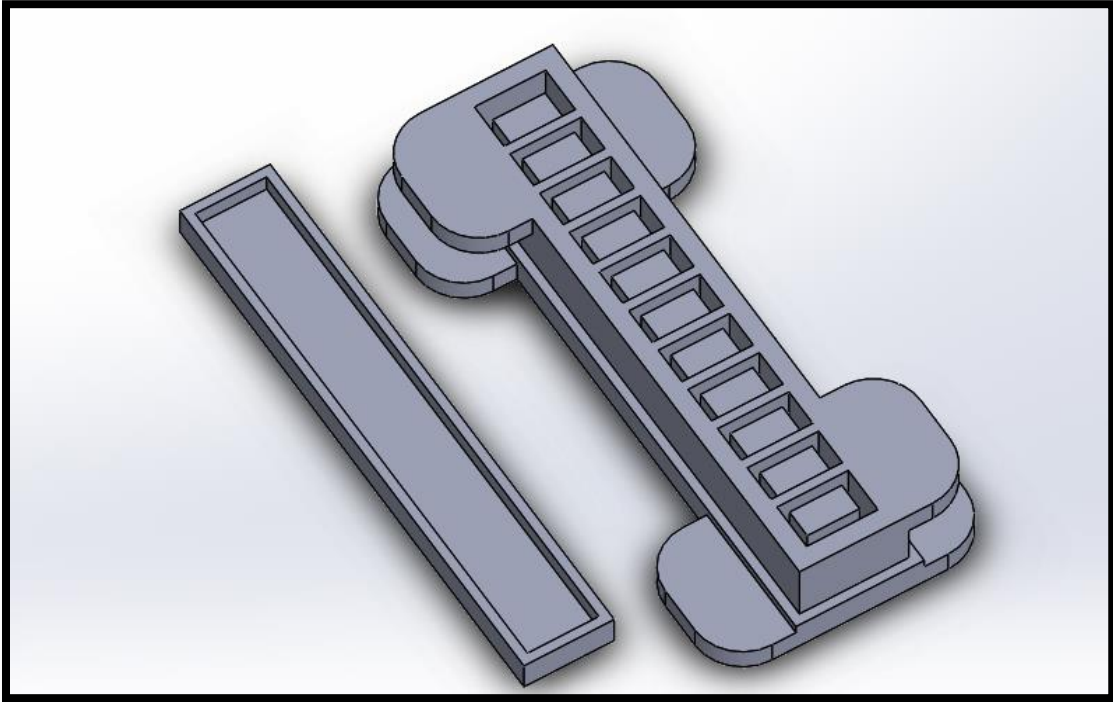


Figure 2. PneuNet actuator SoftRobotics toolkit design.

One model was designed with taper angle $\theta = 3^\circ$, while all other geometric parameters were constant. To be compared with taper angle $\theta = 0^\circ$. The design was made on Solid works software, The SolidWorks design for PneuNet actuator mold with taper angle $\theta = 3^\circ$ is shown in Figure 3.

Three different mold parts were designed to manufacture the actuator. The Bottom part is used to make the cavity of chambers; the top part is used to separate the chambers and the base part was used to unify the top and bottom of the actuator, also to put a layer of fabric on the bottom to restrict linear displacement in the bottom to allow the actuator

to bend. Figure 4 shows the dimensions of the PneuNet soft actuator with taper angle $\theta = 3^\circ$, and illustrates how the taper angle θ affects the design.

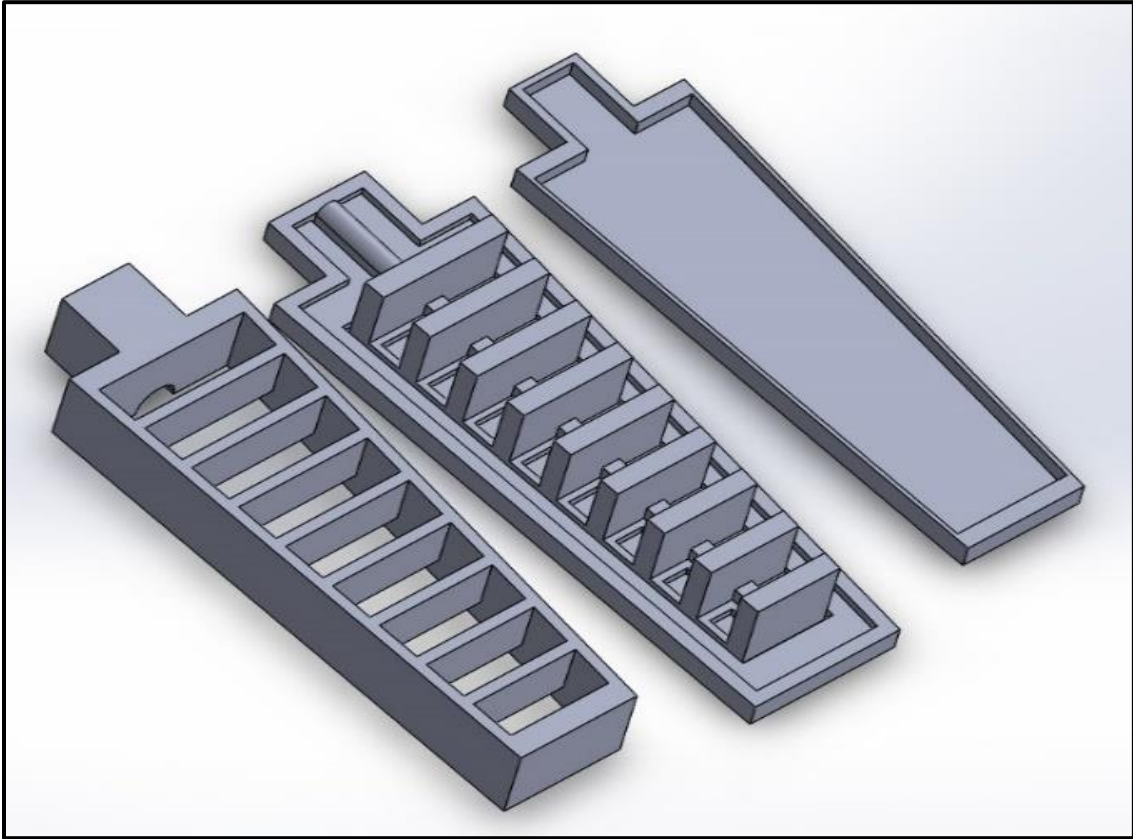


Figure 3. SolidWorks Design mold for $\theta = 3^\circ$.

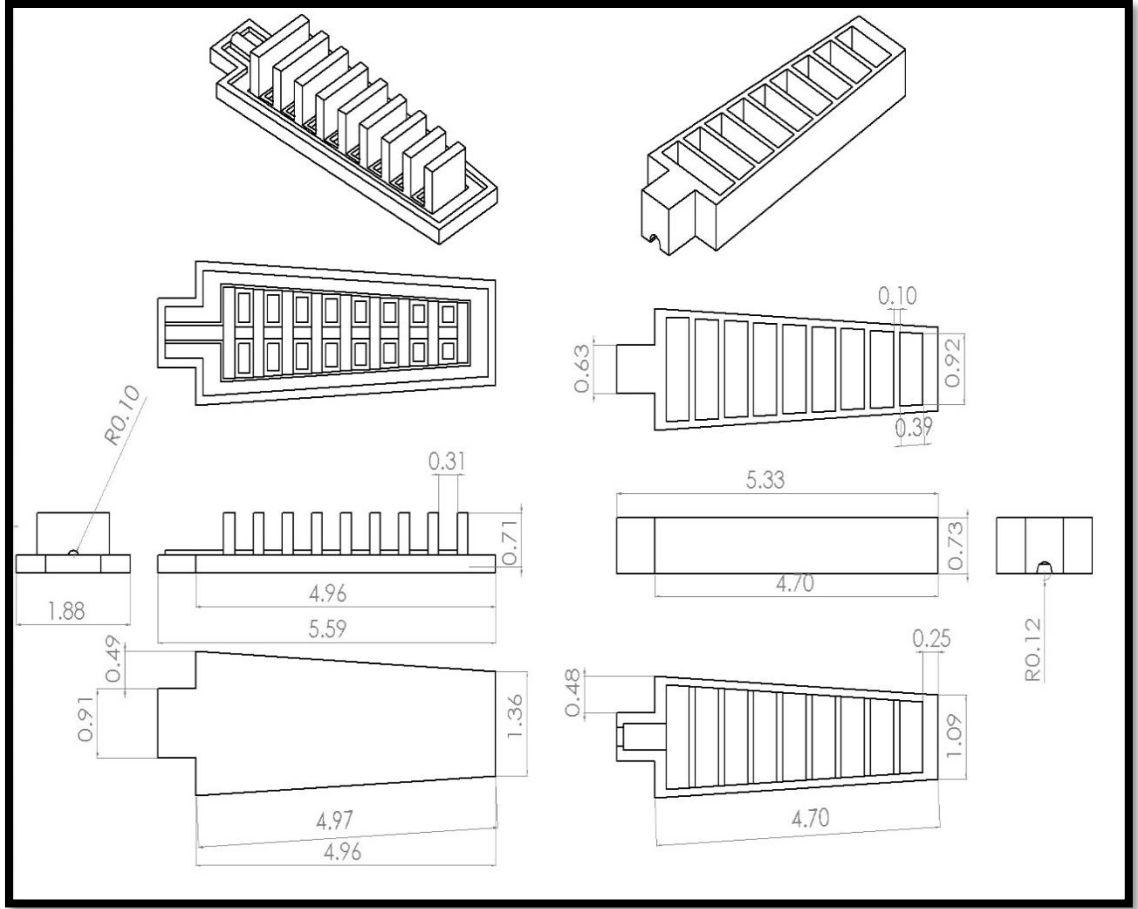


Figure 4. Soft Actuator Dimensions for $\theta = 3^\circ$.

2.2 Fiber-Reinforced Actuator

Named Boa, a carbon-Fiber-Reinforced actuator was the next step after finishing with PneuNet actuator, a stronger actuator was needed that can withstand higher pressures in order to exert higher force and for a better actuation durability. The carbon fiber wrapped around the cylindrical actuator gives it the looks of a Boa snake, hence the name. One degree of freedom actuator was designed, the actuator is conceptualized in [24] shown in Figure 5.

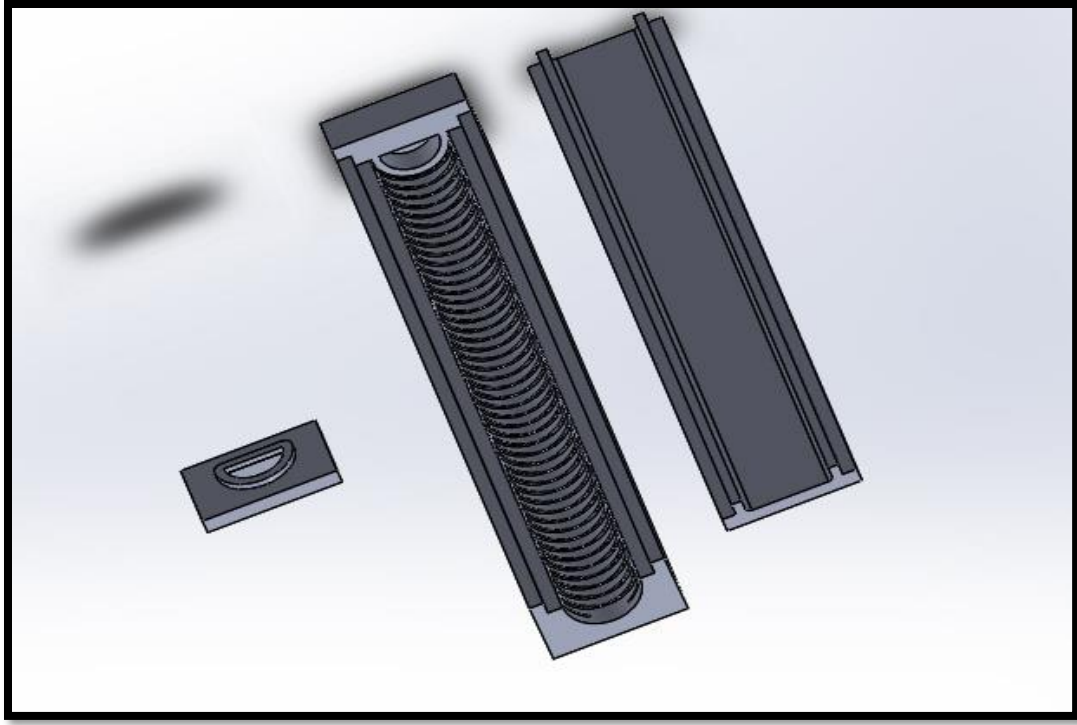


Figure 5. Fiber-Reinforced actuator SoftRobotics toolkit design.

Fiber Reinforced actuators are hollow enclosures made of elastomer surfaces reinforced with fiber [26]. The movement behavior of soft Fiber Reinforced actuators is mainly controlled by: i. Inextensibility of fibers, ii. Incompressibility of fluids, and iii. deformation of the hyperelastic membrane [26]. Fiber Reinforced actuators can do different type of motions depending on the design and fabrication, i. bending only toward the bottom (winded helically with fabric both ways), ii. Extending axially (winded parallelly with fabric), iii. Bending toward the bottom and one of the sides (winded helically with fabric only one way) [27].

In this thesis a bending only soft Fiber Reinforced actuator was made, 4 actuators were made for a thorough study on them, having two different parameters. The mold

consists of four parts, the base, the top, the rod and the cap, figure 6 shows the Fiber-Reinforced actuator design and parts.

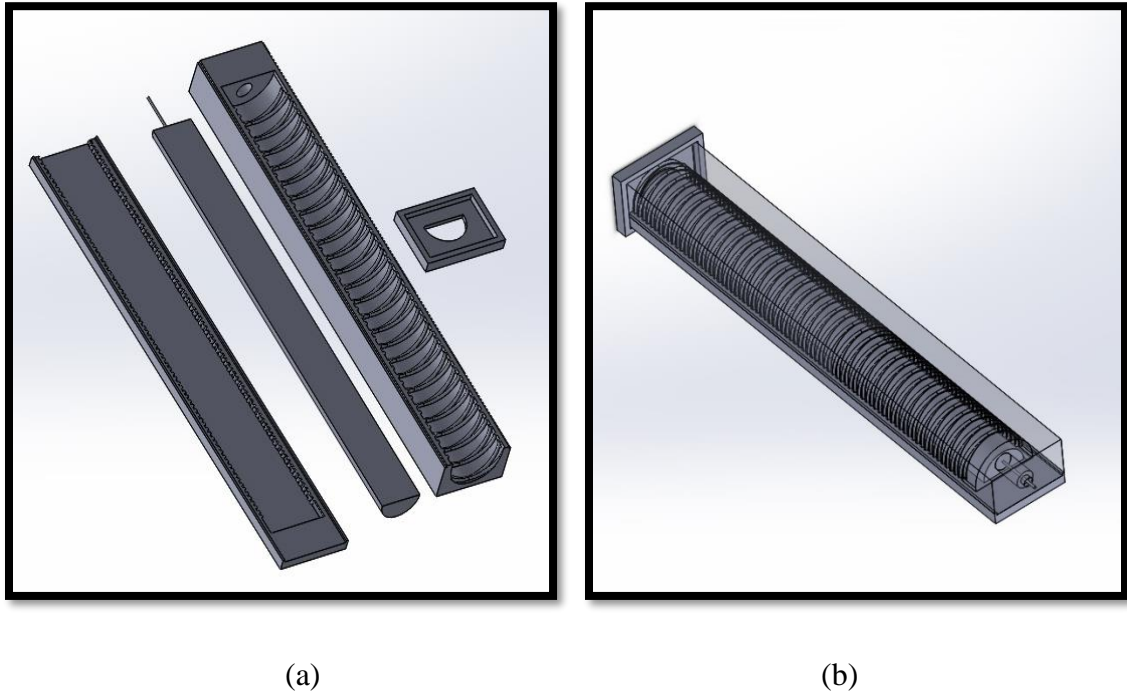


Figure 6. (a)Fiber-Reinforced with $n=25$ windings inner mold design and parts. (b)Reinforced actuator inner mold parts assembled on SolidWorks.

The first parameter was the winding spacing, helically winding around the body of the actuator, a grooving of 2 mm height was designed to ensure even and balanced winding during the fabrication. First a 5-mm winding spacing which is the minimum; less than 5-mm would cause the winding to overlap, results in 40 revolutions of fabric helically along the actuator body. Second an 8-mm winding spacing, results in 25 revolutions of fabric helically along the actuator body. The second parameter was the material which will be discussed in detail in the Fabrication section.

Modifications were made on the actuator design [24] using SolidWorks software, similar with the PneuNet actuator a nozzle was added to allow ease of connect to a tube, a

semi-cylindrical rod was designed to guarantee even hollowness in the body of the actuator, other necessary modifications were made to ensure consistency when changing variables and material. Figure 7 shows the dimensions of 5 mm winding spacing actuator, the 8-mm winding spacing actuator has the same dimension with only the winding spacing being different.

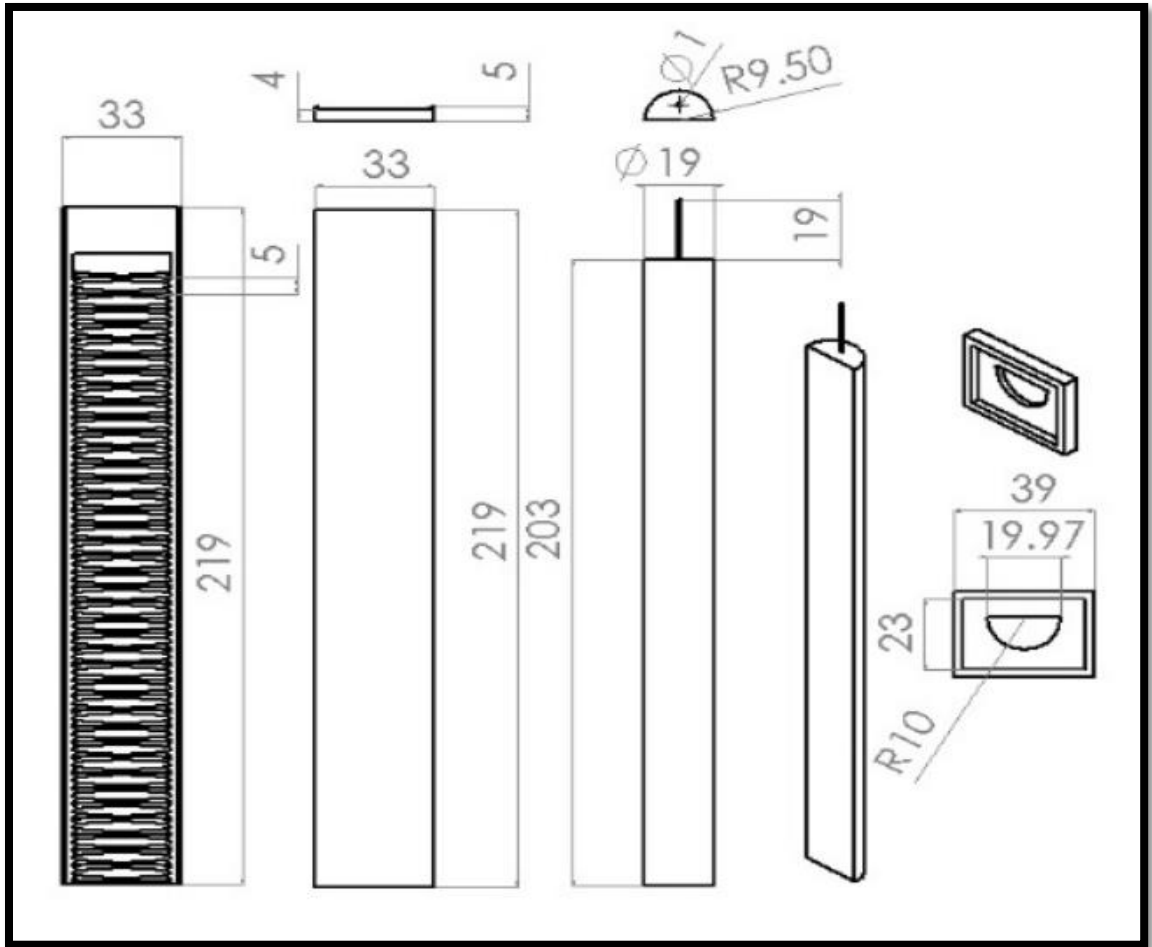


Figure 7. 5-mm winding spacing Fiber-Reinforced actuator inner mold design and dimensions.

Two stages of fabrication are required for the soft Fiber-Reinforced actuator, the first stage uses the design shown earlier to create the body of the actuator. Afterwards the fabric winding, and the bottom fabric layer are added which will be explained in detail in

the fabrication section, another layer of elastomer material need to be casted over to cover the reinforcement and unify them together with the body of the soft Fiber-Reinforced actuator.

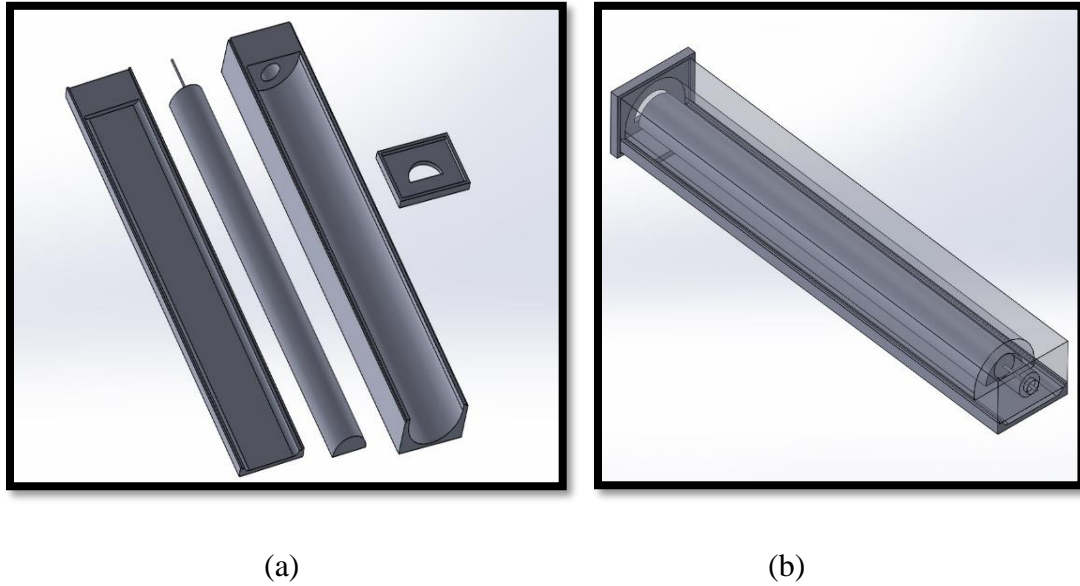


Figure 8. (a)Fiber-Reinforced with 5 mm winding spacing outer mold design and parts. (b)Fiber-Reinforced actuator outer mold parts assembled on SolidWorks.

Therefore, another mold was designed slightly bigger than the first stage mold, the mold consists of four parts, the base, the top, the rod and the cap, figure 8 shows the Fiber-Reinforced actuator design and parts. This design carries more simplicity, a semi-cylindrical base and the same principles as the first stage mold. Figure 9 shows the dimensions of the mold.

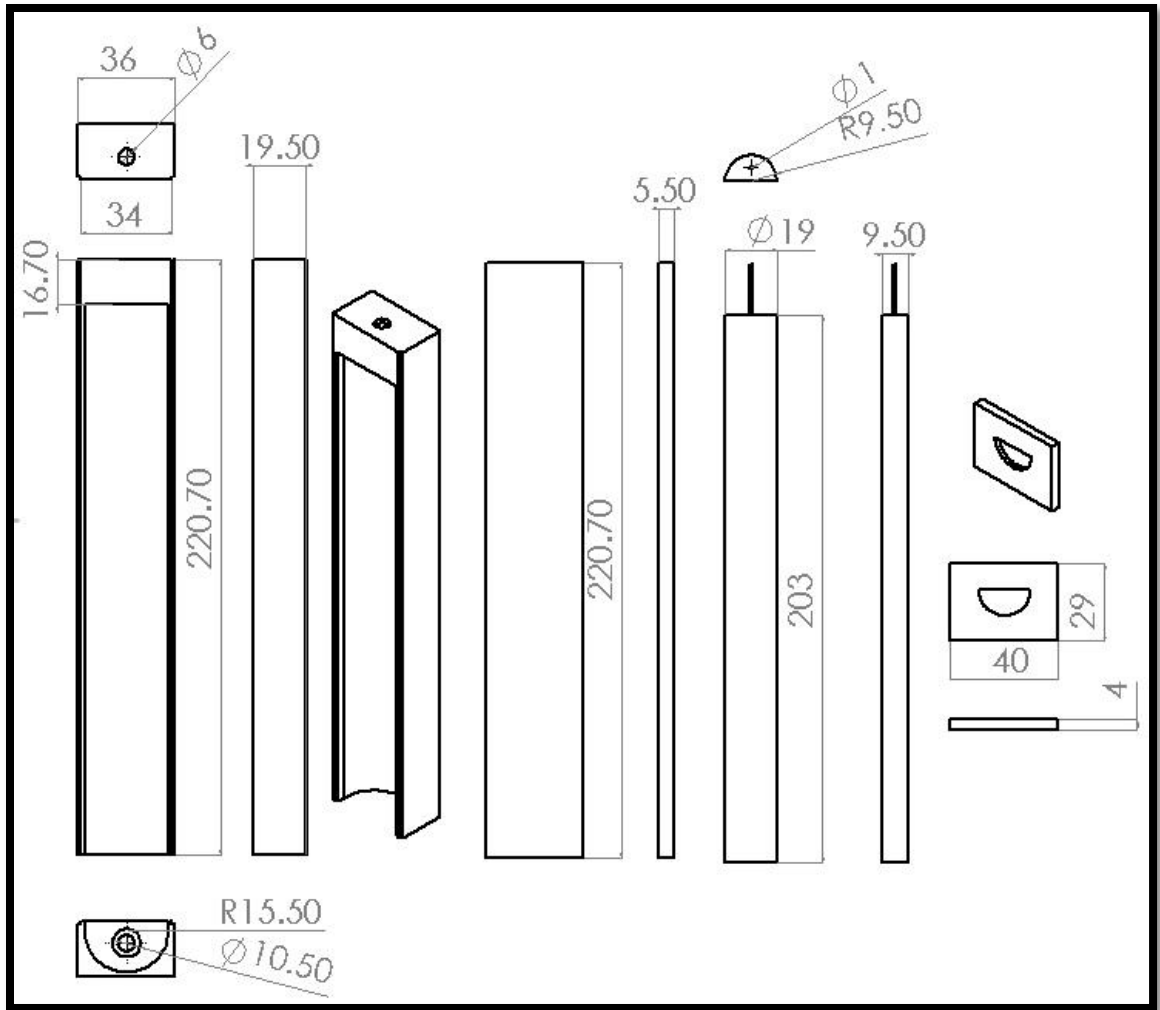


Figure 9. Fiber-Reinforced actuator outer mold design and dimensions.

3 ACTUATOR FABRICATION

Constructing soft actuators involves a number of stages, including: a material ordering process, 3D printing, body fabrication.

3.1 Ordering

Table 1: Itemized Boa Exoskeleton parts list.

Item	Details	Vendor	Quantity	Price
Air compressor with a tank	AC, Bostitch BTFP02012, 6-gallon air tank, 150PSI max, 2.6 SCFM	Amazon	1	\$99.99
Solenoid Air Valve	MettleAir 3V210-08, 3 Way, 2 Position, Solenoid, 12V DC, 1/4" NPT	Amazon	1	\$34.87
Dragon Skin 30	2 cartridges, 1A:1B, (2.0 lb net)	Smooth-On	1	\$32.21
SORTA-Clear 40	2 catridges, 10A:1B, (2.2 lbs net)	Smooth-On	1	\$40.87
Latex Tubing	Lee’s, 1/4" ID, 3/8" OD, 8'	Amazon	1	\$4.66
Pressure Sensor	PRESSURE SENSOR 100PSI GAUGE 5V DIP, SSCDANN100PGAA5	Honeywell	1	33.27
Wrist brace	NEOALLY, M 20.3 cm	Amazon	1	13.99
Total SORTA-Clear	\$227.65	Total Dragon Skin		\$218.99

The components to the proposed Boa Exoskeleton, prices and vendors are detailed in Table.

This is the first step to manufacture, as it helps set the budget and plan for the process.

3.2 3D Printing

In this thesis 2 actuators were designed, each actuator mold consists of several parts, PneuNet actuator and Fiber-Reinforced actuator mold parts listed in Table and Table

respectively, along with the type material used to print and the 3D printer, print quality settings were set high, it was found that the soft material used to fabricate the actuators has lower chances to stick to the mold if the layer height is thin. In general, the SolidWorks model file is saved as an STL file, then uploaded to the software Cura 3, a G code file is then auto generated and sent to the printing machine, Ultimaker 3 [28].

Table 2: 3D printed PneuNet mold actuator components.

Item	Printer	Plastic	Quantity
Bottom Mold Piece	Ultimaker 3	PLA	1
Base Mold Piece	Ultimaker 3	PLA	1
Top Mold Piece	Ultimaker 3	PLA	1

Table 3: 3D printed Fiber-Reinforced mold actuator components.

Item	Printer	Plastic	Quantity
Inner Bottom Mold Piece	Ultimaker 3	PLA	1
Inner Top Mold Piece	Ultimaker 3	PLA	1
Inner Cap Mold Piece	Ultimaker 3	PLA	1
Rod Mold Piece	Ultimaker 3	PLA	1
Outer Bottom Mold Piece	Ultimaker 3	PLA	1
Outer Top Mold Piece	Ultimaker 3	PLA	1
Outer cap Mold Piece	Ultimaker 3	PLA	1

3.3 Actuator Fabrication

Actuators fabrication is a multi-stage process shares some similarities between PneuNet and Fiber-Reinforced actuators that involves putting the mold together, layering the elastomer material and adding the reinforcement material. Be sure to wear the proper personal protective equipment, such as gloves and eye glasses, when working with chemicals. The following two sections will explain each actuator fabrication steps in details. After 3D printing all the parts molds, we made sure that the mold sections are smooth and free of surface defects, then the mold surfaces were sanded to insure softness.

The material used in fabrication are all cold casting material, they harden after getting mixed at the specified mix ratio.

3.3.1 PneuNet Actuator Fabrication

The first step is to put the top part and the bottom part together, as shown in Figure 11, then add a hot glue around the edges of the mold to prevent material leakage. The material used is Ecoflex 00-30 with a shore hardness of (00-30), this scale hardness is based on the manufacturer [29]. Figure 10 shows the shore hardness scale from the manufacturer website.

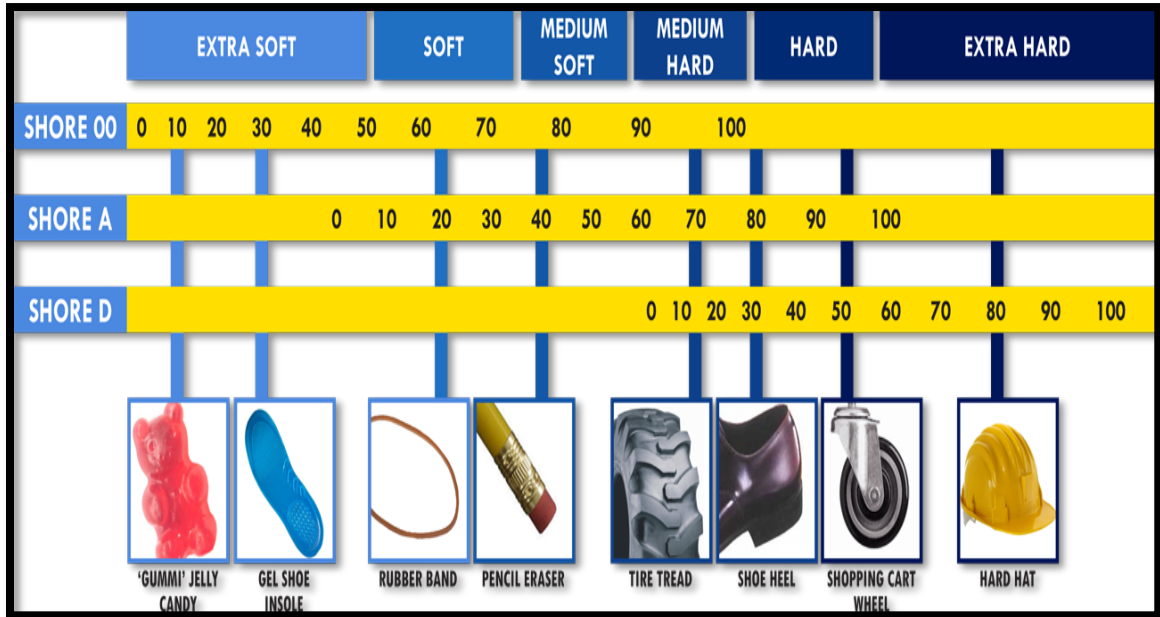


Figure 10. Shore hardness scale based on [28].

Then Ecoflex material comes in two cartridges, A and B, they are mixed together with a ratio of 1:1 either by weight or volume, we choose by weight to be more consistent over the time, after they are combined, we mix them together for about 2 minutes. The mixing will generate air bubbles in the mixed material, using a vacuum pump, we degas

the material from air bubbles for five minutes, this step is very important as the air bubbles causes imperfections in the body of the actuator after molding. Spray all mold parts with a mold release, such as Ease Release 200. After that the material is poured into the mold and left to cure for 8 hours. After the material has cured, carefully detach the top and bottom mold parts that were previously put together, then remove the actuator, take care not to rip the Ecoflex.

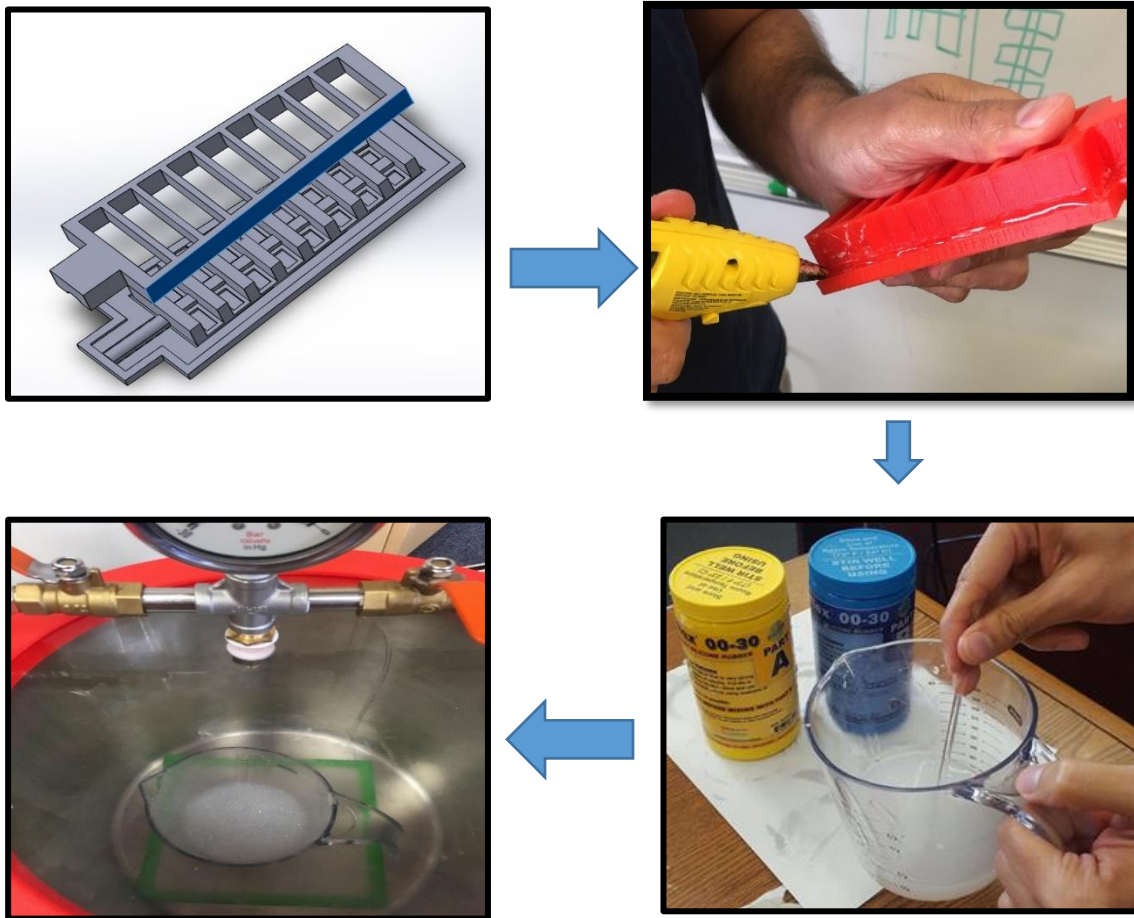


Figure 11. Fabrication steps for molding the PneuNet soft actuator.

The second step is to cut a piece of fabric that has the same size as the bottom of the actuator, then put the fabric in the base mold, pour another thin layer of Ecoflex material

onto the base mold, make sure the fabric is immersed inside the Ecoflex layer. Place the cured molded actuator from step on top and tap down lightly to ensure all the pattern bumps and bonding ridges make contact. Allow to cure for 8 hours, remove mold carefully and check any imperfections.

After molding finishing the steps, PneuNet actuators were made, the results are shown in Figure 12.

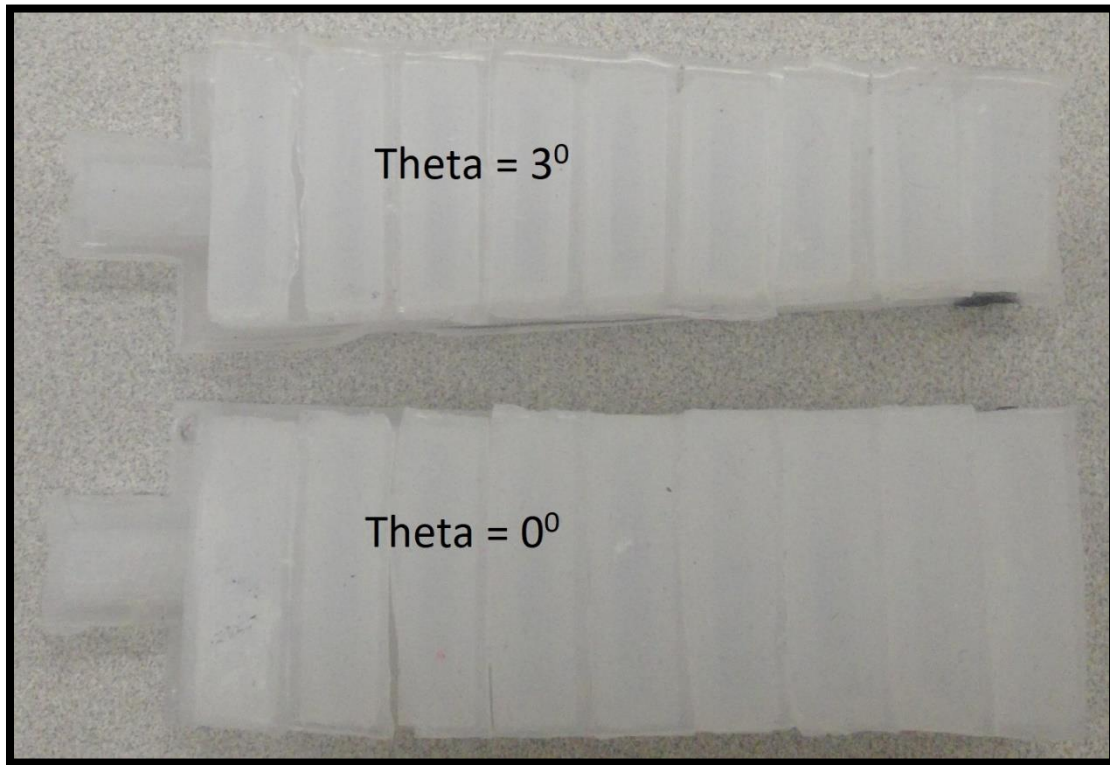


Figure 12. Fabricated PneuNet soft actuators with taper angle 0° and 3° .

3.3.2 Fiber-Reinforced Actuator Fabrication

As stated earlier both actuators share similarities in steps of fabrication. The need for a higher force actuator led us to the Boa actuator. Fabricating the Boa actuator consists of two stages: the first stage we call it the inner part, the second stage is the outer part. Four

actuators were made, varying the material and the winding spacing. Figure 13 shows the classification of the actuators.

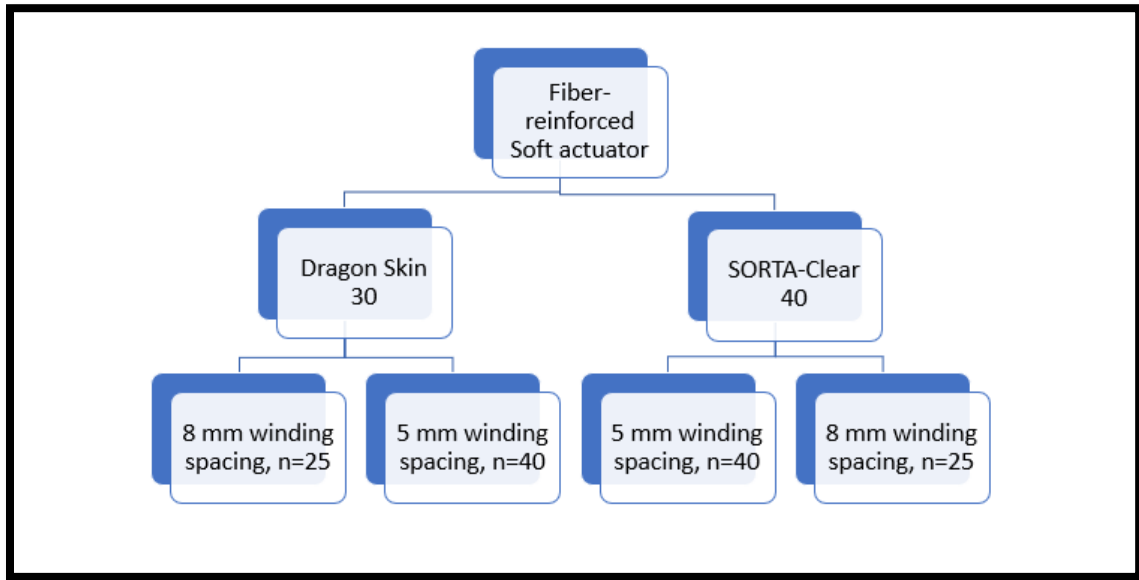


Figure 13. Classification of the four Fiber-Reinforced actuators.

The first stage uses the inner mold which consists of four parts: inner top, inner bottom, inner cap and the rod as shown in Figure 14. The top part and the bottom part are put together, then add a hot glue around the edges of the mold to prevent material leakage.

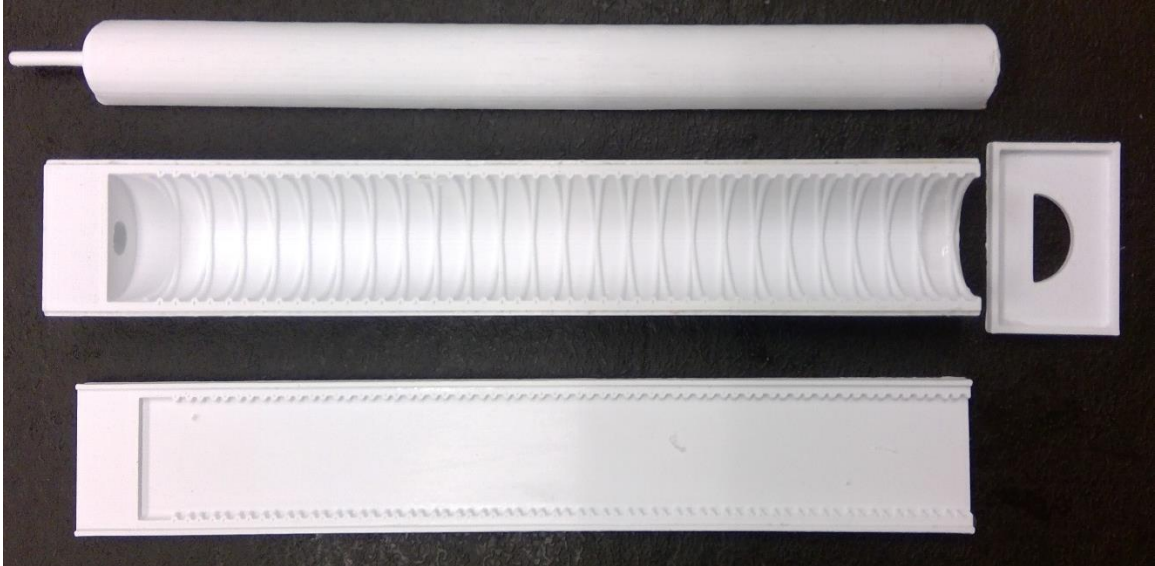


Figure 14. Components of the first stage, the inner mold for Fiber-Reinforced actuator.

Two materials were used to fabricate different actuators, one material for each actuator. This is one of the varying parameters that were studied. Dragon Skin 30 with a shore hardness of 30A comes in two cartridges A and B, mixing ratio of 1A:1B by weight or volume. SORTA-Clear 40 with a shore hardness of 40A, comes in two cartridges as well, mixing ratio of 100:10 by weight only. Weight is chosen for consistency. The material is then mixed together in the proper ratio for five minutes, shown in Figure 15.

The mixing will generate air bubbles in the mixed material, using a vacuum pump, the Dragon Skin material is degassed for 5 minutes, the SORTA-Clear material on the other hand is degassed for 20 minutes or when you see that there are no bubbles left. The longer degassing time is believed to be because of the high viscosity of the material. Spray all mold parts with a mold release, such as Ease Release 200.



Figure 15. Mixing elastomer materials during fabrication.

The material is poured into the mold, then the rod is inserted, and the cap is put to close the mold, care was taken to ensure the rod alignment between both ends of the mold, as the rod function to ensure even hollowness along the actuator. Another possible way would be to pour the material after putting the rod, this needs more time and patience, then adding the cap on top to align the rod and close the mold. The material is left to cure, Dragon Skin 30A requires eight hours, SORTA-Clear 40A requires sixteen hours. After that hot glue was removed, top part was detached carefully, remove the actuator and the result is shown in Figure 16.

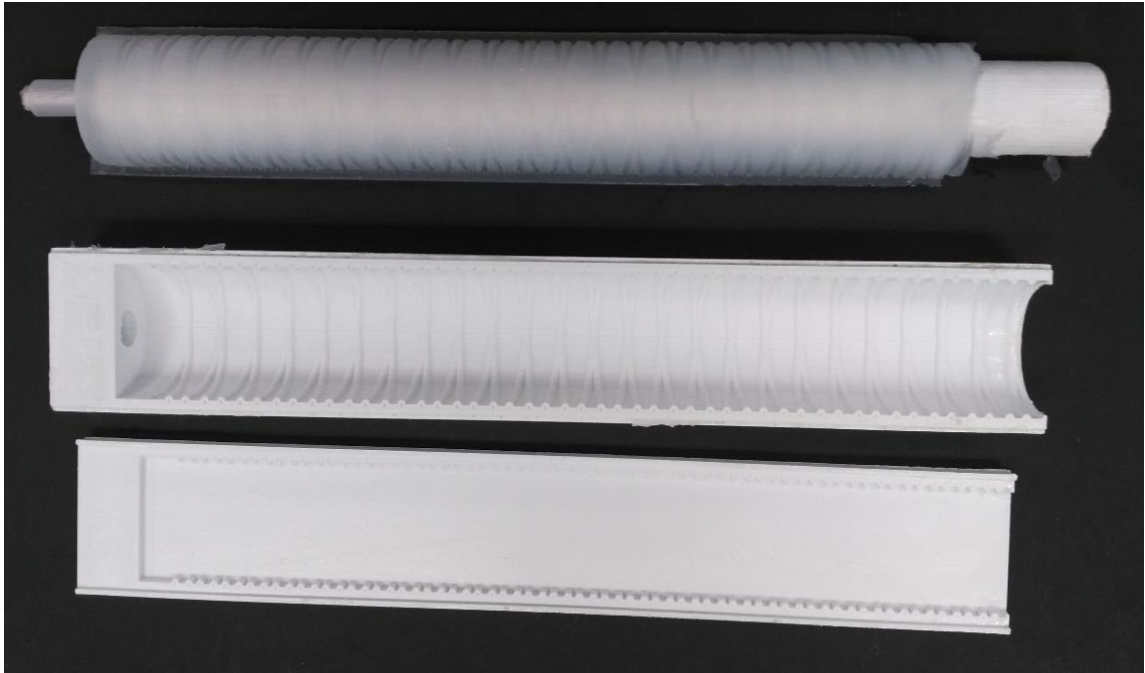


Figure 16. First stage of fabricating Fiber-Reinforced actuator winding spacing 5-mm.

To complete the first stage, the most rewarding part is to reinforce the actuator. First, a piece of fabric layer is cut to the size of the actuator bottom as shown in Figure 17.

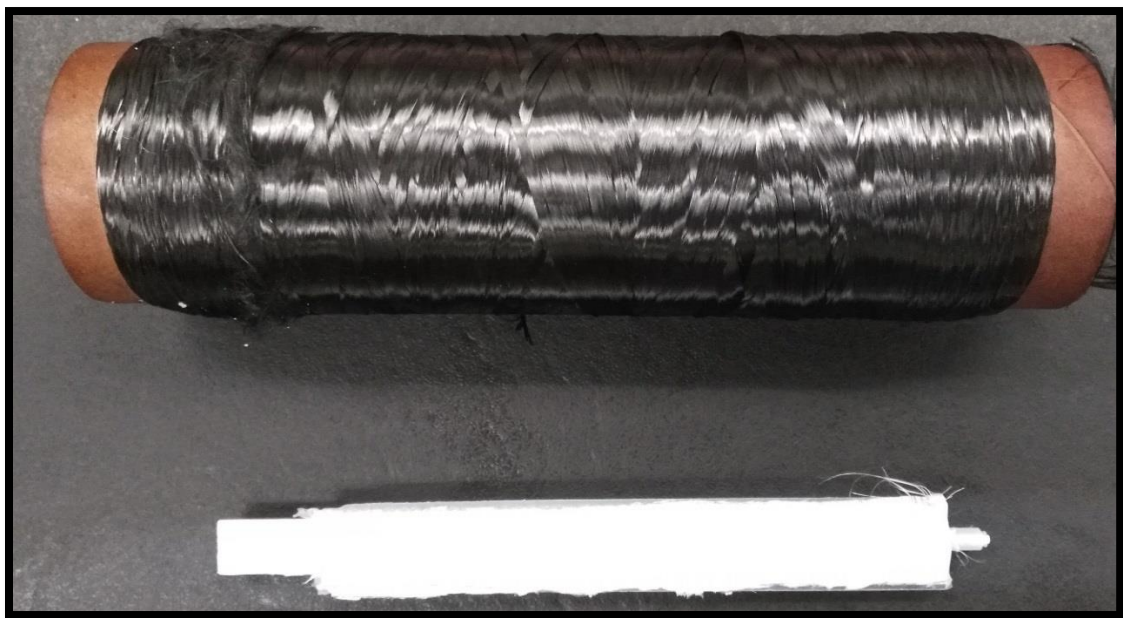


Figure 17. Adding fabric layer to the bottom of the Fiber-Reinforced actuator.

Carbon fiber was used to wrap the actuator helically, the result is shown in Figure 18. Attention was paid to have even wrapping along the actuator that was done with ease due to the designed grooving on the actuator body. The wrapping starts from one end with extra round of wrapping on the end to give reinforcement, then continuing along the actuator to the other end doing the same step, after that wrapping back to the first end.

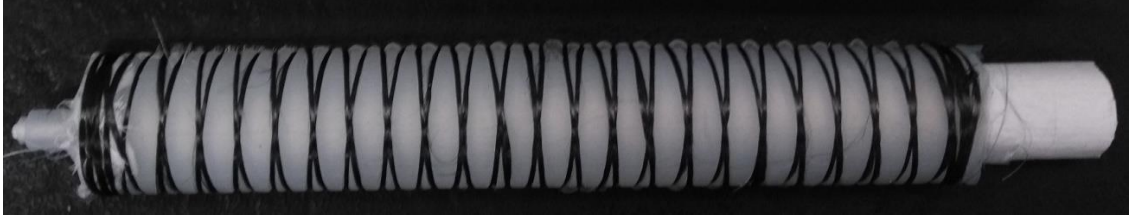


Figure 18. First stage of fabricating fiber-Reinforced actuator.

The second stage will add a layer of elastomer around the actuator to cover the reinforcement. Following the same procedure as before, we start by the outer mold, consists of three parts, shown in Figure 19.



Figure 19. Components of the second stage, the outer mold for Reinforced actuator.

The outer mold is little bigger than the first stage molded actuator, the mold parts are put together and glued, the molded actuator is put inside without removing the rod, as the rod will still be useful to align the actuator inside the mold, then pour the elastomer material following the same steps as earlier. After curing the actuator is shown in Figure 20.



Figure 20. Fiber-Reinforced actuator during process of fabrication.

The final step is to remove the rod, close the actuator from the lower end. Put the actuator standing in a small cylindrical container, pour the elastomer material and leave to cure. Teflon tape can be used to prevent the material from sticking to the actuator from outside, that way we can insure uniformness from outside and inside. Finally, the fabricated actuators are shown in Figure 21.

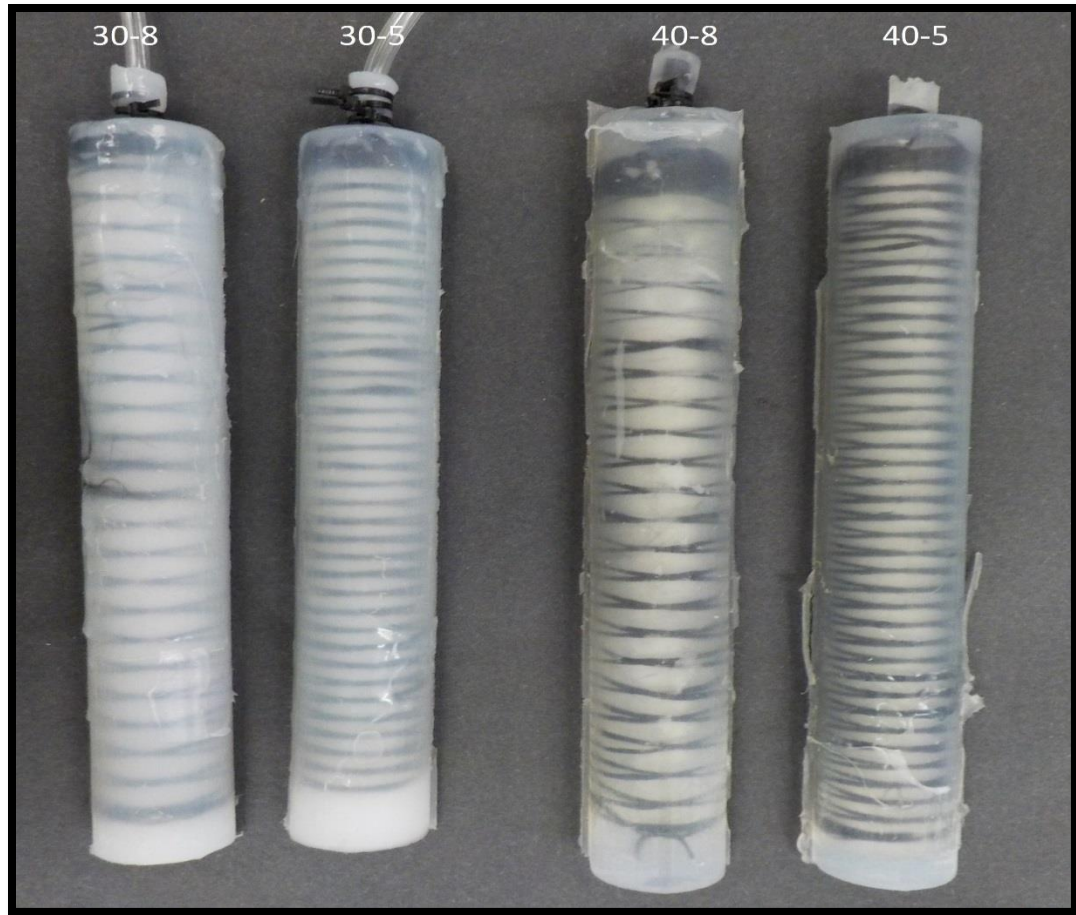


Figure 21. Fabricated Fiber-Reinforced soft actuators.

3.4 Boa exoskeleton arranging

The exoskeleton are considered as a rehabilitation and assistive devices by means of upper limb orthosis; wrist and elbow for instance [30]. Integrating the soft actuators into a brace would create a soft robotic exoskeleton. In this thesis an exoskeleton for wrist was developed, the actuators provide bending movement, it assists the wrist joint moving in palmar or dorsal direction. One or two actuators can be put on each side depending on the assistive force required. The results section will go over this in details. The Boa Exoskeleton is shown in Figure 22. Utilizing two soft actuators.



Figure 22. Boa Exoskeleton.

4 CONTROL AND TESTING

PneuNet and Boa actuators control is detailed in this section, including hardware, connections, Matlab Simulink schematics. The actuators were put to test; the testing station is detailed as well. Some similarities are shared between both actuators.

4.1 PneuNet Actuator

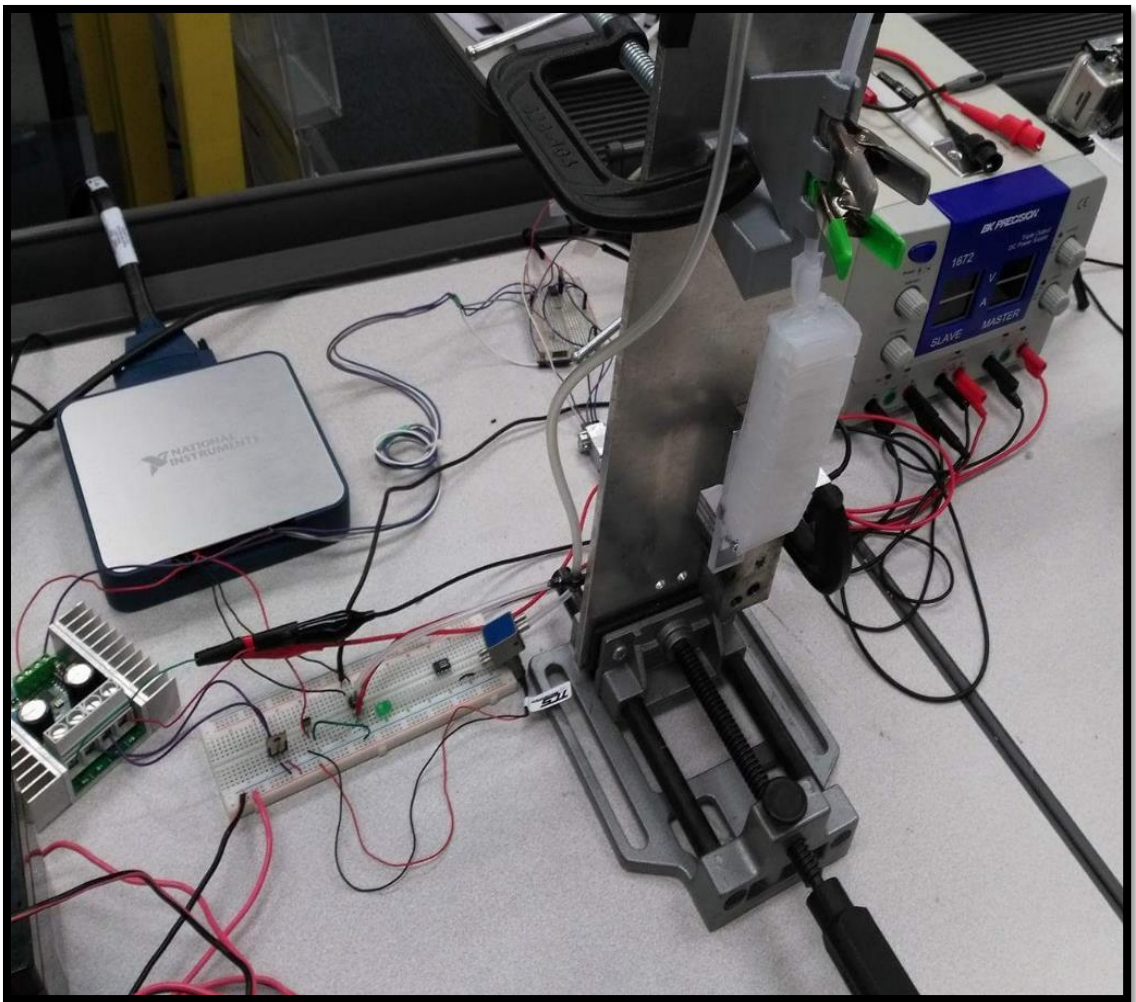


Figure 23. Testing station for PneuNet Actuator.

The testing station consists of a mount for the actuator, a 1 kg load cell (LSP-1 from Transducer Techniques) to record the applied force at the tip of the actuator. A 6V generic air pump to inflate the actuator, a motor driver (Syren 50A) to drive the air pump, a 12V 2-way solenoid valve to direct air flow, a 0-15psi pressure sensor from Honeywell to measure pump pressure and a National Instruments DAQ to integrate all components into the computer for control from Matlab/Simulink. Testing station shown in Figure 23.

The controller was designed using Simulink shown in Figure 24. It is an open loop controller that uses a sine wave input to control the on/off for the air pump, the open/close of the solenoid valve, and to measure the pressure of the air pump and the force applied to the load cell by the actuator. Once the system was assembled the load cell needed to be calibrated. This was achieved by incrementally placing known mass onto the load cell and recording the corresponding output voltage from the load cell. Microsoft Excel provided a linear equation relating the voltage to the applied load with a correlation coefficient of 1.

To gather the data for the experiment the actuator was inflated/deflated twenty times at six different frequencies ranging from 1 to 6 rad/s incremented by 1 rad/s. First, the inflation tube was inserted into the actuator and a zip-tie used to secure it in place. The tip of the actuator was then aligned to a mark on the load cell. The power was turned on and the battery plugged in. Finally, the actuators were tested at a lower frequency of 0.5 rad/sec to find the maximum applied load. For each frequency, the actuator was run for 20 cycles.

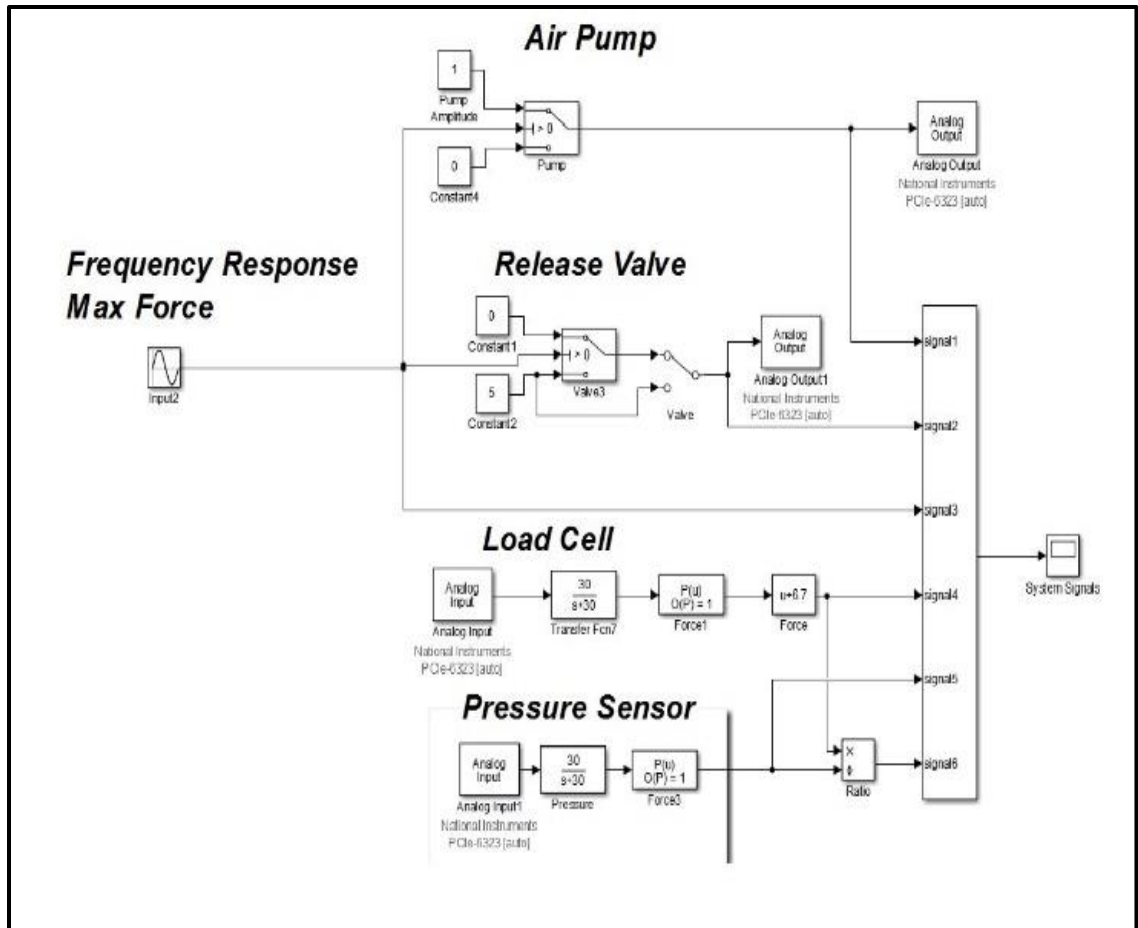


Figure 24. Matlab Simulink controller for PneuNet Actuator.

The actuator was then rotated to enable unconstrained motion and a black dot was marked on the tip. A GoPro HERO 5 was used to record the motion of the actuator when it was inflated to its unrestricted maximum flexion range and then deflated. Care was taken to ensure that the motion of the actuator was planar, in the field of view of the camera. KINOVEA was used to track the planar motion of the black mark on the tips of the actuators. The x-y planar displacement was output to an excel spreadsheet. Figure 25, shows a photo sequence of the actuator during motion.

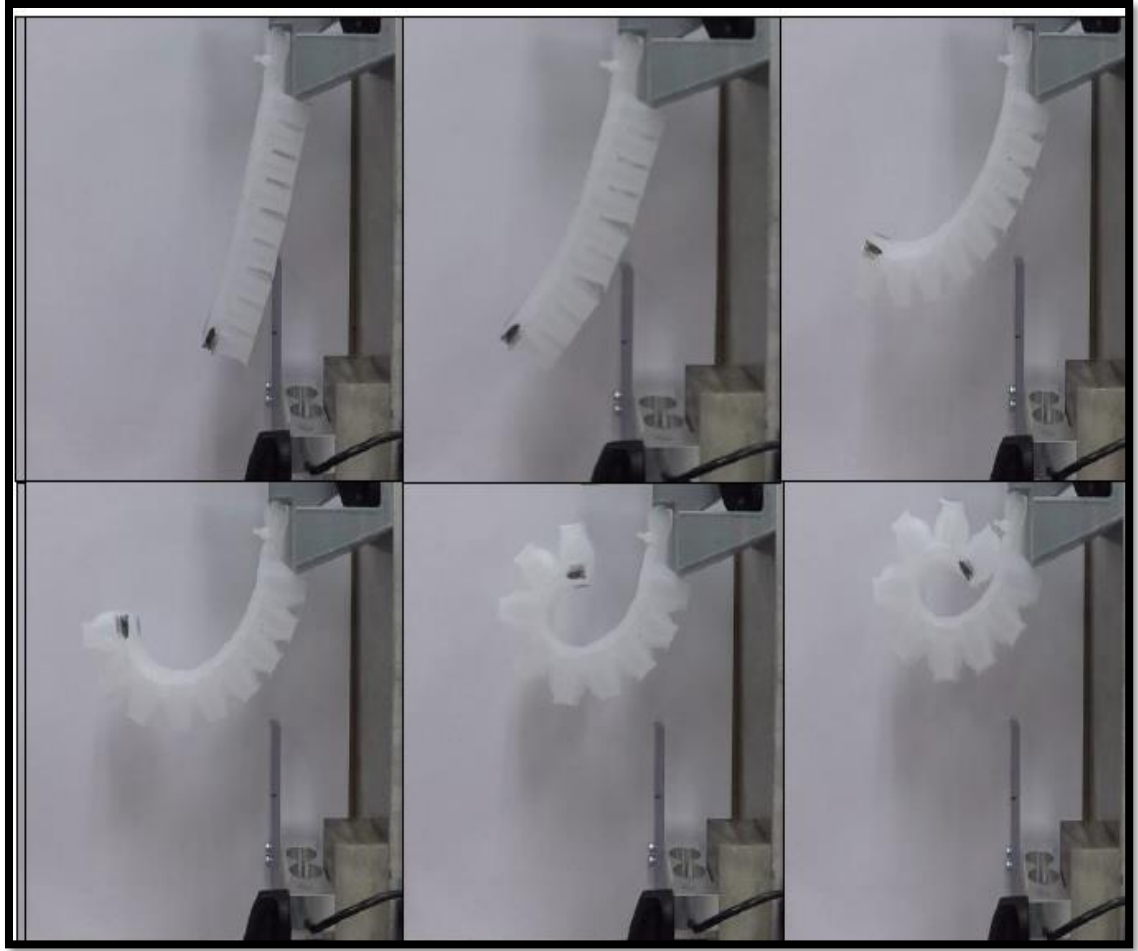


Figure 25. KINOVEA Photo Sequences for PneuNet actuator.

4.2 Boa Actuator

The testing station consist of a mount for the actuator, a 35 kg load cell (ESP-35 from Transducer Techniques) to measure the force applied by the tip of the actuator, a 150 PSI air compressor with an air tank (Bostitch BTFP02012), a 12V DC 3way normally closed solenoid valve (MettleAir 3V210-08) to direct the airflow, a 0-100 PSI pressure sensor from Honeywell to measure the system pressure and a National Instruments DAQ to integrate all components into the computer for control from Matlab/Simulink. The testing station is shown in Figure 26.



Figure 26. Testing station for Boa Actuator.

Matlab/Simulink is also used to design the controller shown in Figure 27. An open loop controller that uses a step input signal to turn on the 3-way valve, and to measure the pressure of the system and the force applied by the tip of the actuator to the load cell

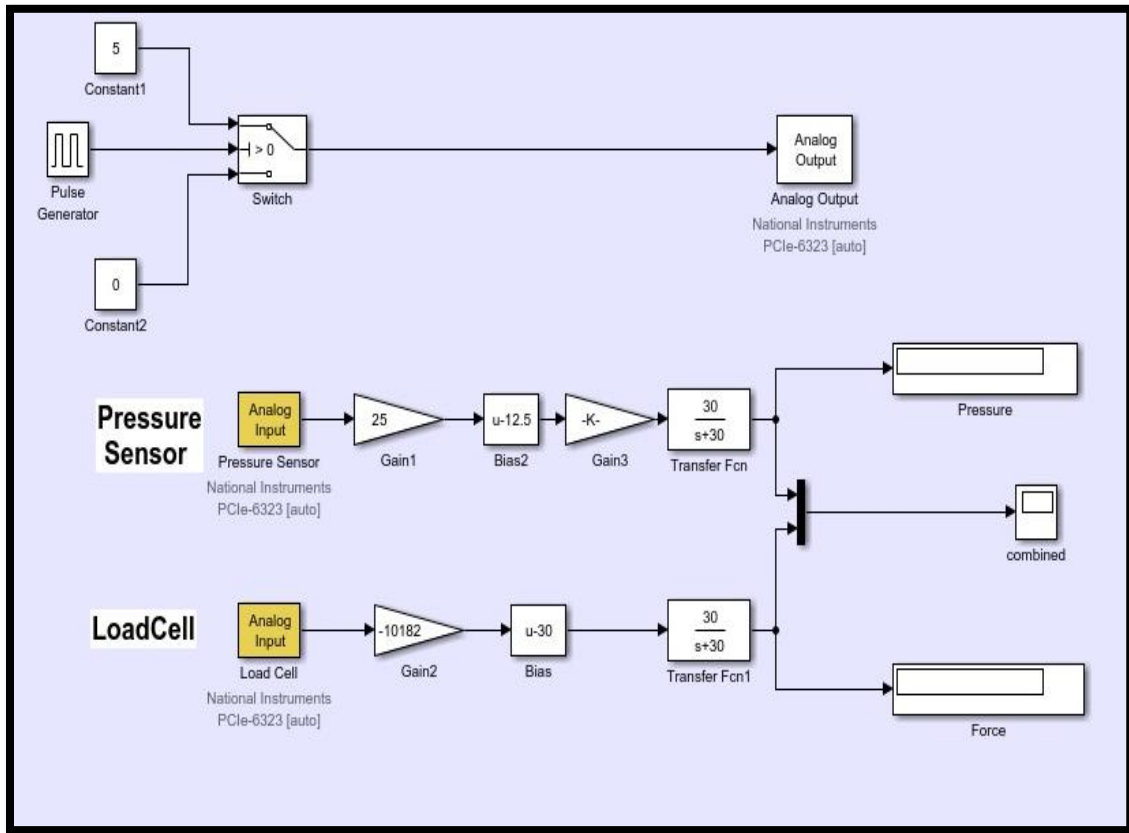


Figure 27. Matlab Simulink controller for Boa Actuator.

Whenever the input signal turns on, it opens the valve allowing the compressed air from the air tank to flow, a regulator before the valve sets a constant desired pressure, the actuator is inflated. When the input signal turns off, it closes the 3-way valve, the air entrapped in the actuator exhaust through exhaust port in the valve deflating the actuator.

Similar calibration method was followed to calibrate the 35 kg loadcell, it was achieved by incrementally placing known masses onto the load cell, only this time heavier masses hence the 35 kg loadcell. Microsoft Excel provided a linear equation relating the voltage to the applied load with a correlation coefficient of 1.

To gather the data for the experiment the actuator was inflated/deflated twenty times at 6 different pressures ranging from 150 KPa to 400 KPa incremented by 50 KPa, the inflation tube was inserted and secured tightly in place to prevent any leakage from high pressure. The tip of the actuator was aligned to a marked calibrated spot on the load cell.

4.3 Boa Exoskeleton

A more simple, compact and cost effective than traditional rigid mechanical exoskeletons, the Boa Exoskeleton shown in Figure 28. The exoskeleton consists of a brace and soft actuators. EMG (Electromyography) is a technique for evaluating and recording the electrical activity produced by skeletal muscles. EMG is implemented in the Boa Exoskeleton for actuation. Four EMG electrodes are placed around the arm muscles. EMG signals triggers the actuation and used to control the degree of bending.



Figure 28. Boa Exoskeleton during testing.

To test the Boa Exoskeleton, the testing station will include the Boa Exoskeleton and Myolab II; utilizes EMG to locate muscle activity down to 0.2 microvolts. Four EMG electrodes were placed on the arm: E_{F1} and E_{F1} were placed around the arm muscles responsible for wrist flexion, E_{E2} and E_{E2} were placed arm muscles responsible for wrist extension. An accelerometer, from (The Computer Group, part #0300-0143), put on the hand, on top of the wrist, to measure the flexion angle ϕ . Added to the testing station used in the Boa actuator testing. Figure 29 shows a diagram of the Boa Exoskeleton testing process.

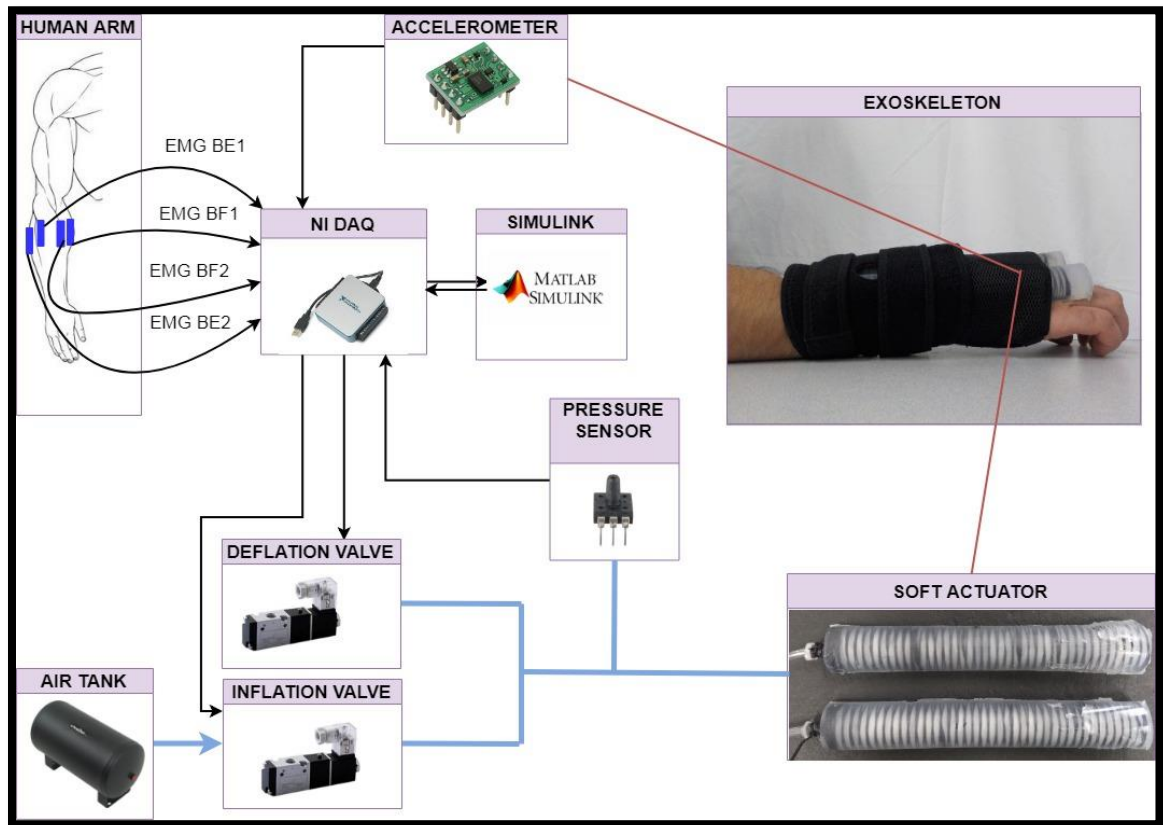


Figure 29. Boa Exoskeleton testing diagram.

The human arm was rested on a platform to prevent undesired motion, accelerometer to measure the flexion angle on the human wrist. A 2.5 lb (1.13398 Kg) weight was placed on the hand. Figure 30 shows Boa Exoskeleton testing station.

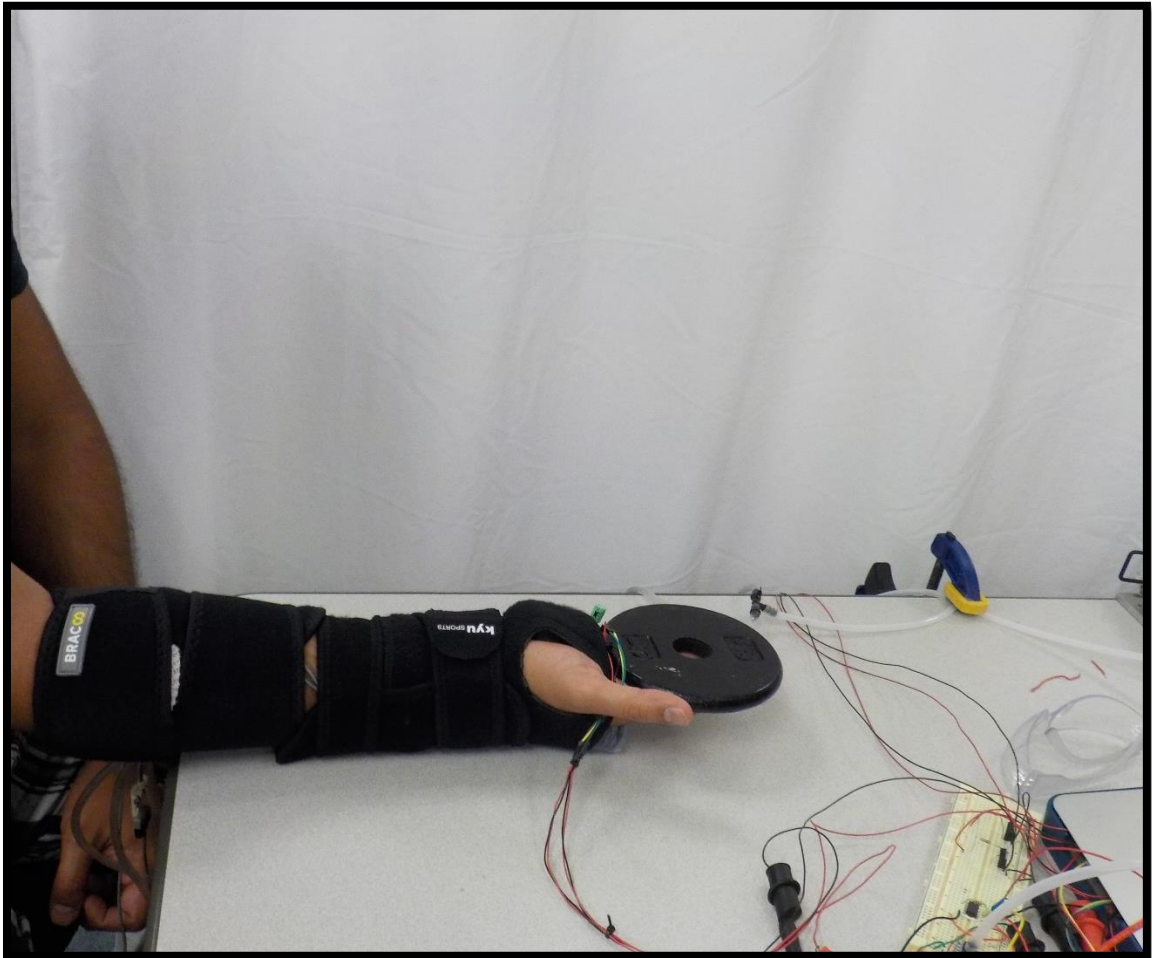


Figure 30. Boa Exoskeleton testing station.

The control was designed on Matlab/Simulink, the diagram is shown in Figure 31.

To test the Boa Exoskeleton, five tests were made as follows:

- 1) Full assistive: the human subject was asked not to move, the Boa Exoskeleton is actuated from the controller, and this is used to find the maximum assistive flexion

angle ϕ of the Boa Exoskeleton, where almost no EMG signals. To be compared with normal human movement EMG signals and angle.

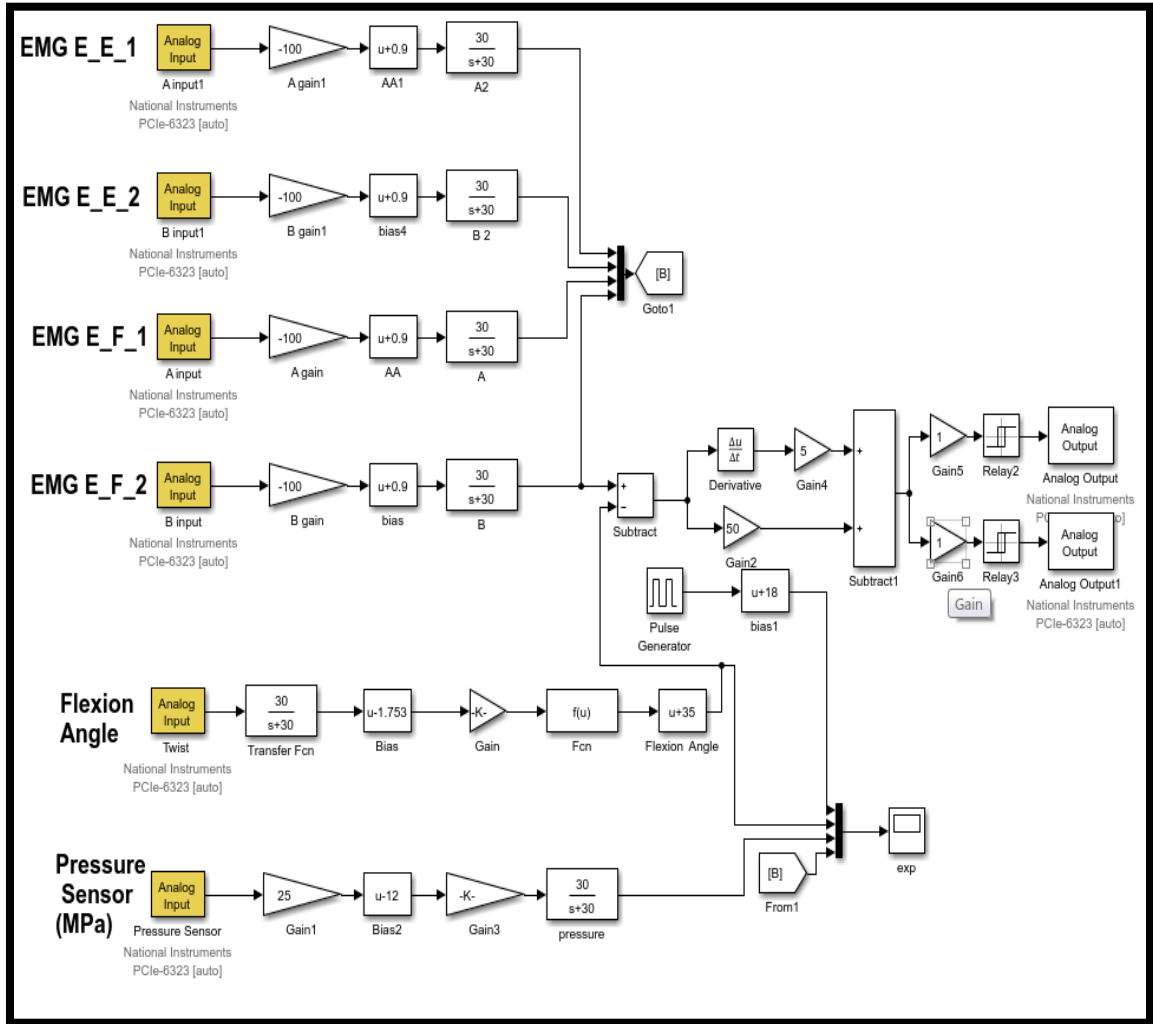


Figure 31. Matlab/Simulink control diagram for Boa Exoskeleton.

- 2) Non-Assistive: EMG signals were recorded for the human arm bending wrist. This meant to measure the EMG signals and the flexion angle ϕ the human exerts to normally bend the wrist.
- 3) No Exoskeleton: The Exoskeleton causes some resistance on bending. This test to measure the EMG signals and the flexion angle ϕ without the exoskeleton.

- 4) No Exoskeleton/No weigh: The purpose of this test is to measure the EMG signals and the flexion angle ϕ without weight for the unrestricted hand.
- 5) EMG actuated: The EMG signals will activate the Boa Exoskeleton that will assist in bending the wrist. This is how the Boa Exoskeleton would function normally. The control system will keep track of the hand, based on the error between the EMG signal and the flexion ϕ angle. When the human exerts EMG more than the flexion angle ϕ it will open the inflation valve, on the other side when the EMG signals are less than the flexion ϕ angle it will open the deflation valve. There is a no-action zone around the error where the Exoskeleton holds its position.

Fatigue was taken into consideration. The “Full assistive” mode does not require any force by the human subject, the “No Exoskeleton/No weight” mode requires minimal effort; hence they were excluded from the combinations. The other three tests make six combinations; therefore, six human subjects were tested according to the following table.

After completing the testing, data will be recorded for analysis. EMG signals and flexion angle ϕ will be compared between the four different scenarios to validate the Boa Exoskeleton.

Table 4: Human subject tests order combinations.

Subject number	First test	Second test	Third test	Fourth test	Fifth Test
One	EMG Actuated	No Exoskeleton	Full Assistive	Non- Assistive	No Exoskeleton /No weight
Two	EMG Actuated	Non- Assistive	Full Assistive	No Exoskeleton	No Exoskeleton /No weight
Three	No Exoskeleton	EMG Actuated	Full Assistive	Non- Assistive	No Exoskeleton /No weight
Four	No Exoskeleton	Non- Assistive	Full Assistive	EMG Actuated	No Exoskeleton /No weight
Five	Non- Assistive	EMG Actuated	Full Assistive	No Exoskeleton	No Exoskeleton /No weight
Six	Non- Assistive	No Exoskeleton	Full Assistive	EMG Actuated	No Exoskeleton /No weight

5 RESULTS

Upon completing the tests, the data was gathered using DAQ through Matlab, all the control was done on Simulink/Matlab. The following sections will show the results for each actuator, compare the data between, eventually choosing the optimum actuator for our Boa Exoskeleton.

5.1 PneuNet Actuator

Soft PneuNet Actuators (SPAs) with a taper angle 3° was designed and tested over 7 input frequencies ranging from 1 rad/s to 6 rad/s in 1 rad/s increment and a minimum frequency of 0.5 rad/s. results will be compared with SPA with a taper angle 0° as a reference.

Figure 32, shows the Force with respect to time for SPA with taper angle 3° , for all seven frequencies 0.5-6 from top to bottom respectively. The graph shows that the maximum force occurs when the frequency is minimum (0.5 rad/s), in general as the frequency increased the force applied by the soft actuator decreased. The lower the frequency the longer the actuation time.

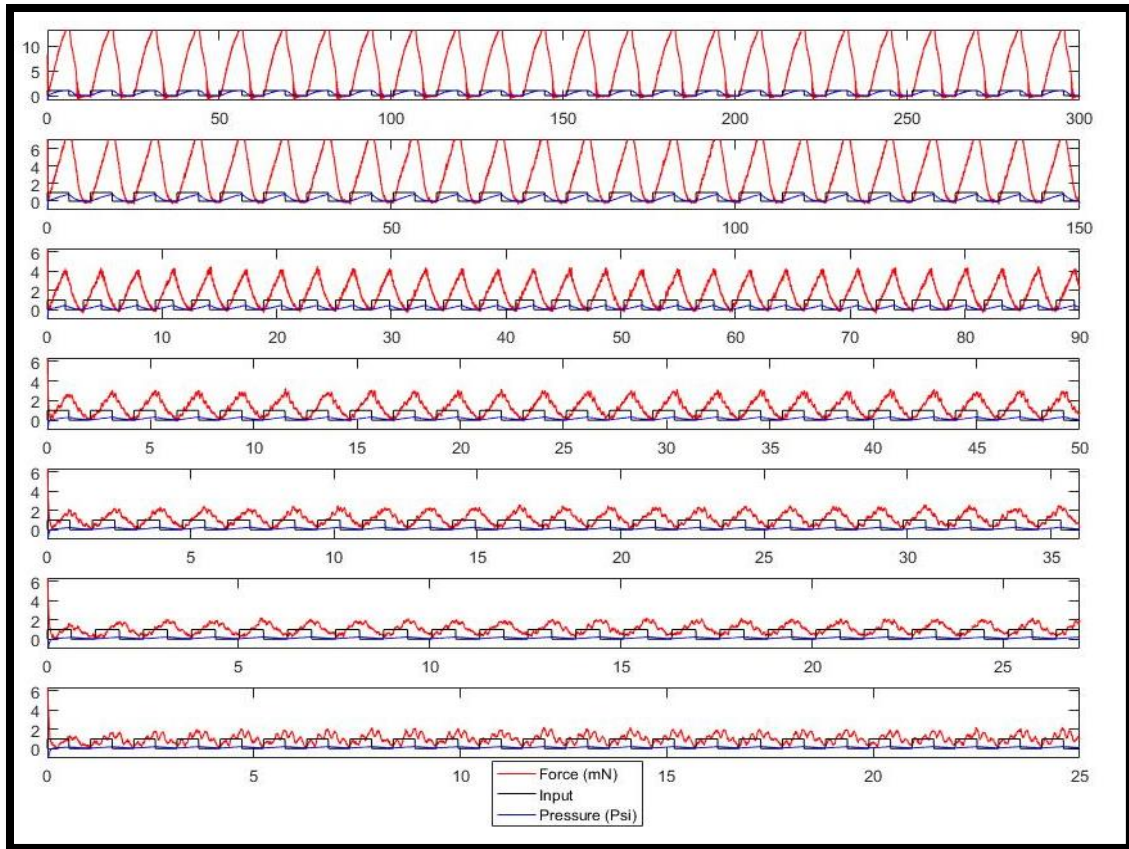


Figure 32. Force for SPA with taper angle 3° . For frequencies 0.5-6 rad/s from top to bottom respectively.

Figure 33 shows a hysteresis loop; the force over pressure in inflation and deflation. The energy losses are maximum when the frequency is minimum.

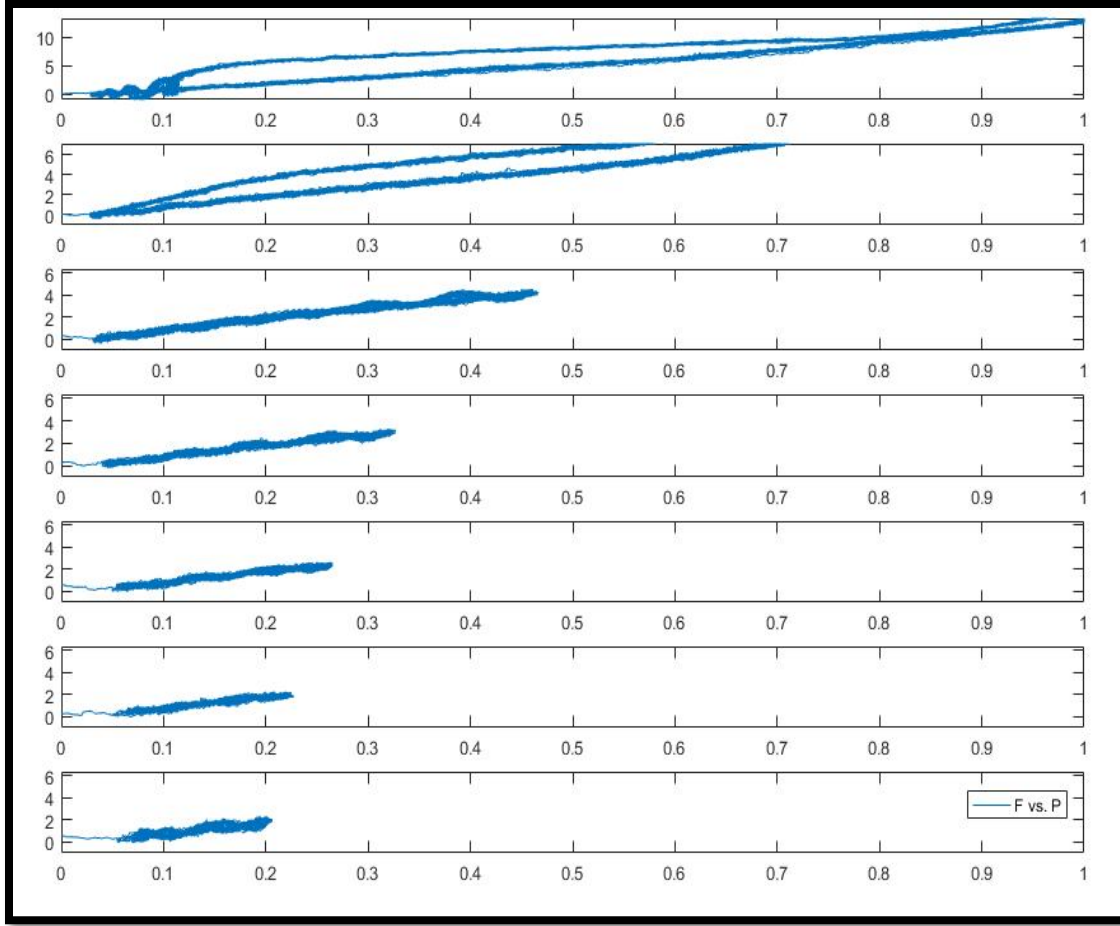


Figure 33. Hysteresis of the soft actuator with taper angle 3° for all frequencies. For frequencies 0.5-6 rad/s from top to bottom respectively

As the frequency increase the energy losses decreases, the reason is when the frequency is the minimum the actuation time is longer in comparison to a higher frequency, which means the energy provided to the system is higher. The input energy to the system is the pressurized air, while the output is the force applied by the soft actuator.

Figures 34 and 35 shows the Mean and standard deviation for maximum forces for SPA with taper angle 3° and 0° respectively, over all the tested frequencies. In general, the highest mean of maximum force is at the lowest frequency as discussed previously.

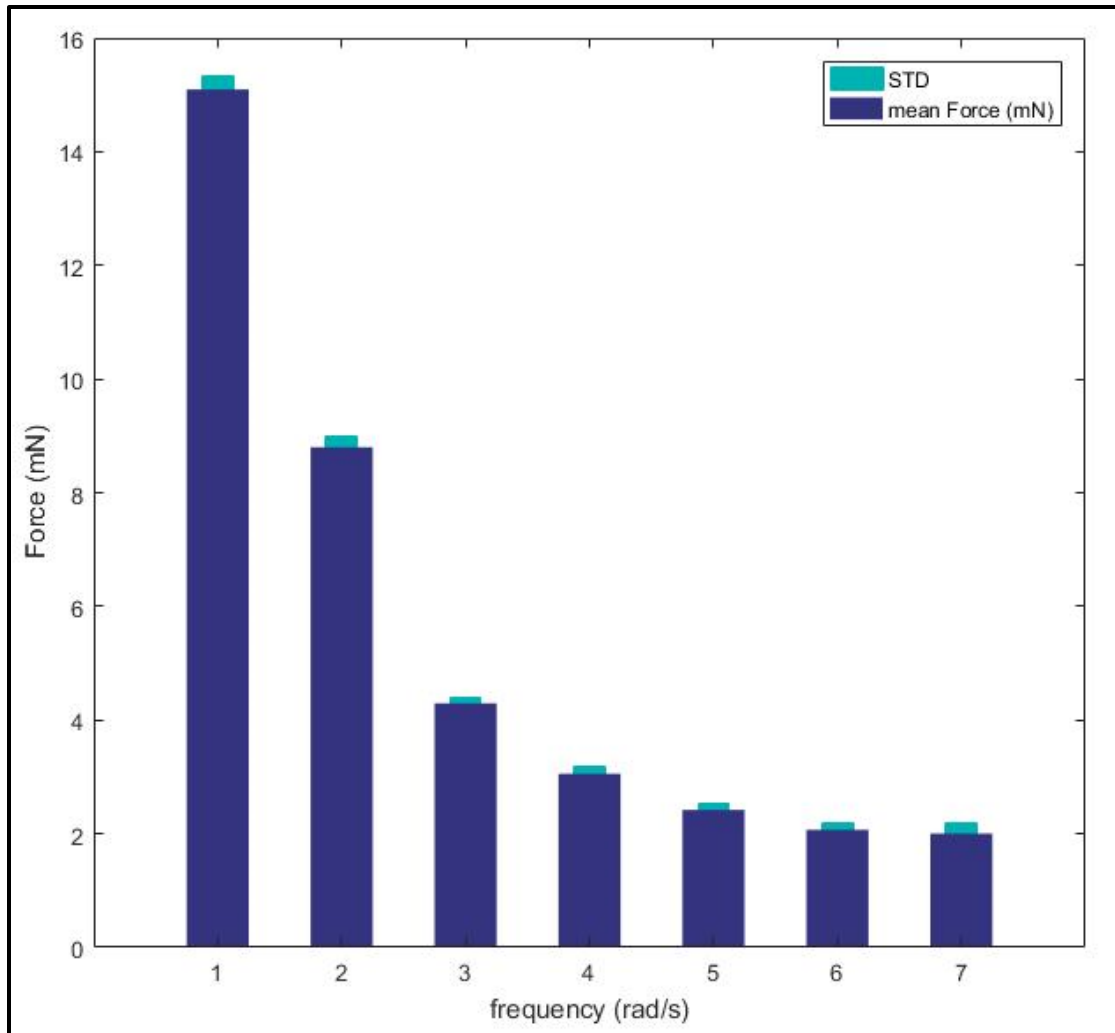


Figure 34. Standard deviation and mean of maximum forces for SPA with taper angle 3° for frequencies 0.5 to 6 rad/s respectively.

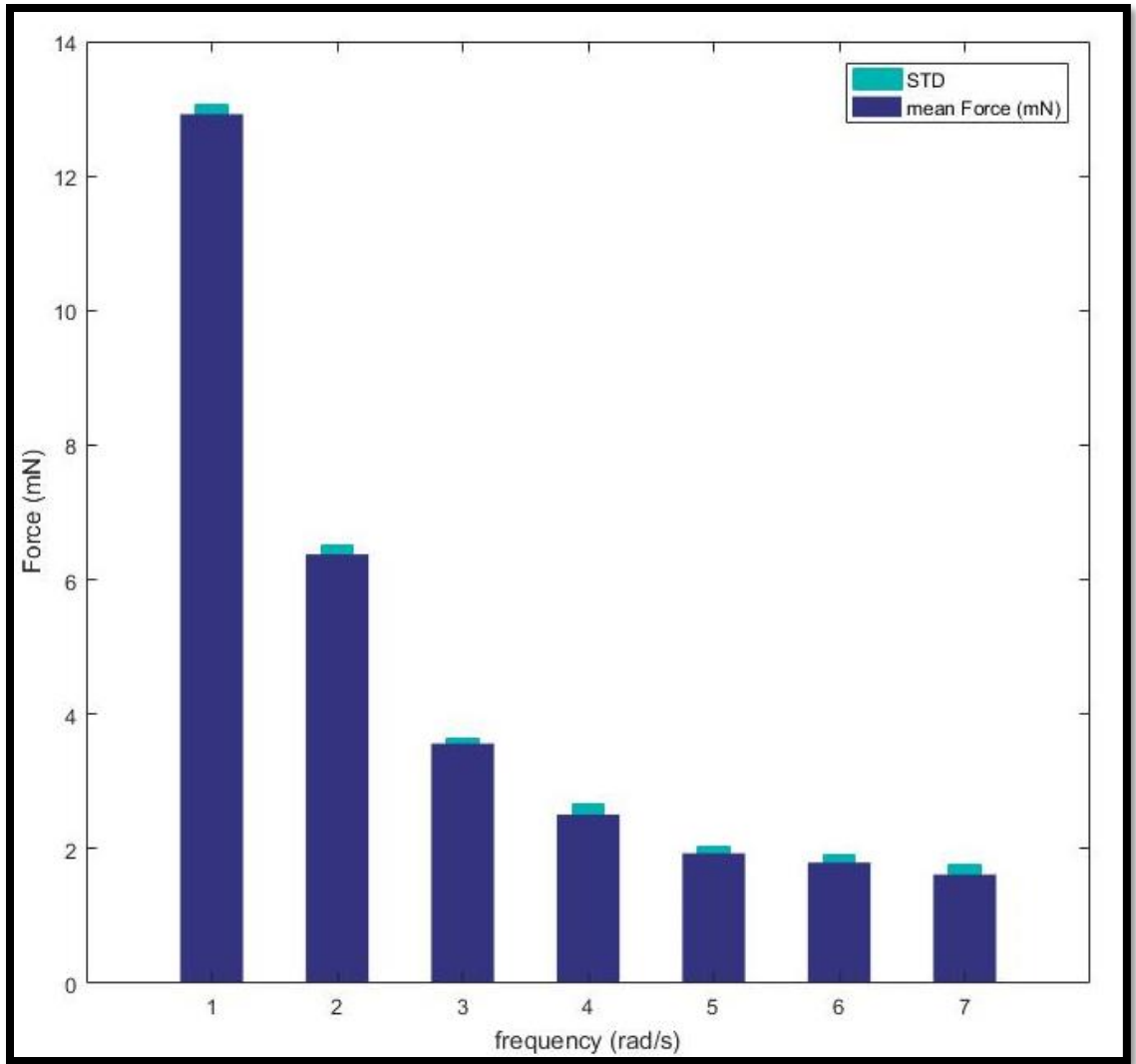


Figure 35. Standard deviation and mean of maximum forces for SPA with taper angle 0° for frequencies 0.5 to 6 rad/s respectively.

The SPAs unrestricted maximum flexion range was found using the method explained in the control and testing. Figure 36 shows the displacement of the soft actuator's tips during inflation in the x-y plane with frequency 0.5 rad/s. The displacement increases as the taper angle increased, with a maximum displacement produced by the actuator with a taper angle 3°.

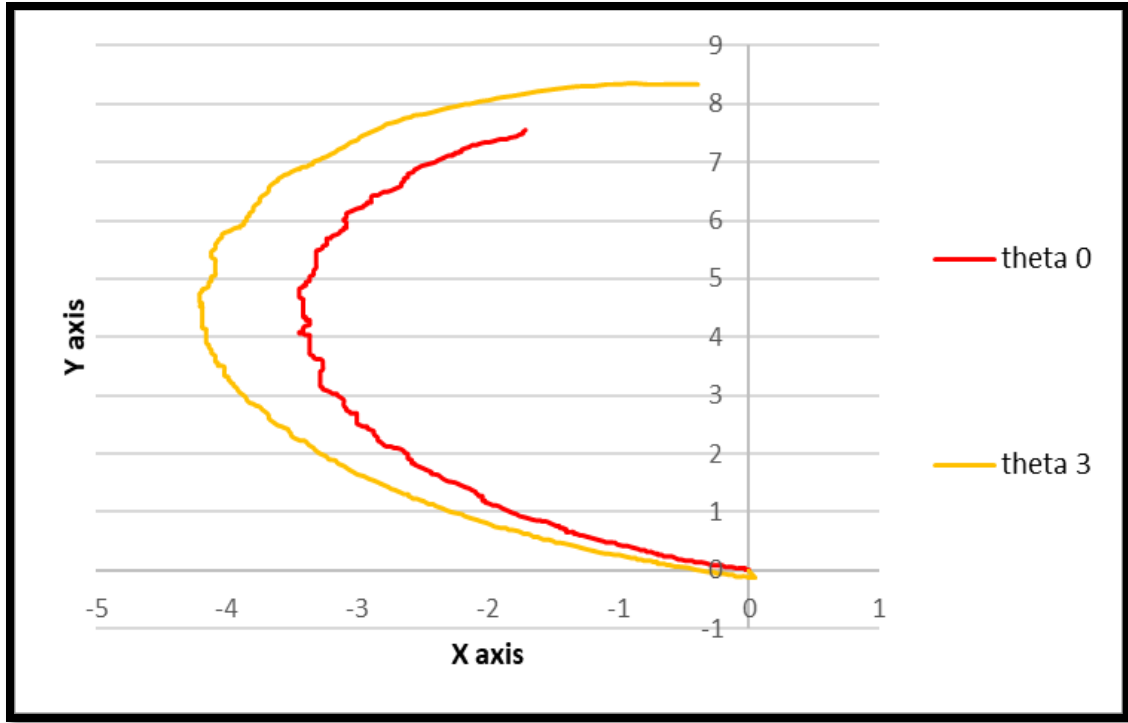


Figure 36. Displacement of the tip of the soft actuators.

Statistical analysis was made on our experiment data for all the group. Table 1 shows the value of one-way analysis of variance (ANOVA1). Since our probabilities (p-value) were less than 0.05, the data is significantly different from each other.

Table 5: ANOVA 1 for PneuNet Actuators

THETA	F	PROB>F
0	19342.32	5.83671E-193
3	18650.12	6.56728E-192

5.2 Fiber-Reinforced Actuator

Four actuators were tested, each actuator was tested at 6 different pressures, from 150 KPa to 400 KPa with an increment of 50 KPa. The tip of the actuator was aligned on

the load cell, the force and Pressure were recorded, as they are the two key values, the input is pressure and the output is force.

Figure 37, shows the force and pressure with respect to time for Boa actuator (30-5) for all tested pressures, it is clear that the force increases when the pressure increase. A minimum force of 2.5 N at 0.15 MPa, and a maximum force of 6 N at 0.4 MPa.

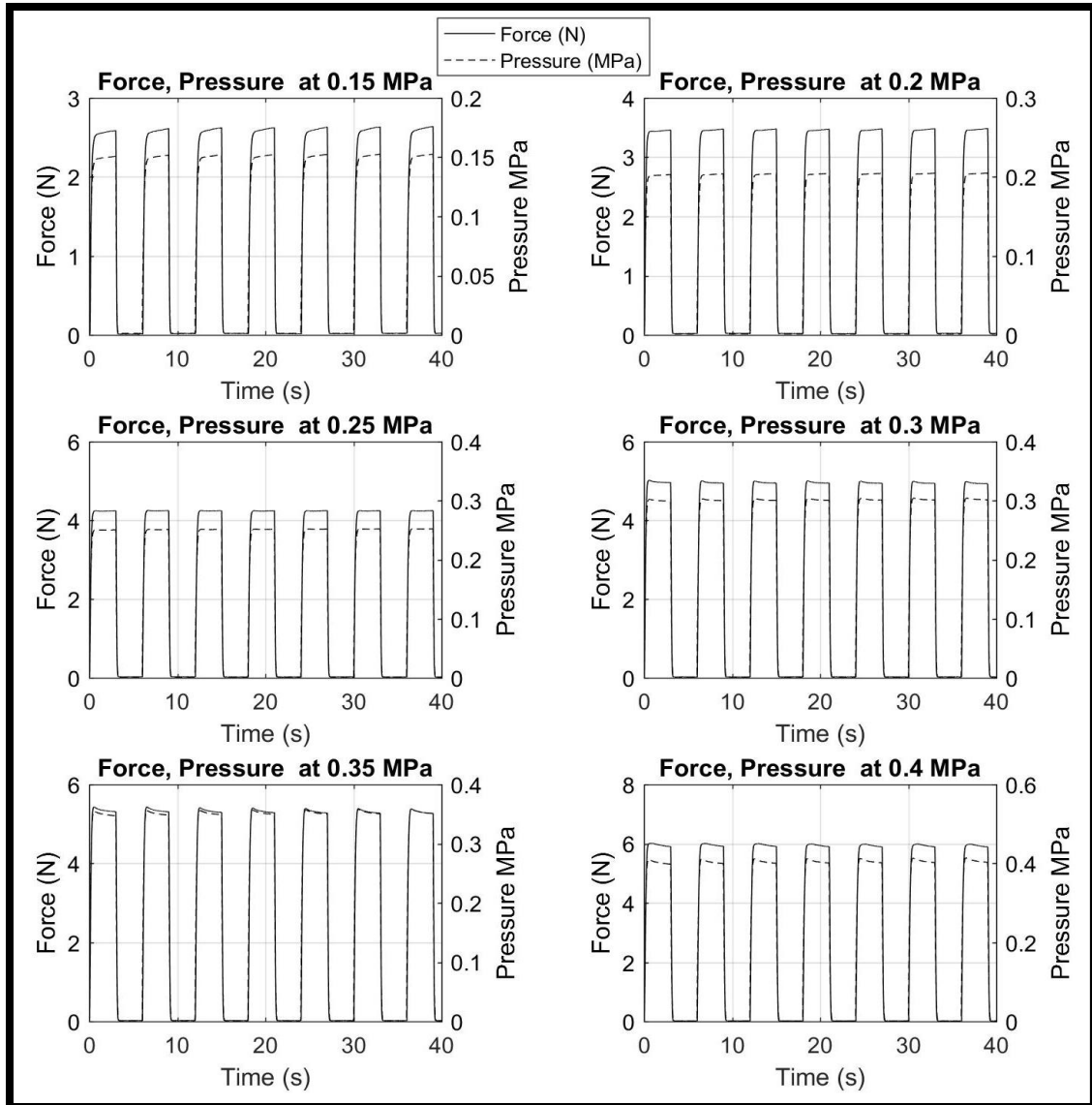


Figure 37. Force (N), Pressure (MPa) with time for Boa (30-5) actuator.

Figure 38, shows the force and pressure with respect to time for Boa actuator (30-8) for all tested pressures, the force increases when the pressure increase. A minimum force of 1.9 N at 0.15 MPa, and a maximum force of 5.1 N at 0.35 MPa. Boa actuator (30-8) exerts less force than Boa actuator (30-5). Boa actuator (30-5) exerts 5.4 N force at 0.35 MPa. Boa actuator (30-8) maximum tested pressure was 0.35 MPa. Considering both are made from same material Dragon Skin 30A, (30-5) has larger number of windings $n = 40$, compared to (30-8) which has $n = 25$, this results in a more reinforced actuator body leading to higher force in this case.

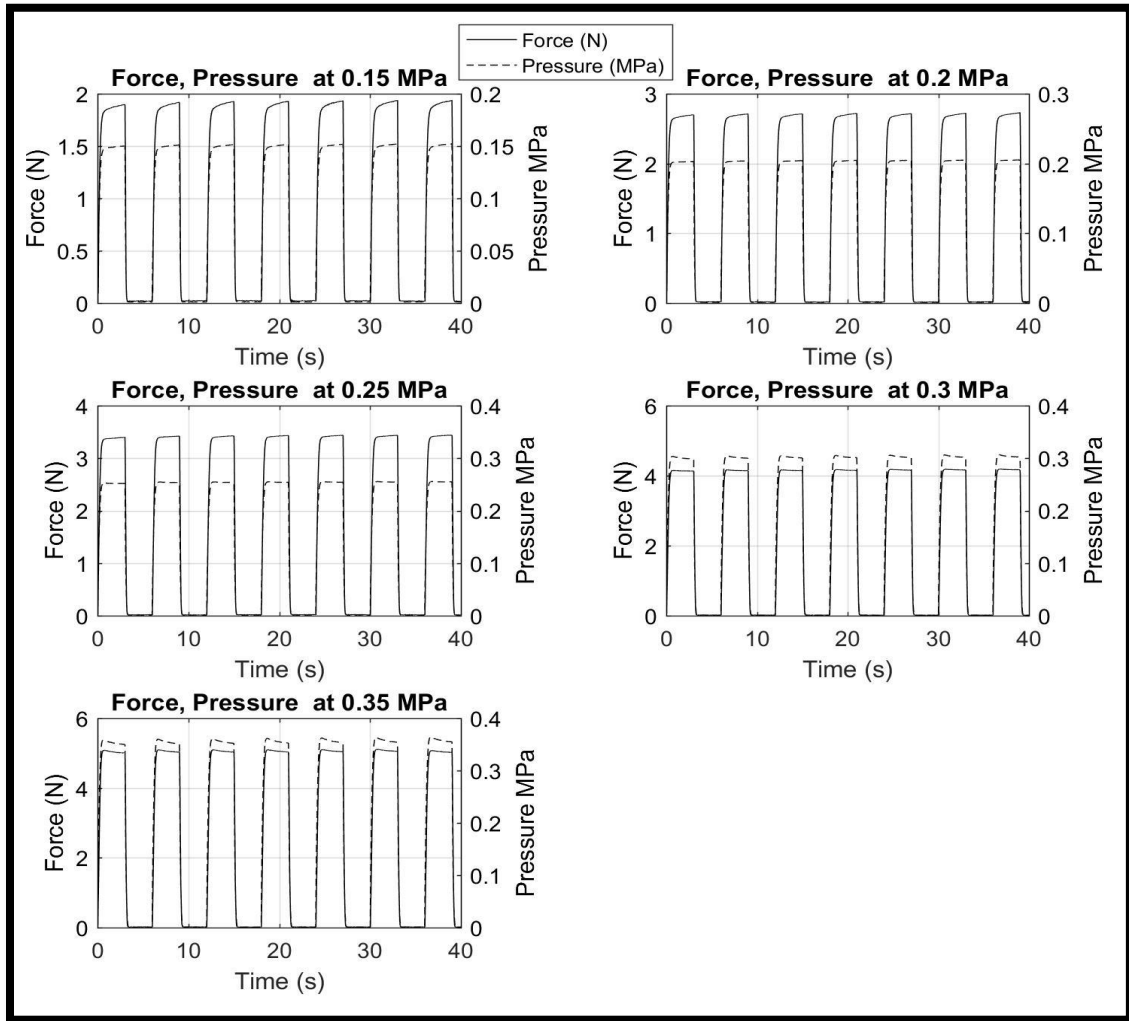


Figure 38. Force (N), Pressure (MPa) with time for Boa (30-8) actuator.

Figure 39, shows the force and pressure with respect to time for Boa actuator (40-8) for all tested pressures. The same behavior noticed here, the force increases with pressure increase. A minimum force of 2.2 N at 0.15 MPa, and a maximum force of 6.6 N at 0.4 MPa.

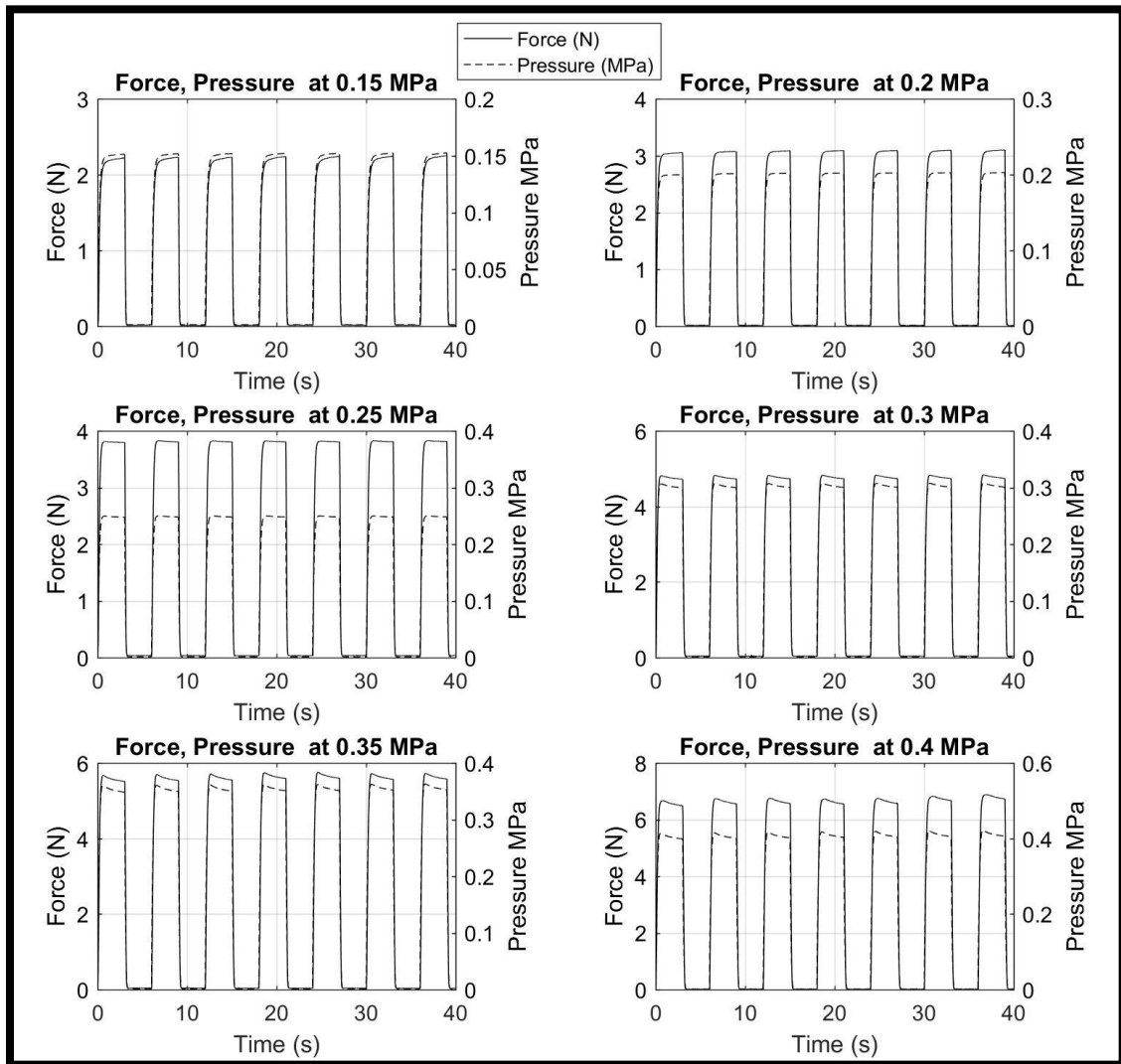


Figure 39. Force (N), Pressure (MPa) with time for Boa (40-8) actuator.

Figure 40, shows the force and pressure with respect to time for Boa actuator (40-5) for all tested pressures, force increases when the pressure increase. A minimum force of

2.2 N at 0.15 MPa, and a maximum force of 6.35 N at 0.4 MPa. Boa actuator (40-8) exerts higher maximum force than Boa actuator (40-8). Considering both are made from same material SORTA-Clear 40A, (40-5) has larger number of windings $n = 40$, compared to (40-8) which has $n = 25$.

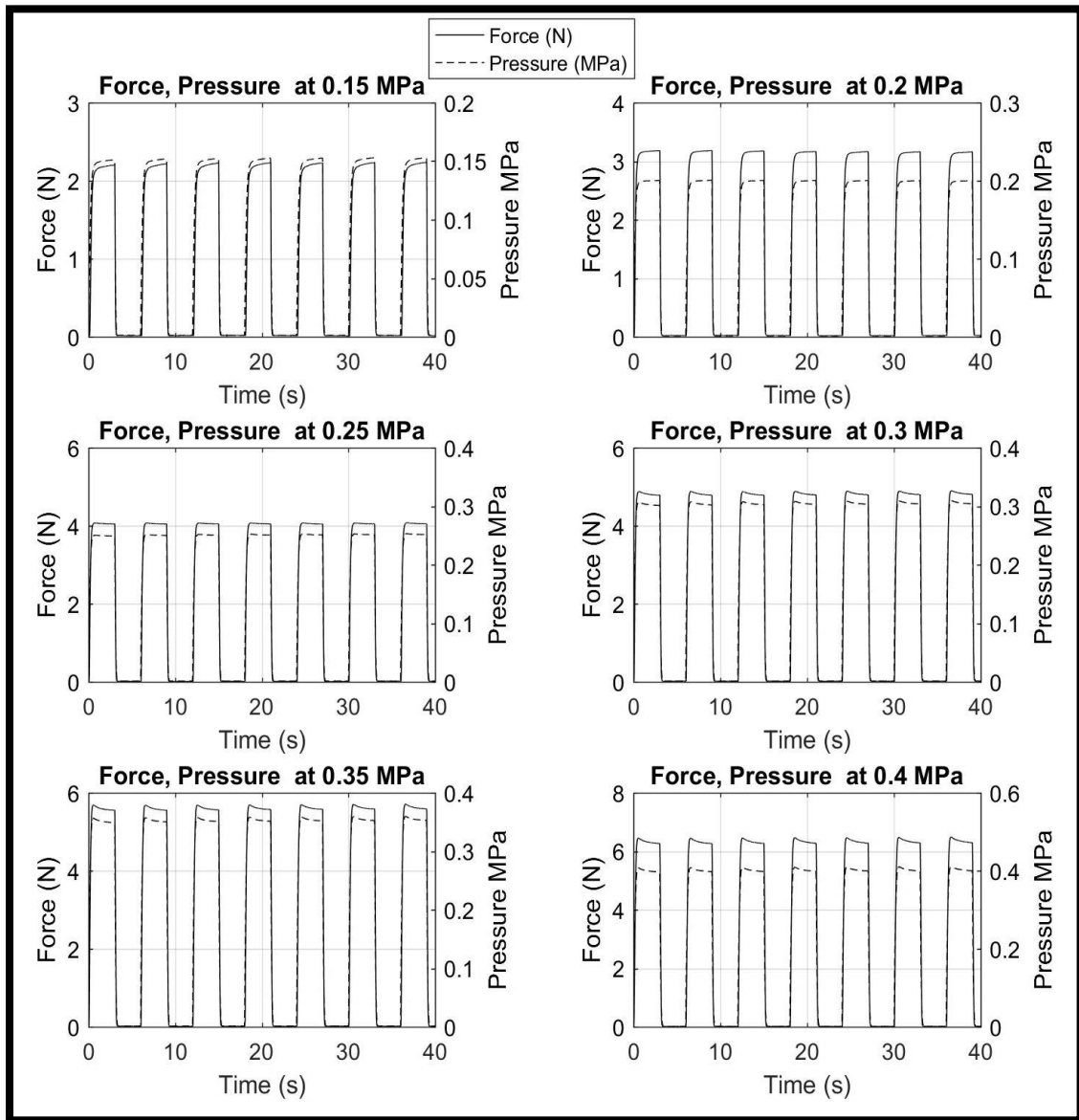


Figure 40. Force (N), Pressure (MPa) with time for Boa (40-5) actuator.

Force is the output of the system, and Pressure is the input, studying the relation between them gives us a good understanding of how the actuators behave. Results for pressure versus time are shown for all four Boa actuators. Figure 41 shows the force versus pressure for Boa actuator (30-8) for all the tested pressures.

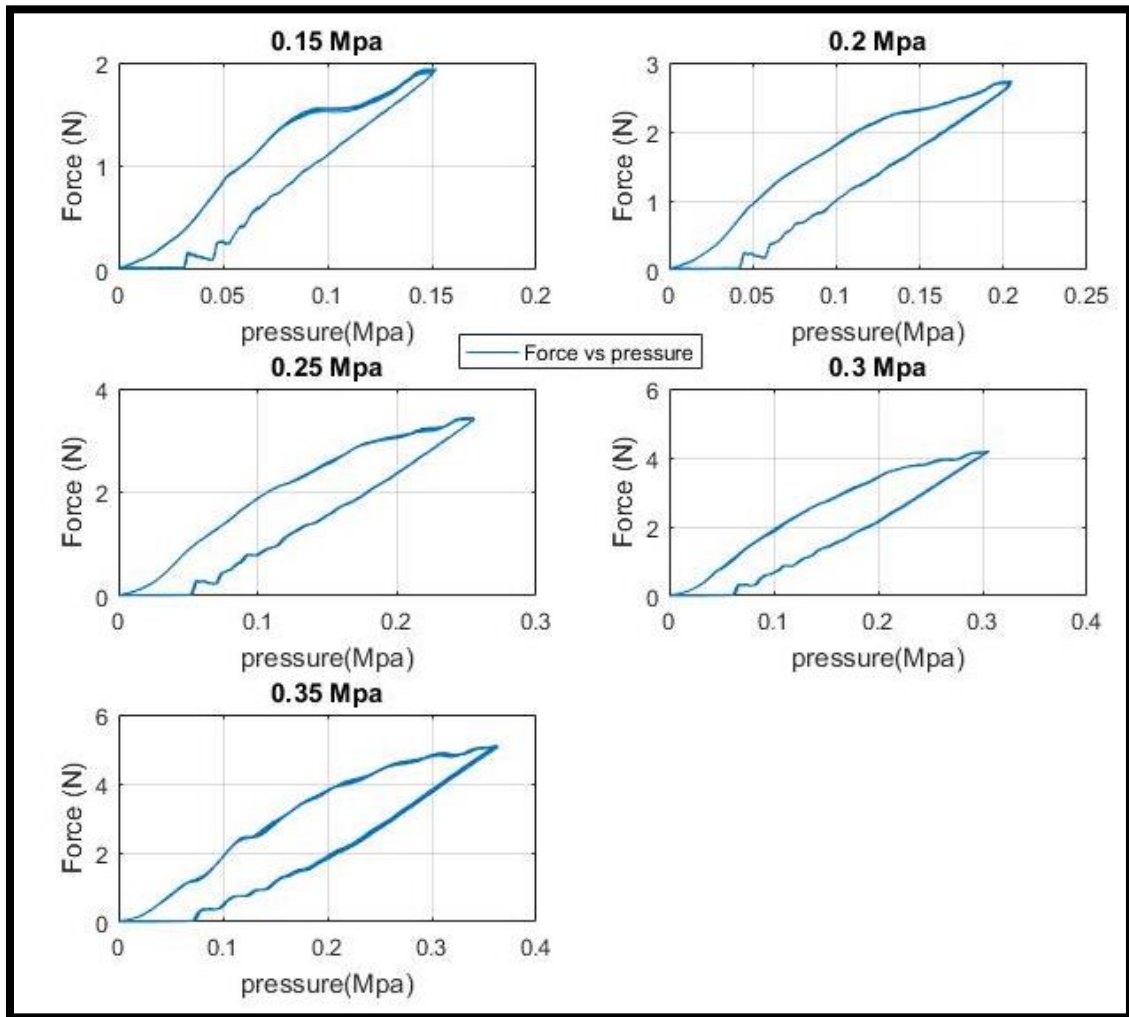


Figure 41. Force vs Pressure for Boa actuator (30-8).

The inflation is the bottom part of the plot, while the deflation is the top part. The inflation has lower force/pressure ratio than deflation, which can be because of the immediate deflation. When the valve turns on the actuator inflate gradually reaching its

maximum value, and when the valve shuts the input pressure and deflate the actuator through the exhaust port, it causes a sudden drop of pressure, causing the force/pressure ratio to be relatively higher than inflation. Force vs pressure for Boa actuator (30-5) is shown in Figure 42 for all pressures.

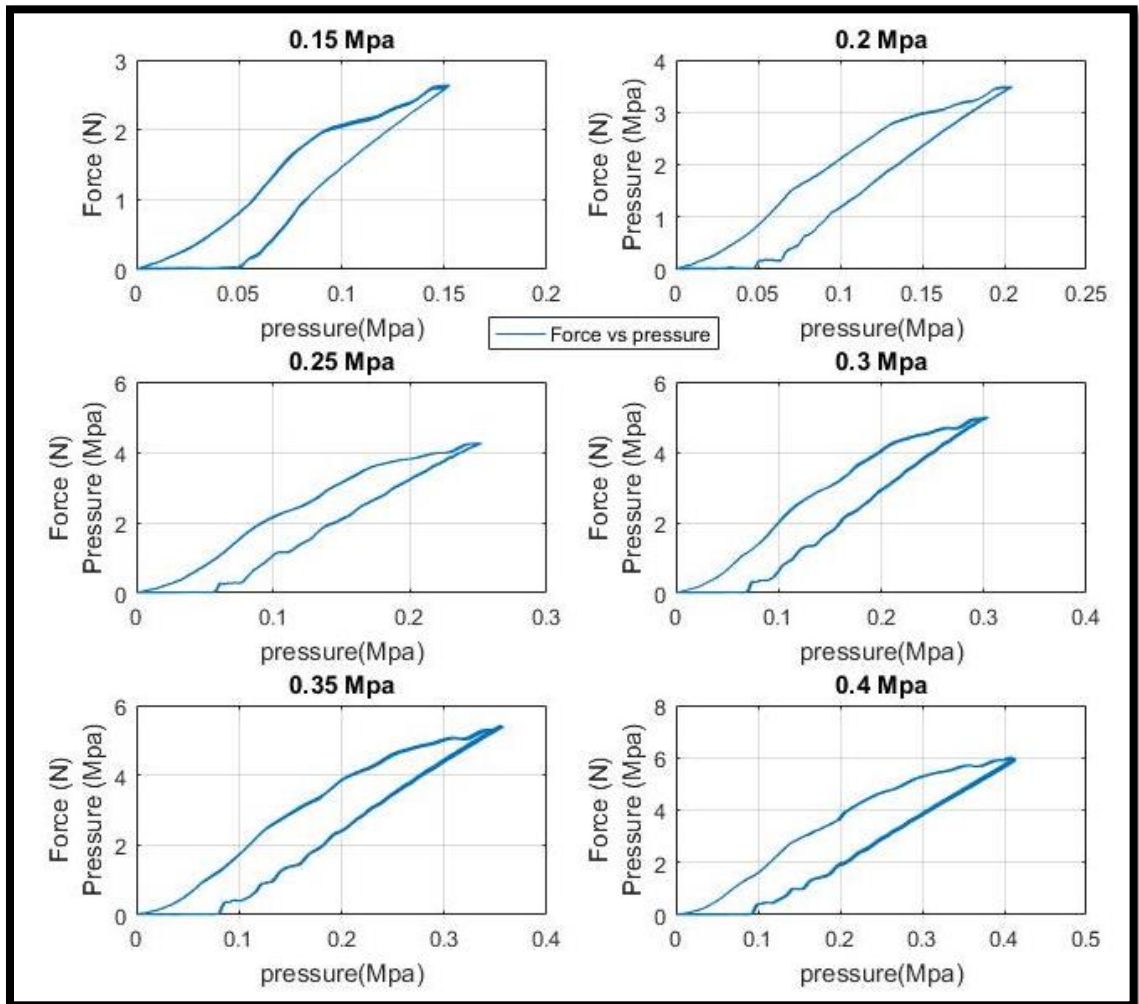


Figure 42. Force vs Pressure for Boa actuator (30-5).

The same behavior was noticed with the PneuNet actuators, and noticed for all the Boa actuators. Figures 43 and 44 shows the Force vs pressure for all tested pressures for Boa actuators (40-8) & (40-5) respectively.

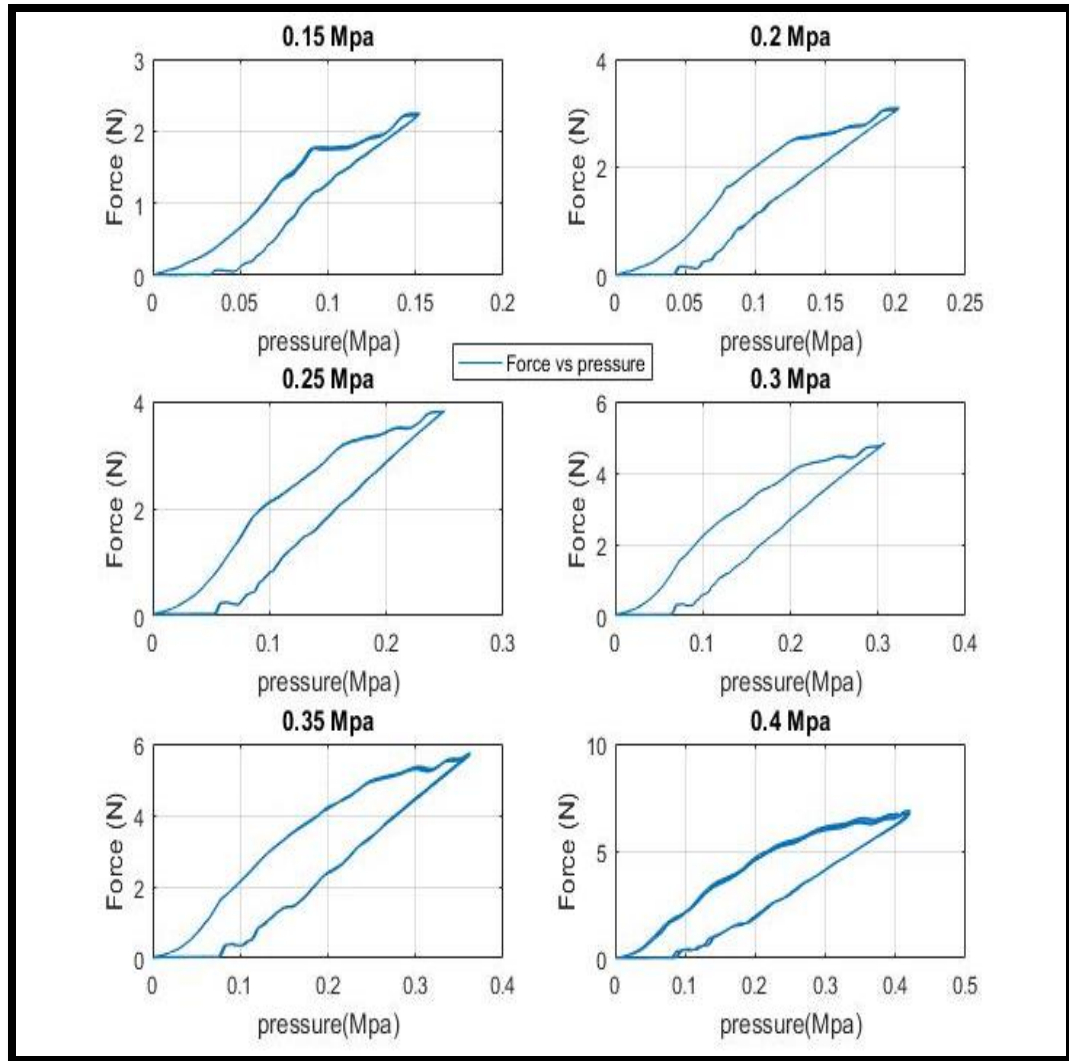


Figure 43. Force vs Pressure for Boa actuator (40-8).

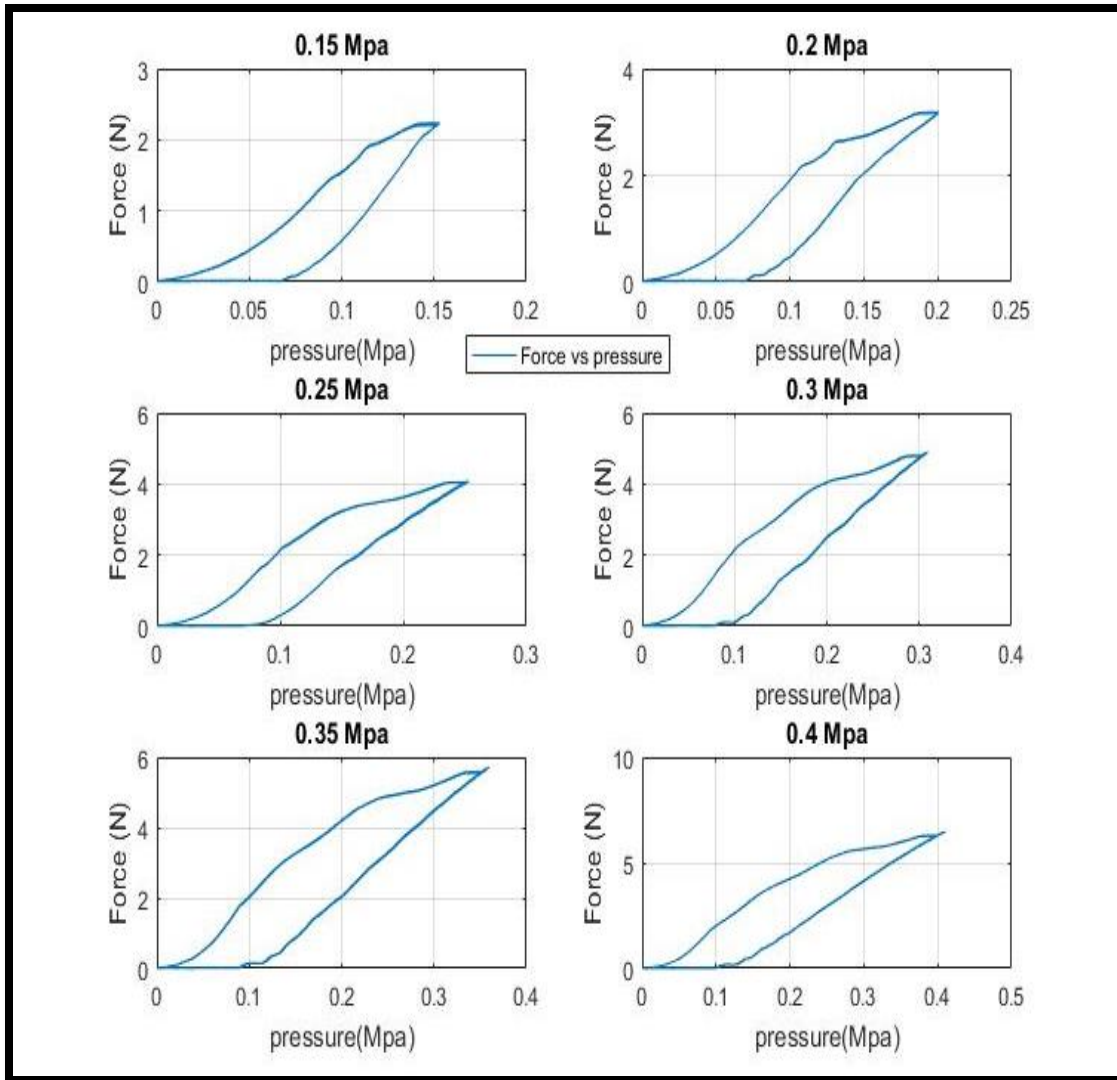


Figure 44. Force vs Pressure for Boa actuator (40-5).

The previous graphs show the relation between force and pressure for the four studied Boa actuators over all tested pressures. An important observance was noted, the relation between force and pressure is very close to linear. To study that, all the data for inflation was separated from deflation, then scatter-plotted for each actuator at all tested pressures. Figure 45 shows the force vs pressure at inflation and deflation at all tested pressures for Boa actuator (40-5).

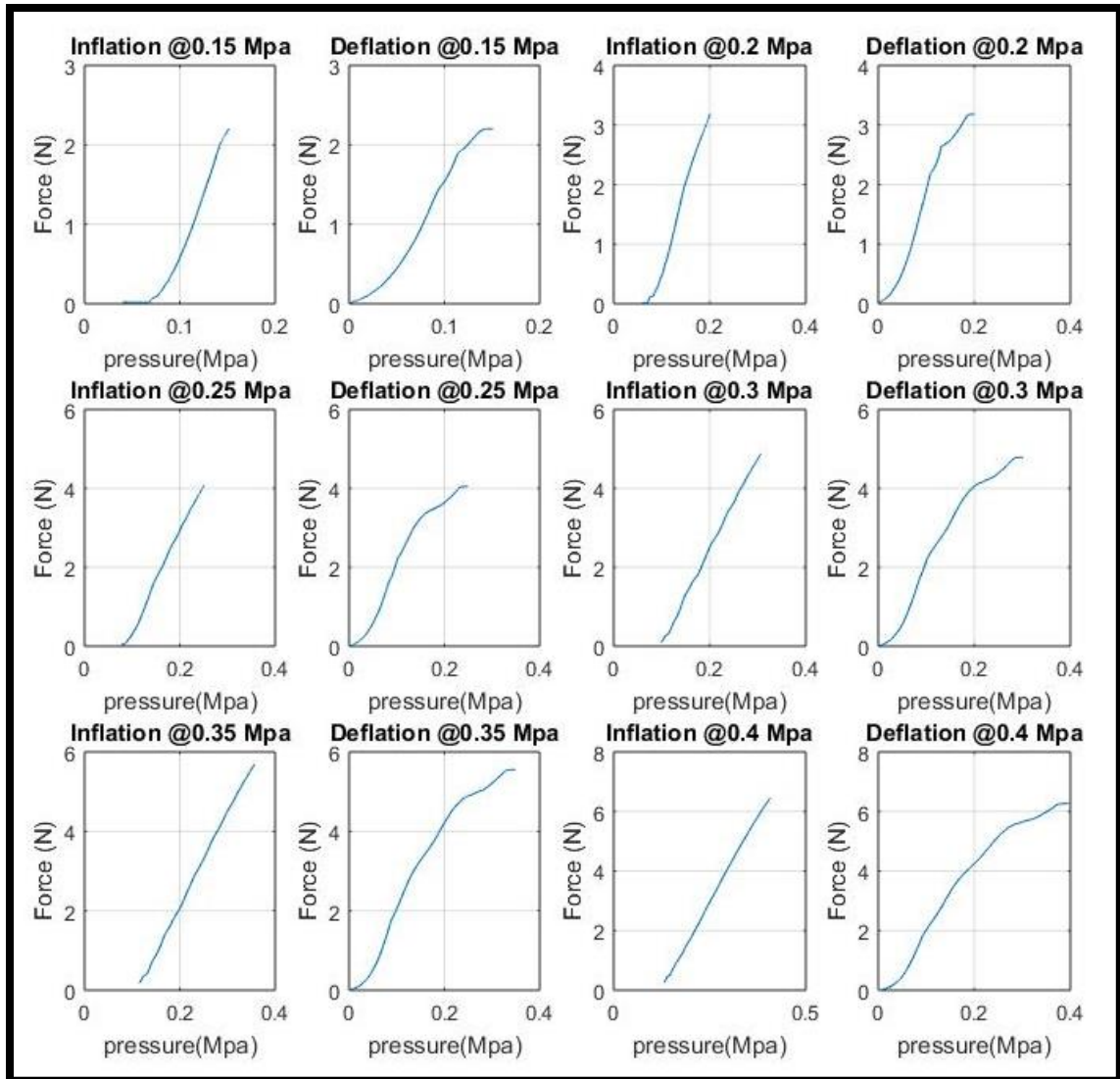


Figure 45. Force vs Pressure at inflation and deflation for Boa Actuator (40-5).

It can be noticed that the Force/Pressure relation is closer to linear at inflation than deflation. The noise could be due to the sudden air exhaustion through the solenoid valve, friction between the actuator and the load cell plate or the vibration that happens when the actuator hits the load cell plate.

Based on that a linear relationship was developed between force and pressure for all Boa actuators, as a ($y=mx+b$) straight line form; where x is the pressure in (MPa). This

relation would be very useful for the Boa Exoskeleton. The following tables shows the linear coefficients for the Boa actuators.

Table 6: Force as a linear relation of pressure coefficients for Boa actuator (30-8).

Pressure (KPA)	Y=mx+b	INFLATION		DEFLATION	
		m	b	m	b
150	Y=	16	-0.51	14	0.0059
200	Y=	16	-0.66	15	0.012
250	Y=	17	-0.98	15	0.01
300	Y=	18	-1.3	15	0.012
350	Y=	20	-1.9	16	0.011
avg	Y _{avg} =	17.4	-1.07	15	0.01018

Table 7: Force as a linear relation of pressure coefficients for Boa actuator (30-5).

Pressure (KPA)	Y=mx+b	INFLATION		DEFLATION	
		m	b	m	b
150	Y=	24	-1.1	18	-0.02
200	Y=	22	-1	18	-0.0058
250	Y=	21	-1.1	18	-0.0051
300	Y=	21	-1.3	18	-0.011
350	Y=	19	-1.4	17	0.01
400	Y=	20	-2	16	-0.013
avg	Y _{avg} =	21.16667	-1.31667	17.5	-0.00748

Table 8: Force as a linear relation of pressure coefficients for Boa actuator (40-8).

Pressure (KPA)	Y=mx+b	INFLATION		DEFLATION	
		m	b	m	b
150	Y=	20	-0.81	15	-0.016
200	Y=	20	-0.91	16	-0.01
250	Y=	20	-1.2	17	0.011
300	Y=	20	-1.4	17	0.019
350	Y=	21	-1.7	18	0.01
400	Y=	22	-2.4	18	0.015
avg	Y _{avg} =	20.5	-1.40333	16.83333	0.004833

Table 9: Force as a linear relation of pressure coefficients for Boa actuator (40-5).

Pressure (KPA)	Y=mx+b	INFLATION		DEFLATION	
		m	b	m	b
150	Y=	26	-1.7	15	-0.026
200	Y=	25	-1.8	17	-0.025
250	Y=	24	-2	18	-0.026
300	Y=	23	-2.2	17	-0.017
350	Y=	23	-2.5	18	-0.015
400	Y=	23	-2.7	48	0.015
avg	Y _{avg} =	24	-2.15	22.16667	-0.01567

For a complete comparison between all the actuators, 16 repetitions were taken for each boa actuator at every tested pressure, the mean of the maximum forces was calculated, and figure 46 shows the mean of the maximum forces for all the Boa actuators and the standard deviation.

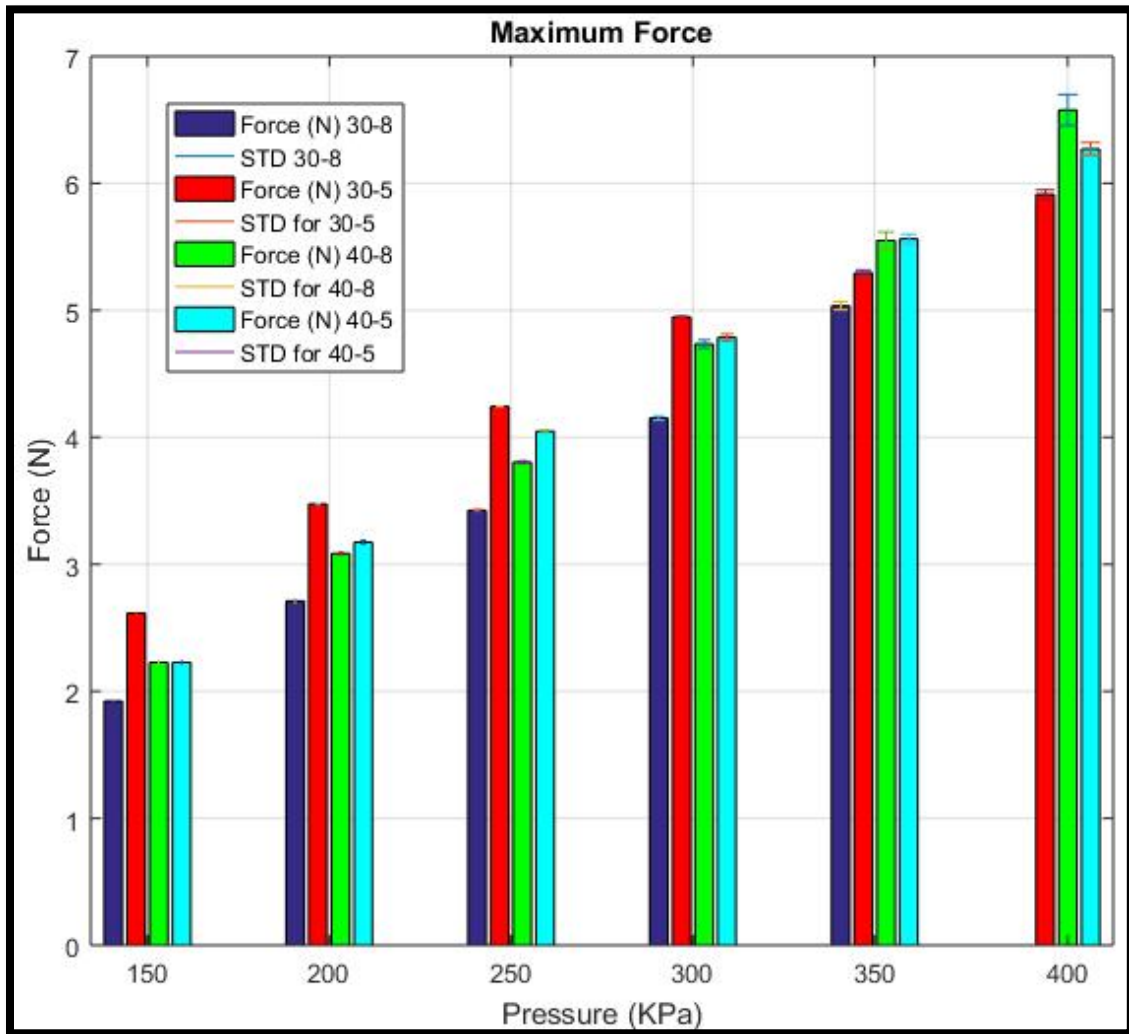


Figure 46. Mean of maximum forces for all Boa actuators with STD.

It can be noticed from the figure that for Dragon skin 30A material actuator (30-5) performs better than actuator (30-8) at all pressures. For SORTA-Clear 40A material, actuator (40-5) performs better than actuator (40-8) at all pressures except maximum

pressure 400 KPa. Actuators (30-5) performs the best at low pressures, while actuator (40-8) performs the best at high pressures.

Also, it can be noticed that the standard deviation for the mean of maximum forces is relatively small in value that would mean that the Boa actuators can produce repeatable consistent output through experiments. STD is higher on high pressures than it is for lower pressures.

Statistical analysis was made on our experiment data for all actuators. Table 1 shows the value of one-way analysis of variance . Since our probabilities (p-value) were less than 0.05, the data is significantly different from each other.

Table 10: One-way ANOVA for Boa Actuator.

Actuator	F	PROB>F
30-5	36134.57	1.55099e-65
30-8	34365.76	1.93481e-54
40-5	20371.44	4.67233e-61
40-8	5583.06	6.03023e-51

Two-way analysis of variance was made for the data we have. Table 2 shows the data for ANOVA2. We can conclude that our data is significantly different for all the mean forces of the actuators.

Table 11: Two-way ANOVA for Boa Actuator.

Source	SS	Df	MS	F	Prob>F
Columns	1814.764	4	45.4409	281320.7	2.868e-237
Rows	9.222	3	3.0741	19031.58	1.754e-160
Interaction	1.911	12	0.1592	985.87	1.007e-113
Error	0.019	120	0.0002		
Total	192.916	160			

5.3 Boa Exoskeleton

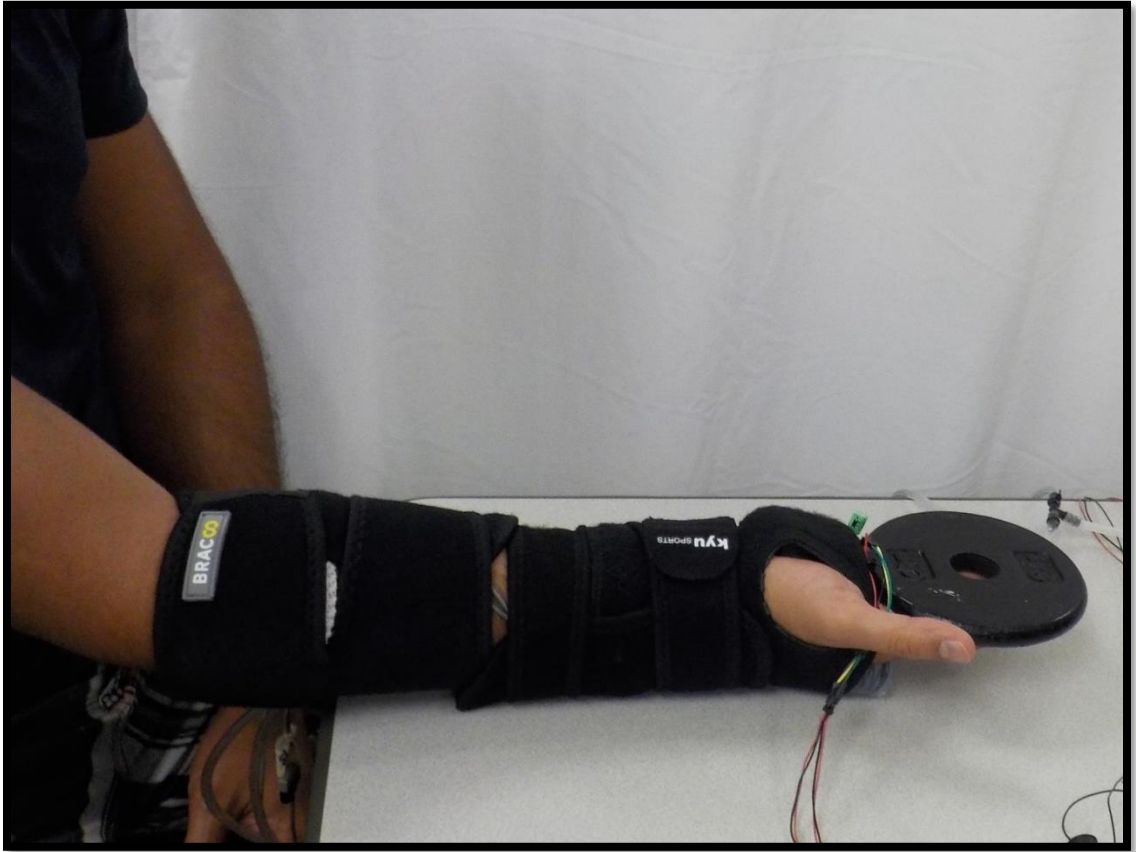


Figure 47. Boa Exoskeleton during testing in BioRobotics Lab,FAU.

The Boa exoskeleton is an approach to apply the soft actuators in rehabilitation, we designed and tested the actuators on an exoskeleton for human wrist. The assistive force of the Boa Exoskeleton can be controlled through controlling the actuators, the output force of the actuator is almost linear to the input pressure, thus by controlling the pressure we can control the assistive force of the Boa Exoskeleton.

After a full study on two types of actuators, Fiber-Reinforced actuators were chosen due to their higher forces and linearity between input and output. The testing was done on 0.4 MPa pressure. SORTA-Clear 40A was the material for the Boa actuators, Boa actuator 40-5 was used in the Boa Exoskeleton.

Five tests were made as described in the control and testing section. Six human subjects were tested accordingly. Figure 48 shows the data for “EMG Actuated” test on human subject 1. The human subject is asked to follow a pulse signal throughout the testing. The pulse signal has a maximum of 47 and a minimum of 19. The exoskeleton tracks the wrist bending through the error of the EMG signals and the flexion angle that can be seen in the second plot, where the pressure changes accordingly.

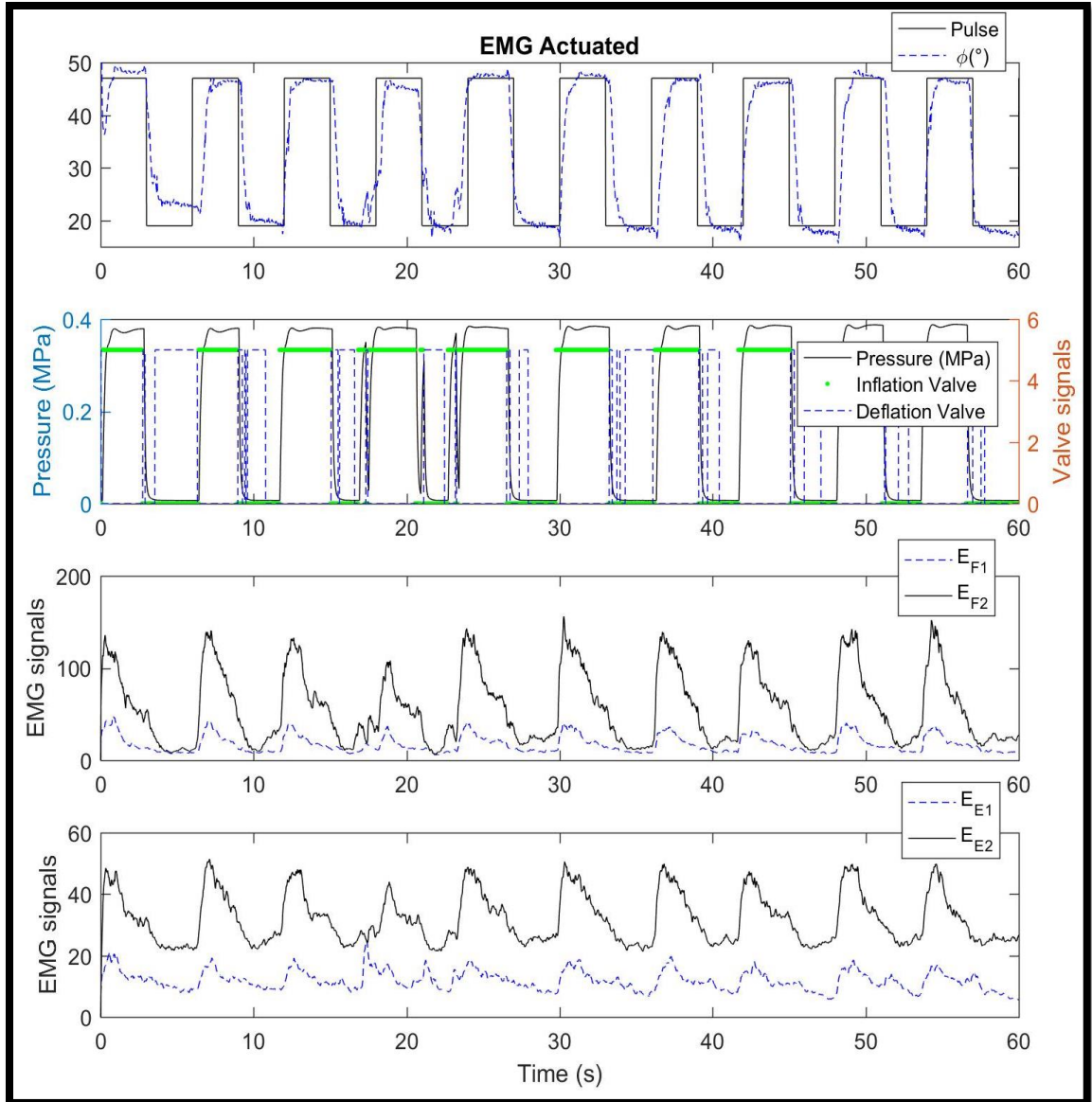


Figure 48. Boa Exoskeleton “EMG Actuated” tests on subject 1.

The flexion EMG signal E_{F1} is the pilot signal to trigger the actuation. The flexion EMG E_{F2} signal can be seen following the same pattern. The extension EMG signals follows the same pattern as well.

Figure 49 shows the data for “No assistive” test on human subject 1. It can be seen that the flexion EMG signal E_{F1} is greater in this test than the “EMG Actuated” test. This

will be further compared in a later figure. The Human subject follows the same impulse signal throughout all the tests to maintain the same flexion angle.

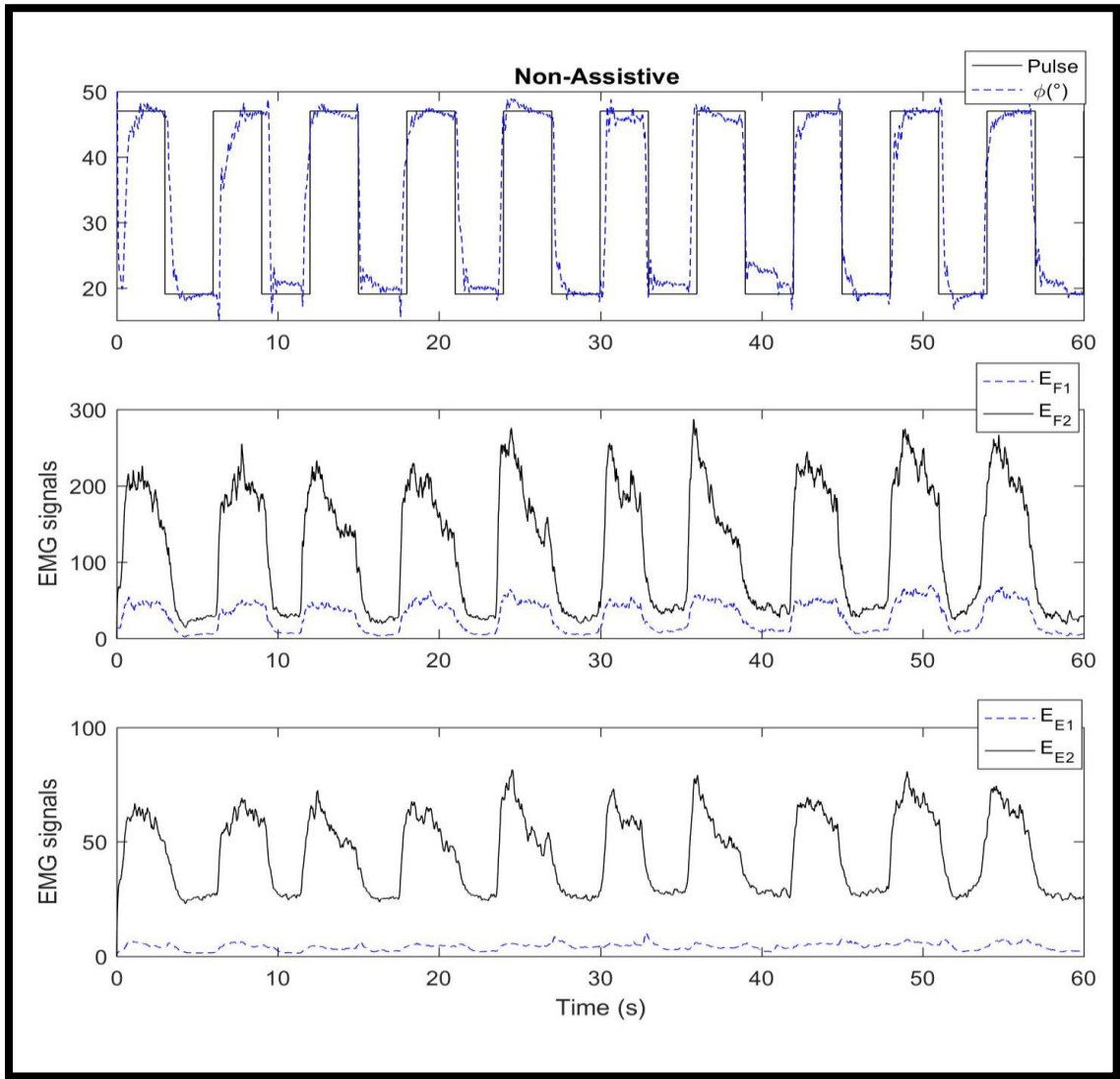


Figure 49. Boa Exoskeleton test "Non-Assistive" on subject 1.

Figure 50 shows the data for "Full Assistive" test on human subject 1. The subject does not reach the impulse target. This test shows the degree of the assistance to the human subject by the Boa Exoskeleton. It can be noticed that the flexion EMG signal E_{F1} is very

low relative to previous tests. The small amount of EMG signal can be due to the weight placed on hand.

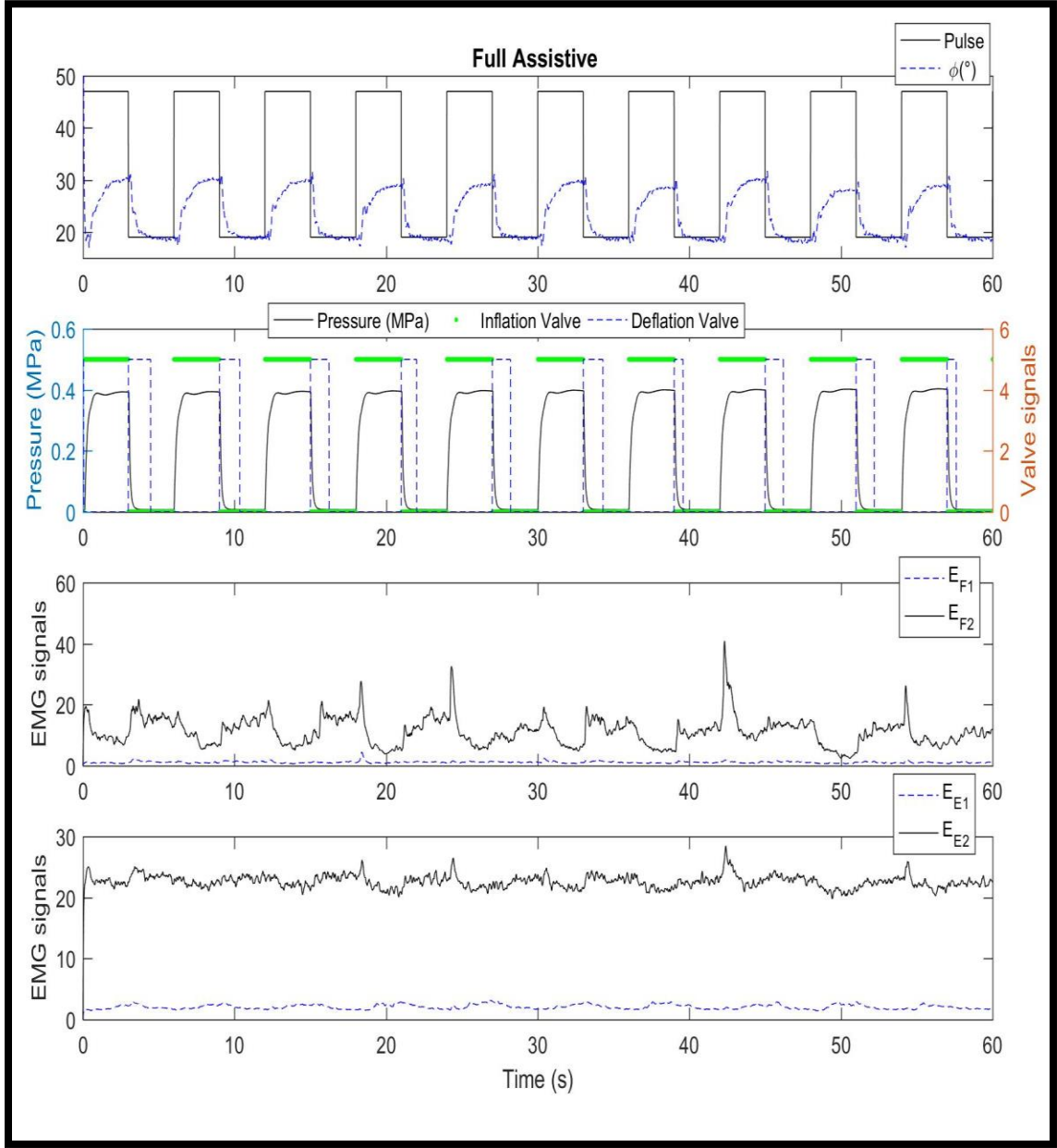


Figure 50. Boa Exoskeleton test "Full Assistive" on subject 1.

Figure 51 shows the data for “No Exoskeleton” test on human subject 1. This test is to be compared with “Non-Assistive”, since the exoskeleton poses restriction on the

wrist. The human subject follows the impulse target. The EMG flexion signal E_{F1} is to be compared later.

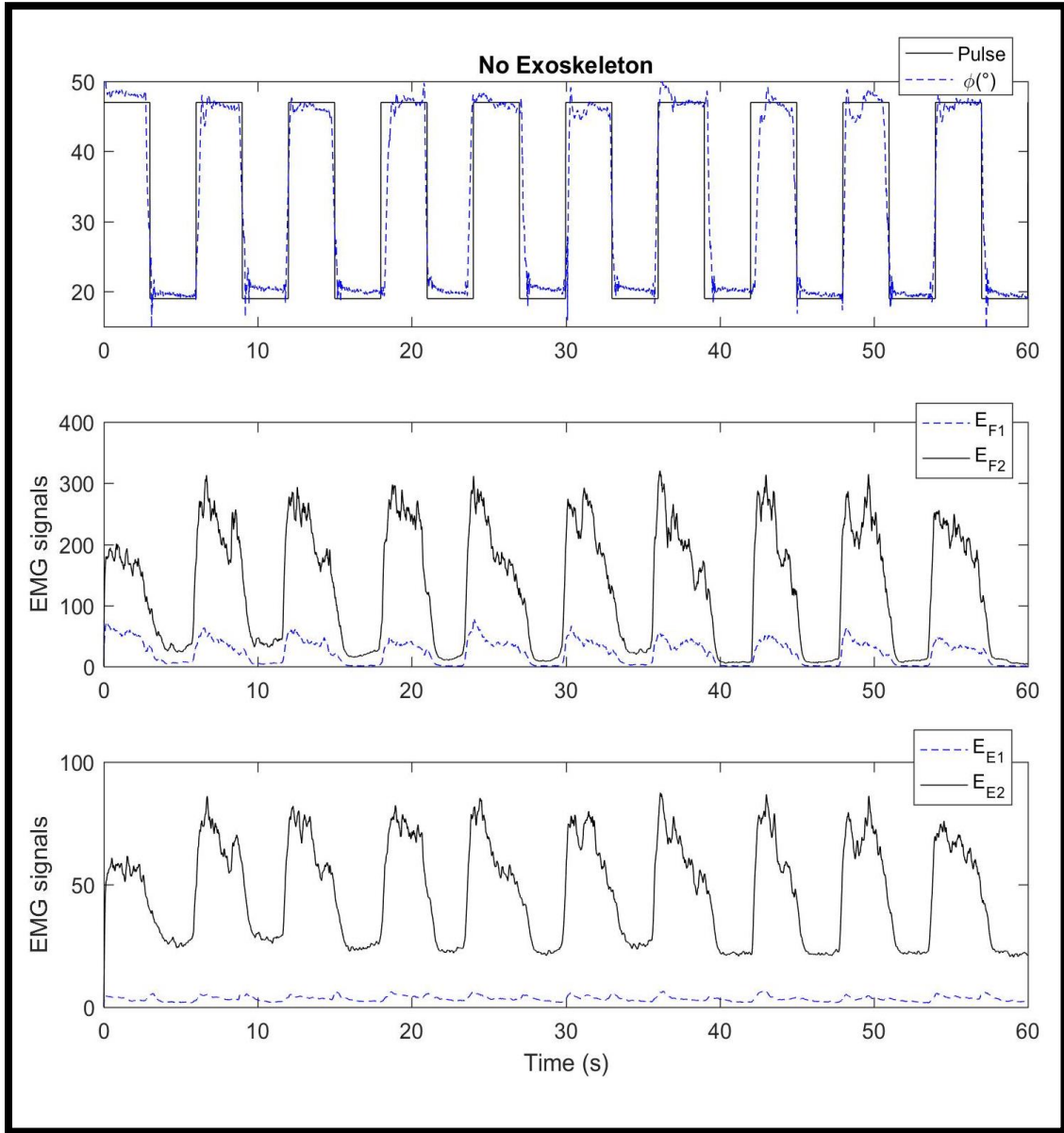


Figure 51. Boa Exoskeleton test "No Exoskeleton" on subject 1.

Figure 52 shows the data for “No Exoskeleton/ No Weight” test on human subject

1. Following the same impulse signal, this data demonstrates the EMG signals when the hand bends with no restrictions.

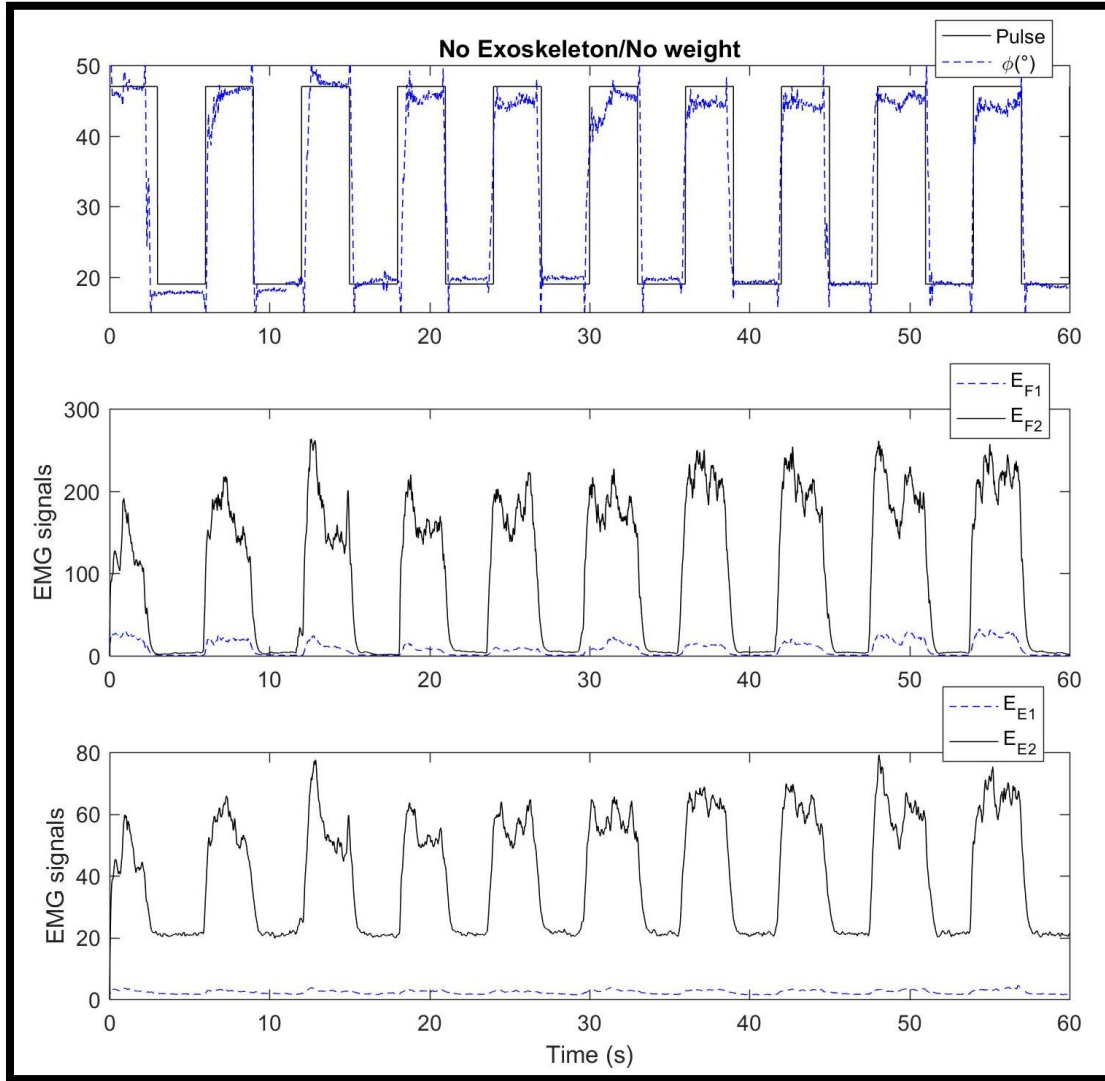


Figure 52. Boa Exoskeleton test "No Exoskeleton/ No Weight" on subject 1.

To have a better understanding of EMG signal difference between tests, Figure 53 shows the EMG flexion signal E_{F1} comparison. The ratio of EMG over Flexion angle ϕ is an indicator of the amount of EMG needed to attain a degree of bending. It can be noticed

that the ratio in the “Non-Assistive” test is higher than the “EMG Actuated” test. This means that wearing the Boa Exoskeleton allows human to exert less EMG signals to attain the same degree of bending than not wearing the Bo Exoskeleton.

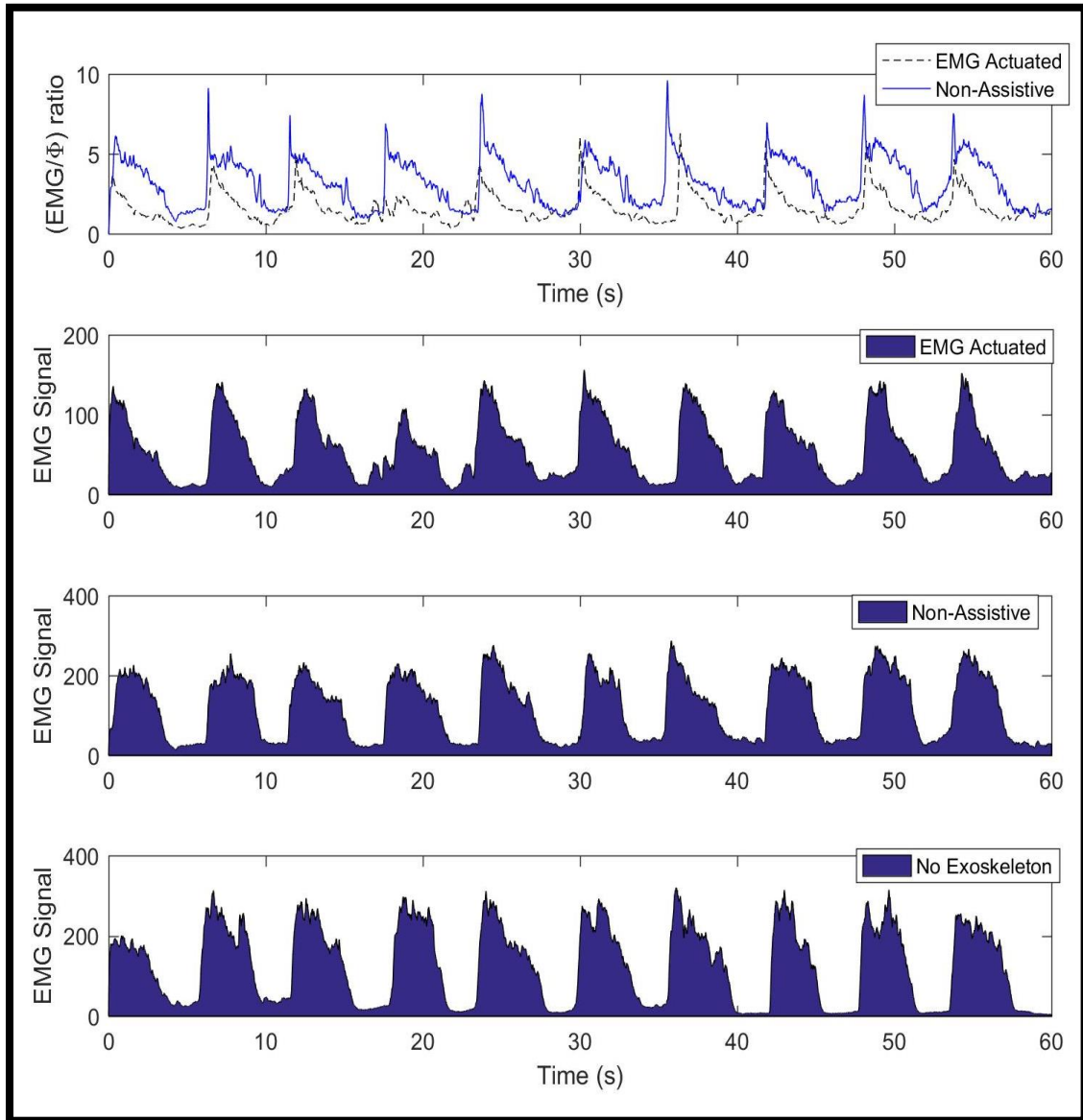


Figure 53. EMG comparison for human subject 1.

Figure 54, 55 and 56 consequently shows the EMG flexion signal E_{F1} comparison for human subject 2, 3 and 4. The data generally follows the same pattern. Values of EMG signals are different between human subjects.

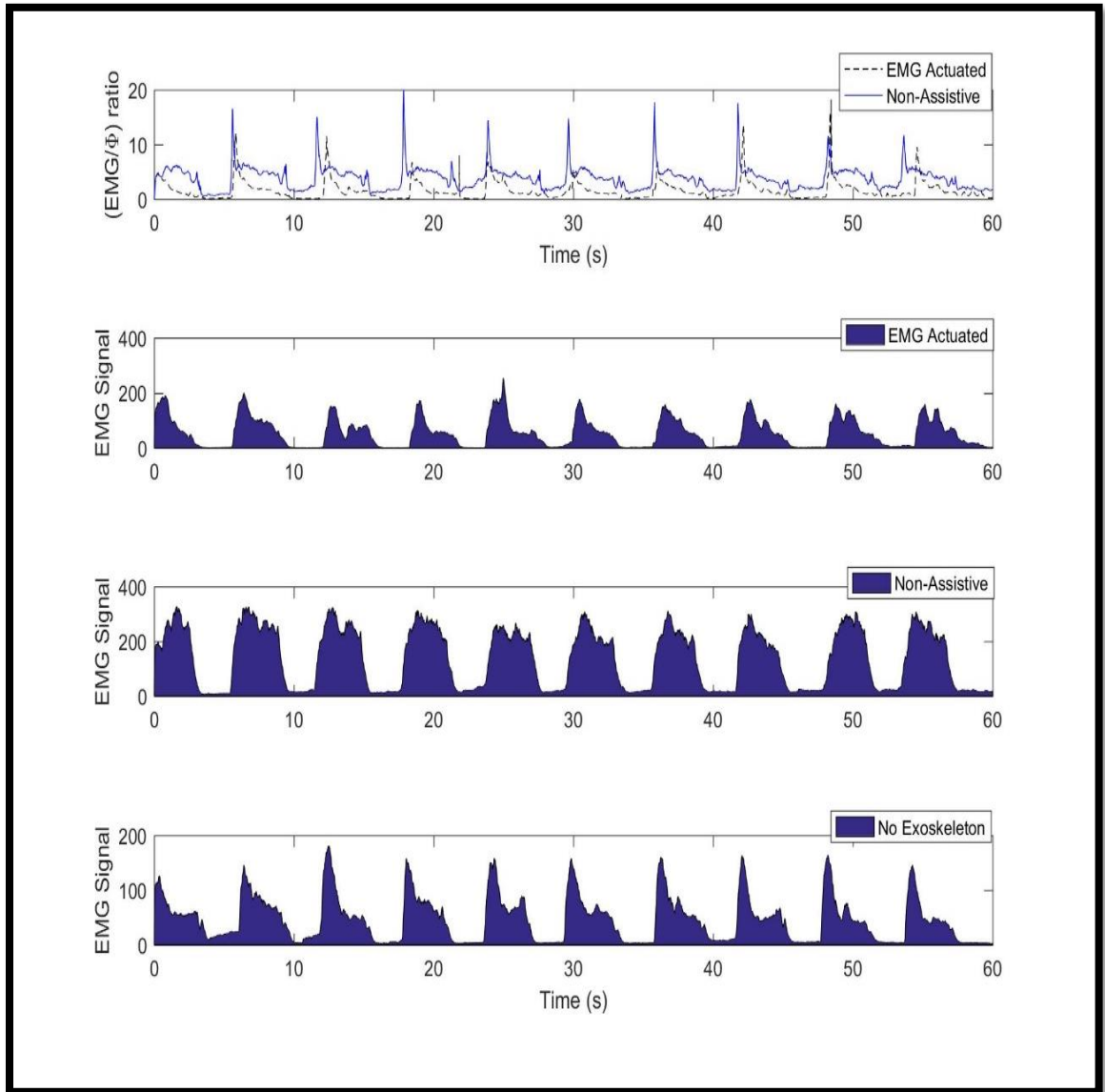


Figure 54. EMG comparison for human subject 2.

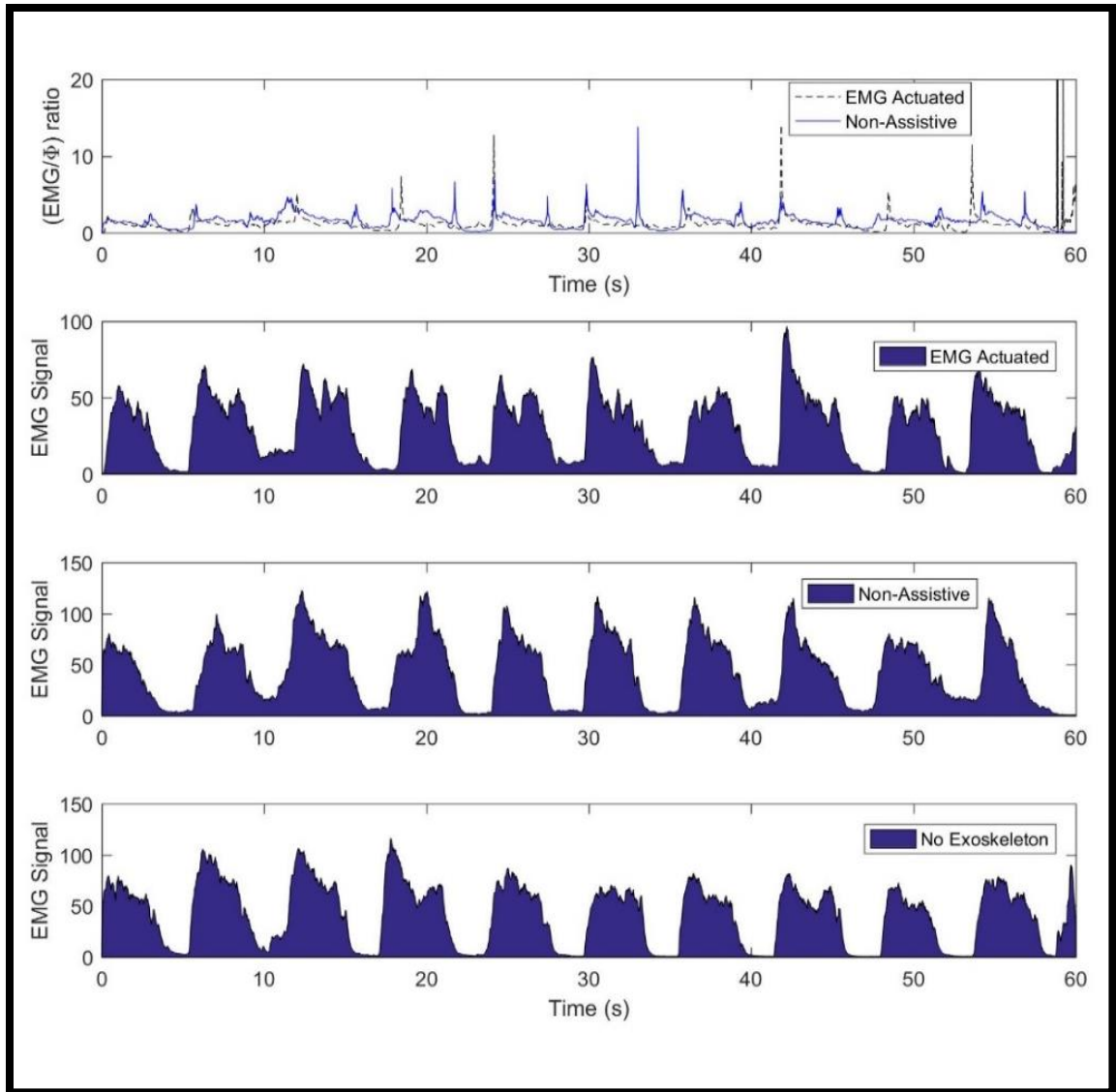


Figure 55. EMG comparison for human subject 3.

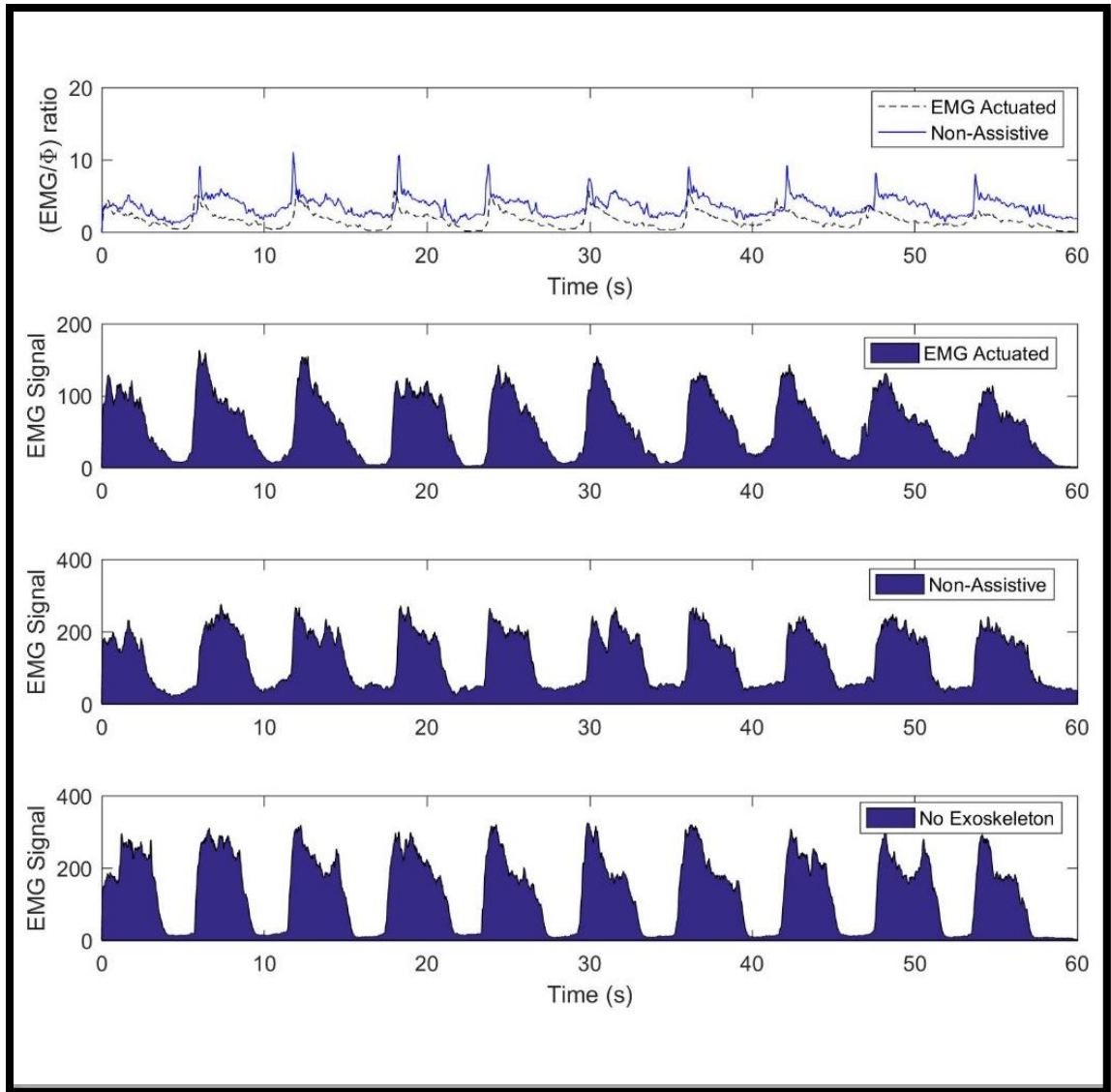


Figure 56. EMG comparison for human subject 4.

To bend the wrist, the human uses a combination of muscles movement. Adding all the studied EMG signals together will give us a different perspective. Figure 57 shows the ratio of combined EMG signals in both tests, MG Actuated and Non-Assistive, to the Flexion Angle ϕ for all human subjects. It can be noticed that the ratio in Non-Assistive test is higher than EMG Actuated test for all human subjects.

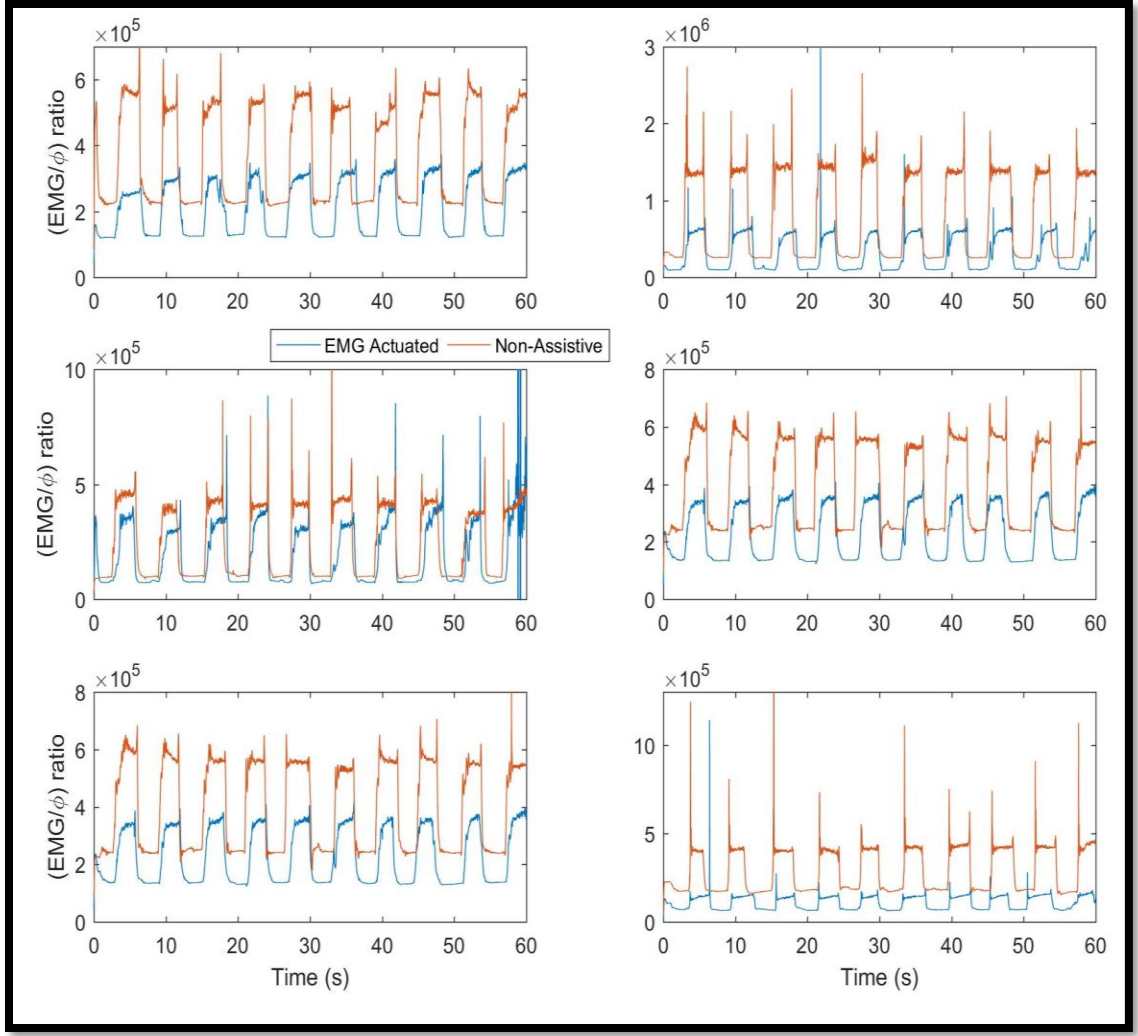


Figure 57. Ratio of combined EMG signals to the Flexion Angle ϕ for all human subjects.

To investigate further in the EMG signals, the area under the curve of the EMG flexion signal is an indicator of how much EMG exerted by the human subject during the sixty seconds tests, following the same pulse signal. Table 12 and Figure 58 shows the area under the curve for flexion signal E_{F1} .

The root mean square is also calculated. Table 13 and Figure 59 shows the root mean square of flexion signal E_{F1} for all tests, for all human subjects tested.

Table 12: Area under the curve of EMG flexion signal E_{F1} .

Human	AREA UNDER THE CURVE				
Subject number	EMG Actuated	Full Assistive	Non- Assistive	No Exoskeleton	No Exoskeleton/ No Weight
One	3.3744e+06	0.6728e+06	7.1053e+06	7.5965e+06	5.6904e+06
Two	3.2012e+06	0.1983e+06	8.2451e+06	2.8040e+06	1.4916e+06
Three	1.8047e+06	0.1285e+06	2.6489e+06	2.4877e+06	1.2567e+06
Four	3.5736e+06	0.9055e+06	7.5416e+06	7.9319e+06	5.4507e+06
Five	2.3631e+06	0.3905e+06	5.9031e+06	5.8760e+06	3.8861e+06
Six	1.5223e+06	0.5934e+06	5.6418e+06	3.4318e+06	3.6330e+06

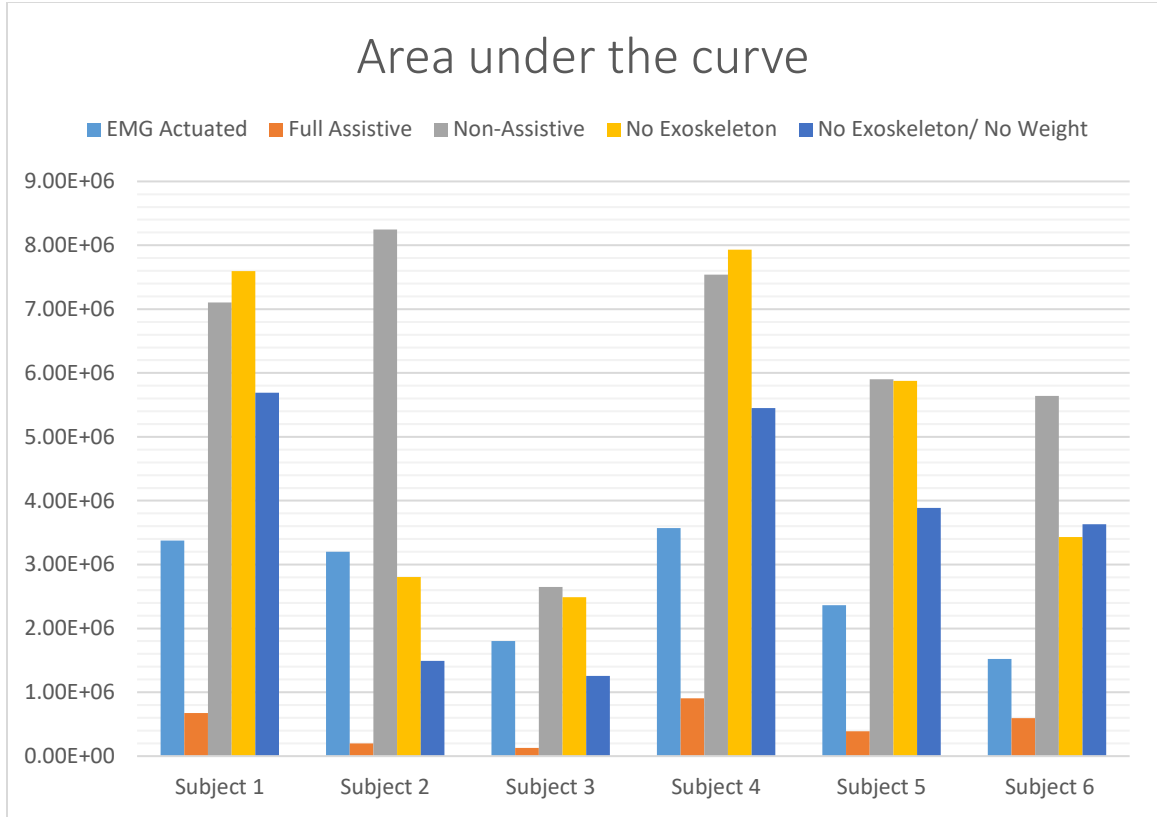


Figure 58. Area under the curve of EMG flexion signal E_{F1} .

Table 13: Root Mean Square of EMG flexion signal E_{F1} .

Human	ROOT MEAN SQUARE				
Subject number	EMG Actuated	Full Assistive	Non-Assistive	No Exoskeleton	No Exoskeleton/ No Weight
One	68.7742	12.1222	143.2030	160.5872	130.0890
Two	75.1805	4.4196	175.6135	63.0432	34.9371
Three	36.7220	3.4992	55.2034	51.5356	27.9256
Four	73.3699	17.5422	146.8328	168.6378	124.0092
Five	54.8512	9.7381	122.4179	119.4873	91.9221
Six	61.5782	11.6598	113.4649	77.3979	86.9132

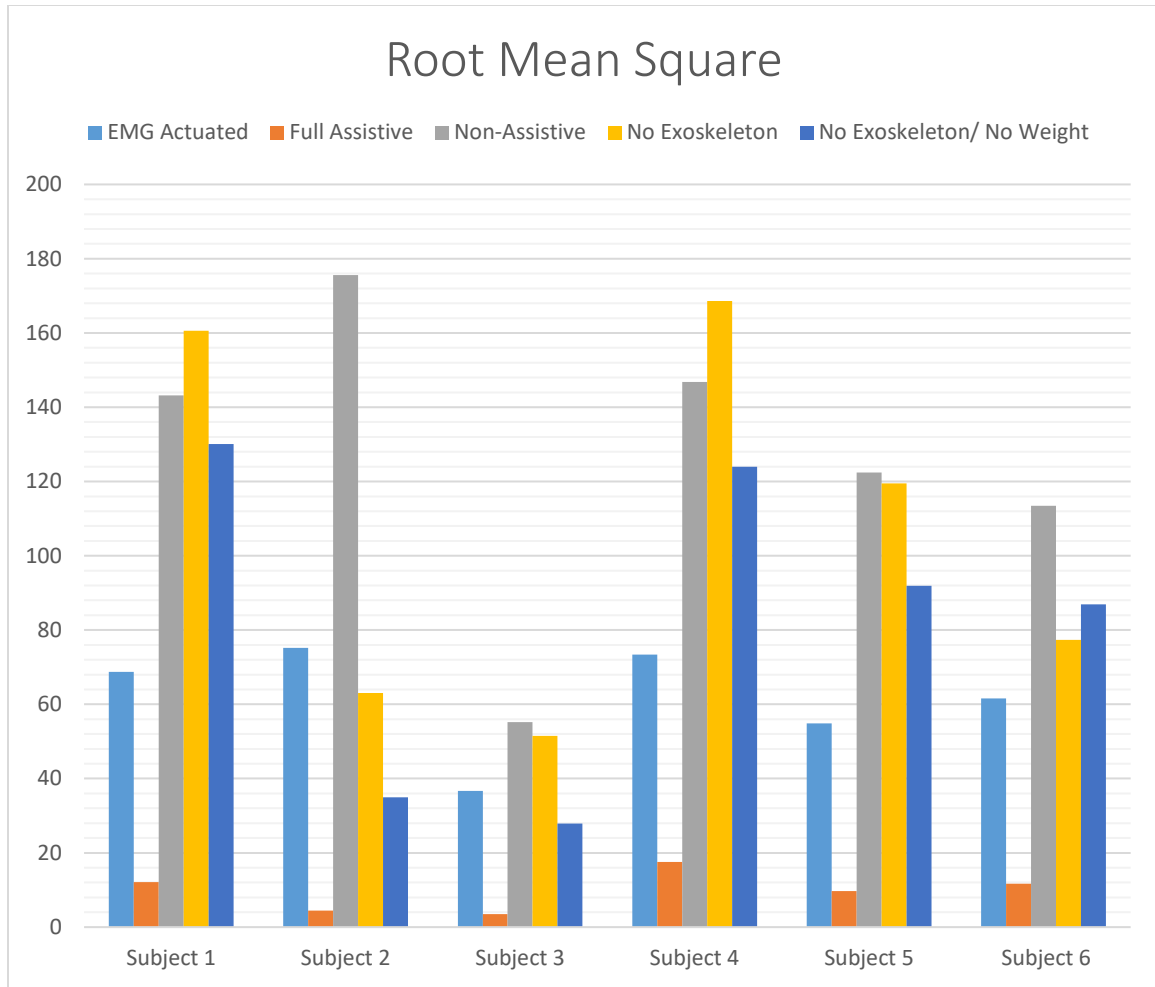


Figure 59. Root Mean Square of EMG flexion signal E_{F1} .

Figure 60, represents a complete comparison of all EMG signals studied between different tests made on all subjects. In all human subjects tested, except subject 2; The assist of the Boa Exoskeleton in lifting the weight, “EMG Actuated” test, can results in a lower EMG signals than lifting the weight without wearing the Exoskeleton,” No Exoskeleton’ test. In some cases, it is lower than “No Exoskeleton/No Weight”.

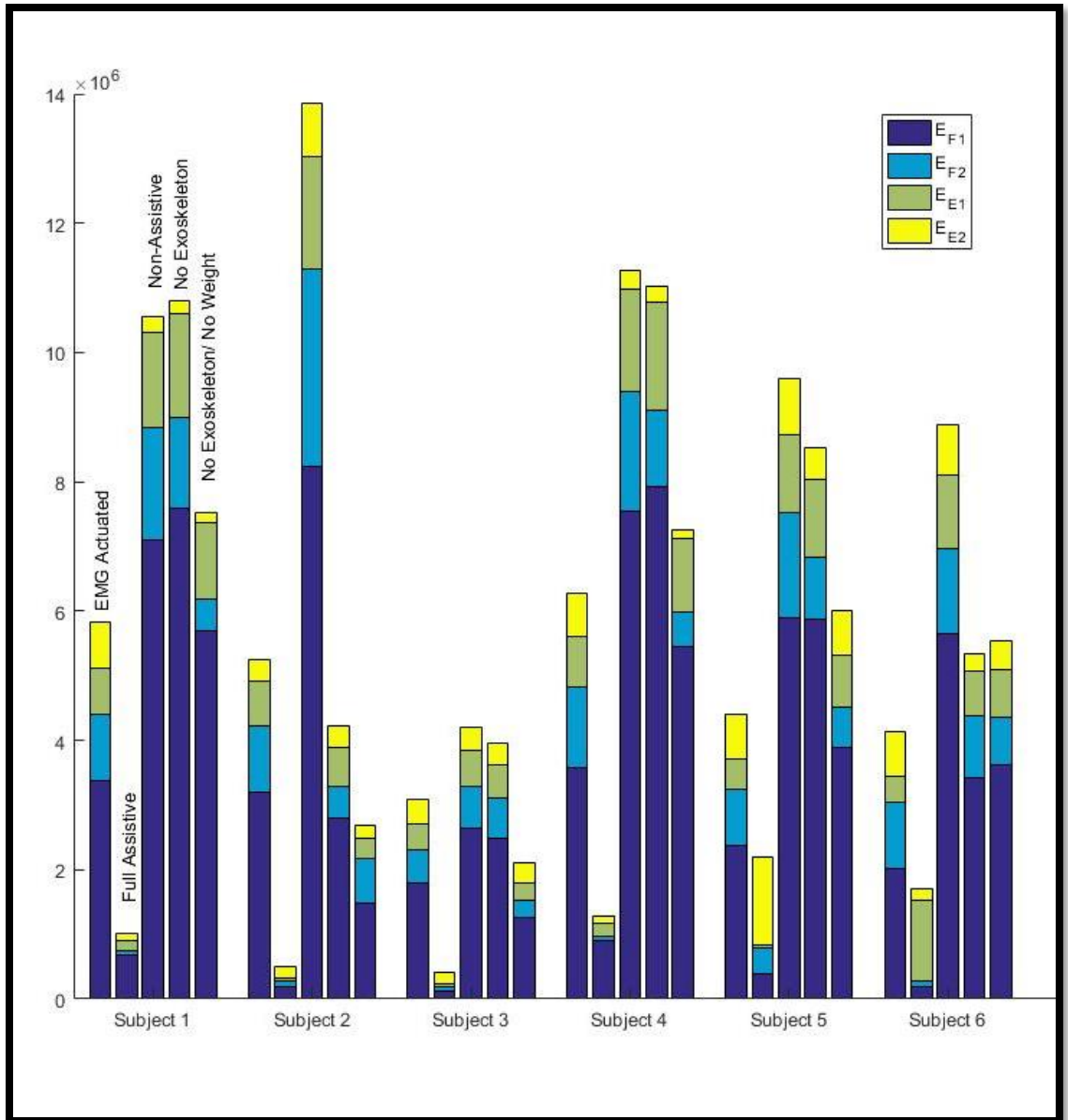


Figure 60. Area under the curve of all EMG signals for all tests, for all human subjects.

6 DISCUSSION

In evaluating actuators for human exoskeleton purpose, the testing was done on two types of soft actuators: Fiber-Reinforced and PneuNet soft actuators. The fiber-Reinforced soft actuator was chosen for the human exoskeleton due its much higher force. Testing the Fiber-Reinforced soft actuator focused on two parameters, the material and the number of winding, while all other parameters were constant. Any change in any parameter might affect the outcome of the actuators. There could be an elastomer material that can outperform the materials we tested. We tested materials with shore hardness 40A and 30A. The second parameter is the winding spacing. We only tested two cases, number of windings $n=40$, and $n=25$. Varying the number of windings in a different pattern for a future study might give different results.

Actuator (30-8) was tested for its maximum pressure (0.35 MPa). After that, higher pressure bursts the actuator. A safety factor can be introduced into real life applications of the actuators, even though the burst actuator does not do damage to a human being, but it might in different circumstances.

The design of the Boa actuators was constant. Changing some parameters of the design might also produce different outcomes and behavior. The outer layer of the actuator does not do anything more than unify the reinforcement with the actuator body. This outer layer can be minimized in size to produce smaller actuators with the same performance. A linear relationship was found between force and pressure. This proposes a possibility of controlling the output force by controlling the actuator pressure.

An electronic air pressure regulator with high precision can be introduced to the control system, allowing to precisely control the outcome of the actuator, most importantly force and displacement.

Actuators were then implemented in a human exoskeleton for real life applications. The exoskeleton consisted of a regular wrist brace; a special design wrist brace can be made to improve the performance of the exoskeleton, such as having stronger material that can provide support to the actuators in the needed areas, or having braces tailored to the size of the human wrist. This way, the actuators can fit in with ease and to prevent any undesired movement. Designing exoskeletons that are made from an elastomer material, allows the exoskeleton to be casted in the same mold with the actuators, producing a unified body exoskeleton.

Investigating other parameters of the actuators can lead us to smaller actuators with similar performance, thus more actuators can be utilized in one exoskeleton, allowing more usage for other joints.

EMG signals are a great indication of muscle movement, these signals can be integrated more in the system, to achieve certain degree of bending or direction. Using EMG signals to control the actuation of the exoskeleton proved its effectiveness, although there might be another way to actuate the exoskeleton. Four EMG receptors were used, that can be increased in case of higher accuracy movement or for more than one degree of freedom actuation.

7 CONCLUSIONS

Two types of actuators were designed, built, controlled and tested. It has been shown that changing the taper angle of the soft Pneumatic actuators affect the performance of the actuators in different ways. In this case, the force output by the actuator with a taper angle of 3° produced a larger force and more displacement than the actuator taper angle of 0° . Four Fiber-Reinforced soft actuators were evaluated in this thesis, varying the material and the winding spacing. It has been shown that the actuators made of SortA-Clear 40A produce larger force on high pressure, while Dragon Skin 30A produce larger force on lower pressure. Material SortA-Clear 40A is more durable than Dragon Skin 30A and can withstand higher pressure. Increasing the winding number would add more reinforcement to the actuator on the expense of the bending. Fiber-Reinforced actuators were implemented in a human wrist exoskeleton. Five tests were performed on six human subjects. EMG Signals were studied in four locations of the arm. It was found that, human subjects wearing the Boa Exoskeleton uses less EMG signals than not wearing it, to perform the same degree of wrist bending.

9 APPENDIX

Data for tests on the five human subjects that were not displayed in results.

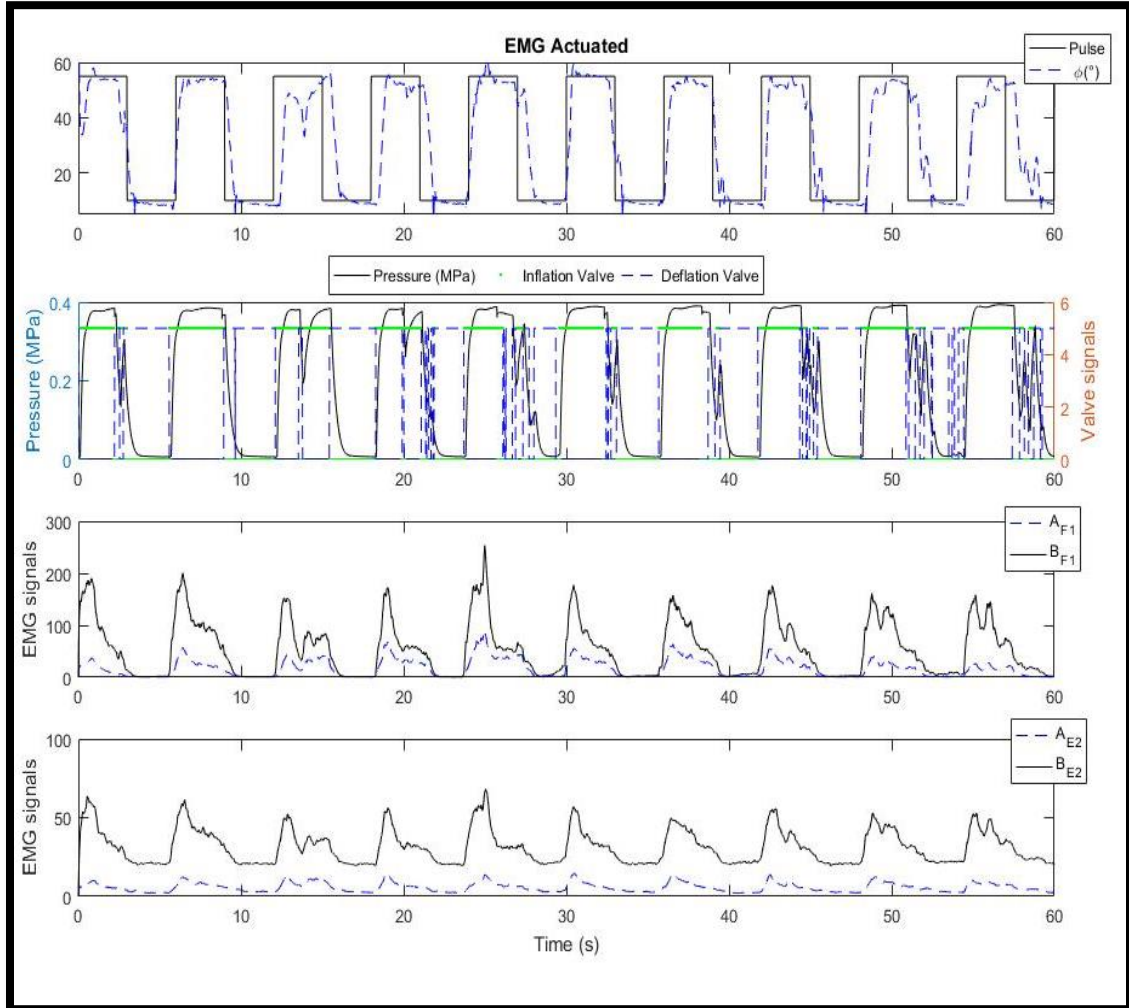


Figure 61. Boa Exoskeleton “EMG Actuated” tests on subject 2.

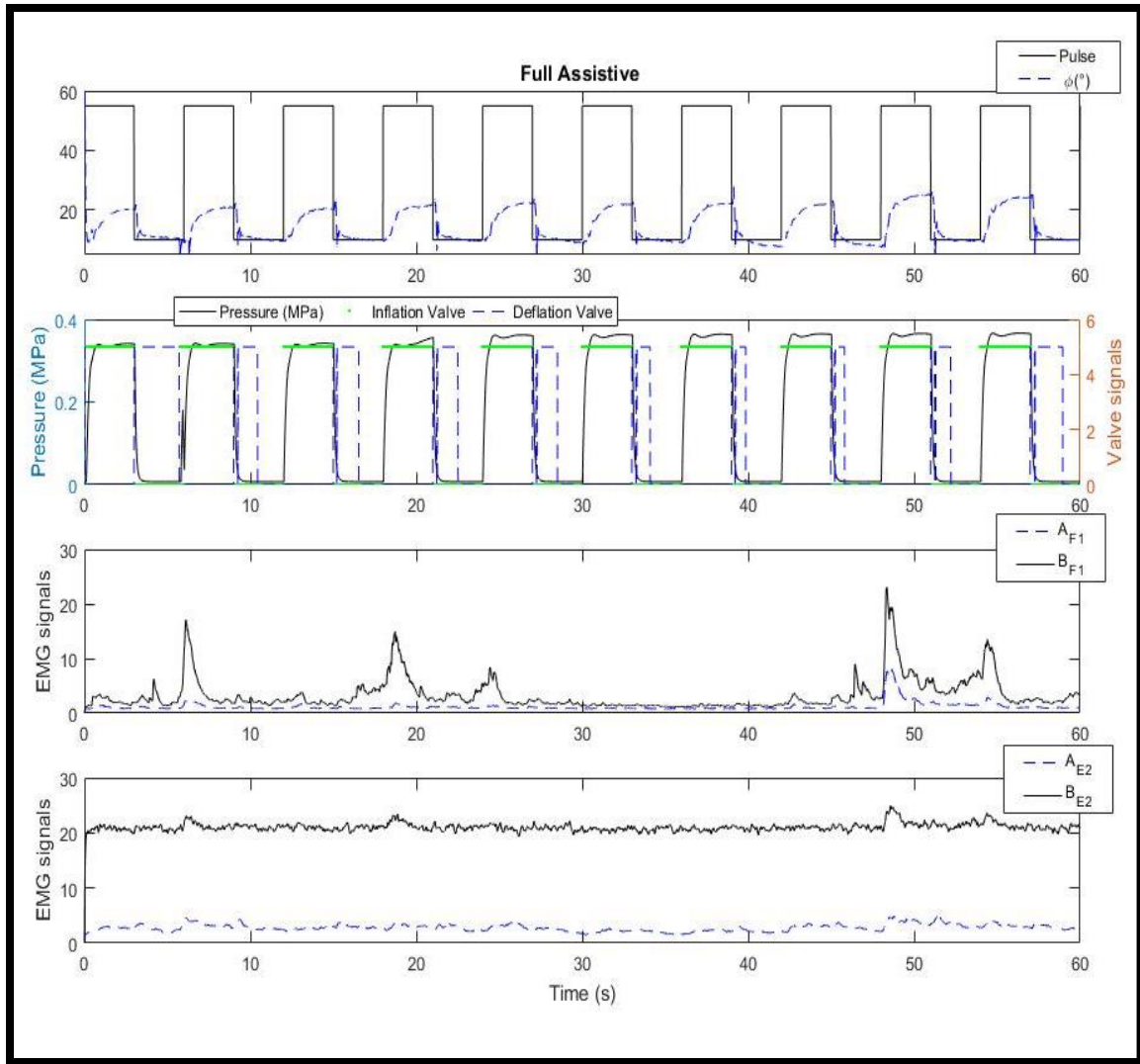


Figure 62. Boa Exoskeleton “Full Assistive” tests on subject 2.

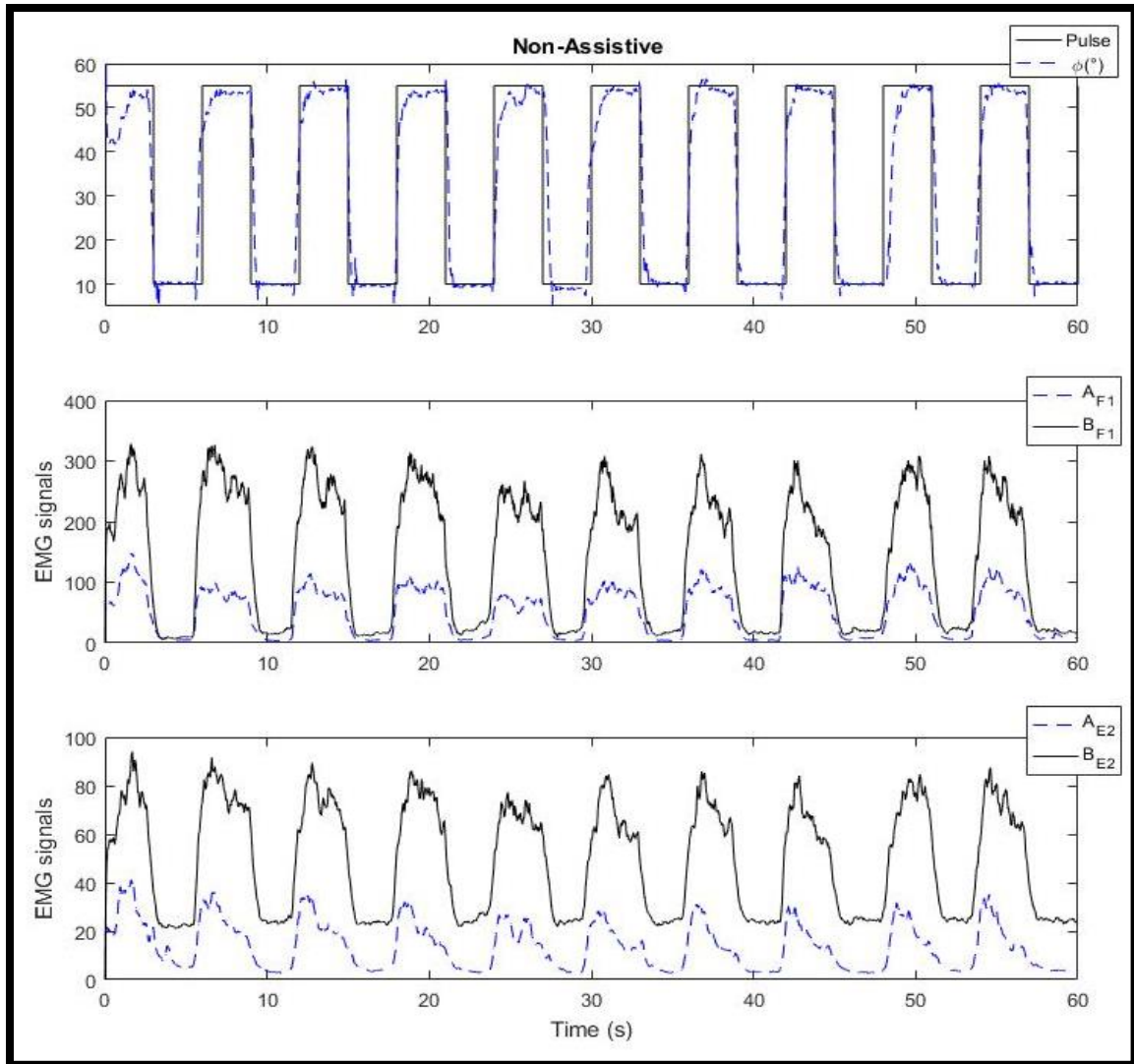


Figure 63. Boa Exoskeleton “Non-Assistive” tests on subject 2.

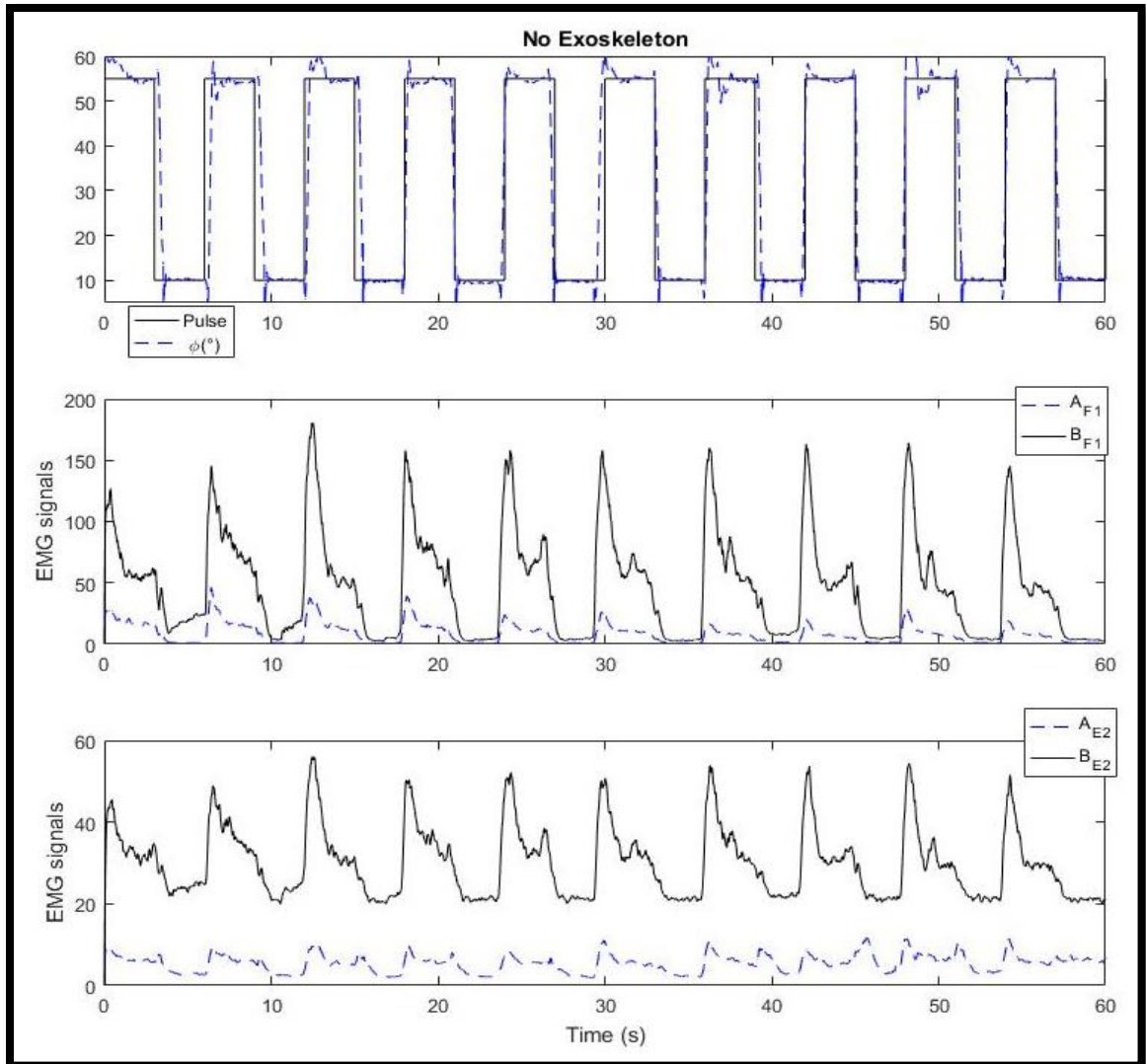


Figure 64. Boa Exoskeleton “No Exoskeleton” tests on subject 2.

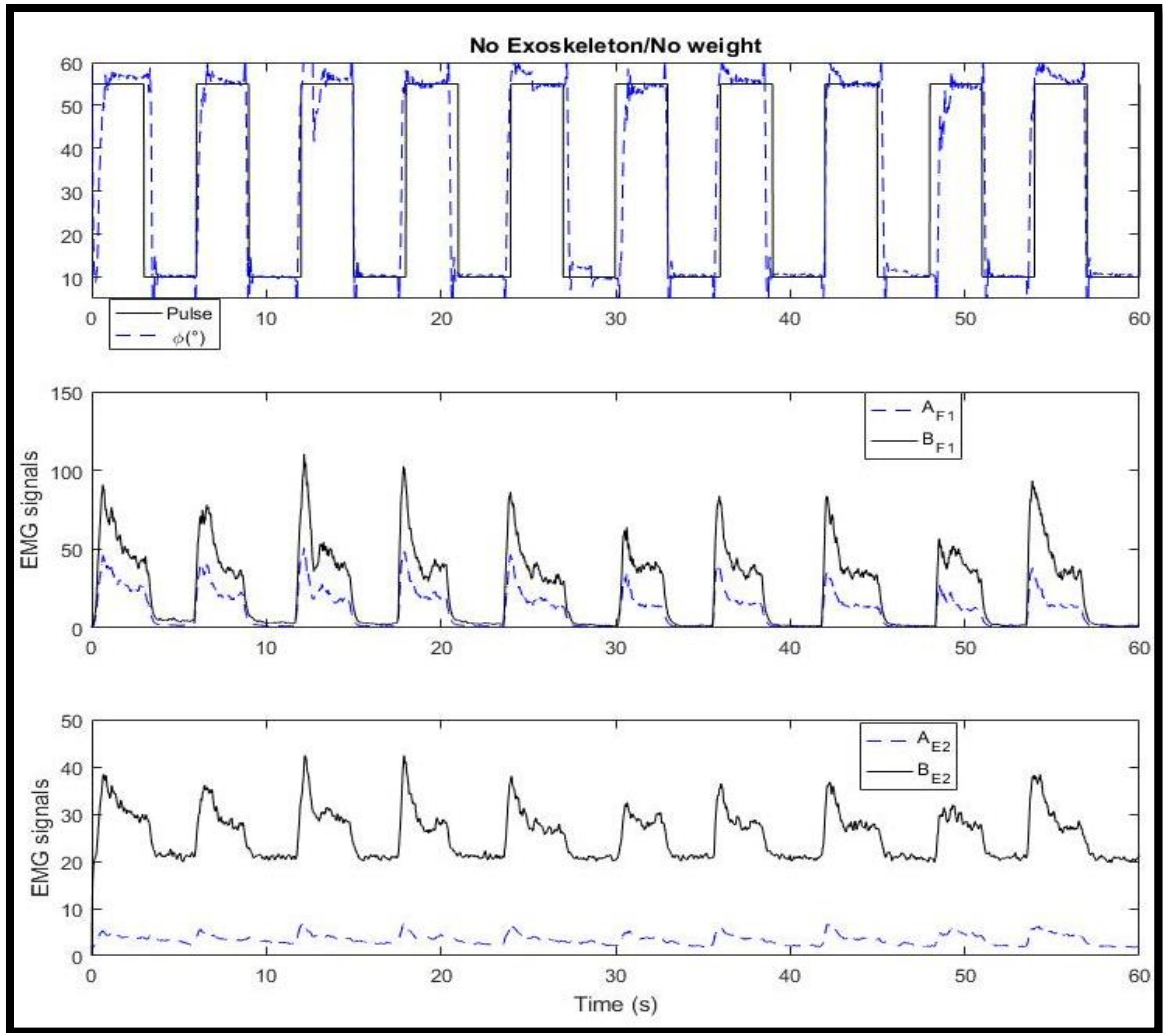


Figure 65. Boa Exoskeleton “No Exoskeleton/ No Weight” tests on subject 2.

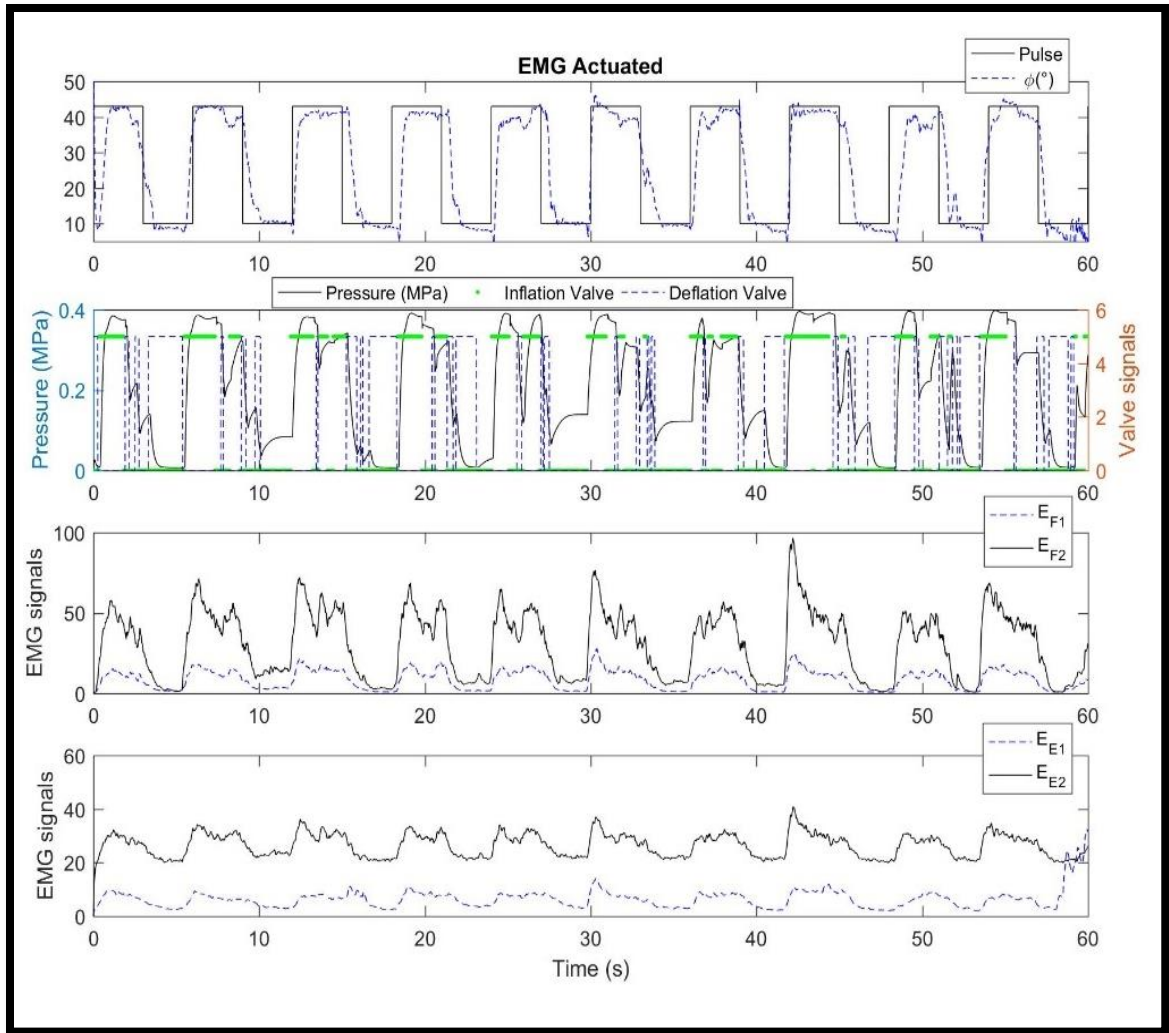


Figure 66. Boa Exoskeleton "EMG Actuated" tests on subject 3.

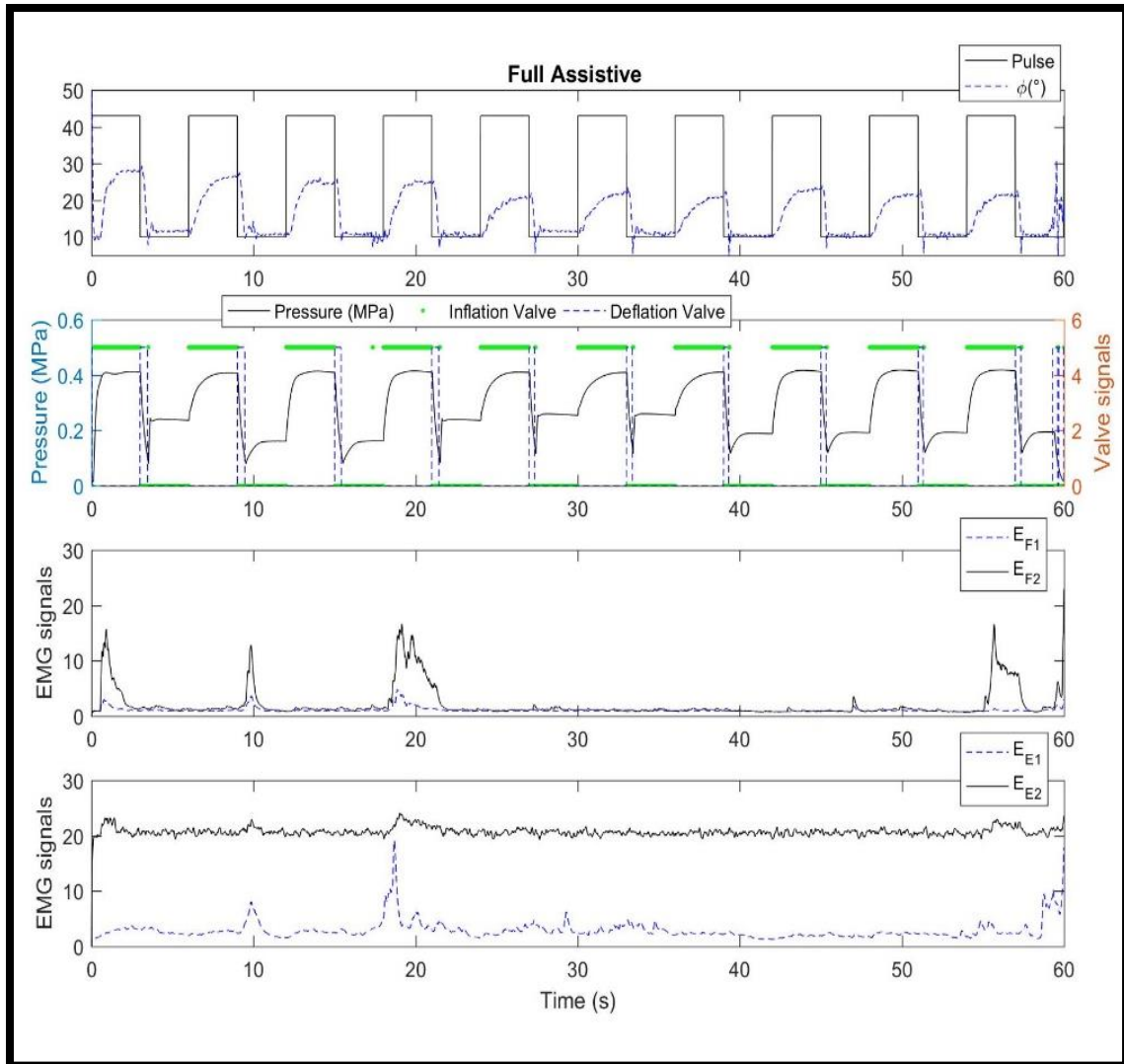


Figure 67. Boa Exoskeleton "Full Assistive" tests on subject 3.

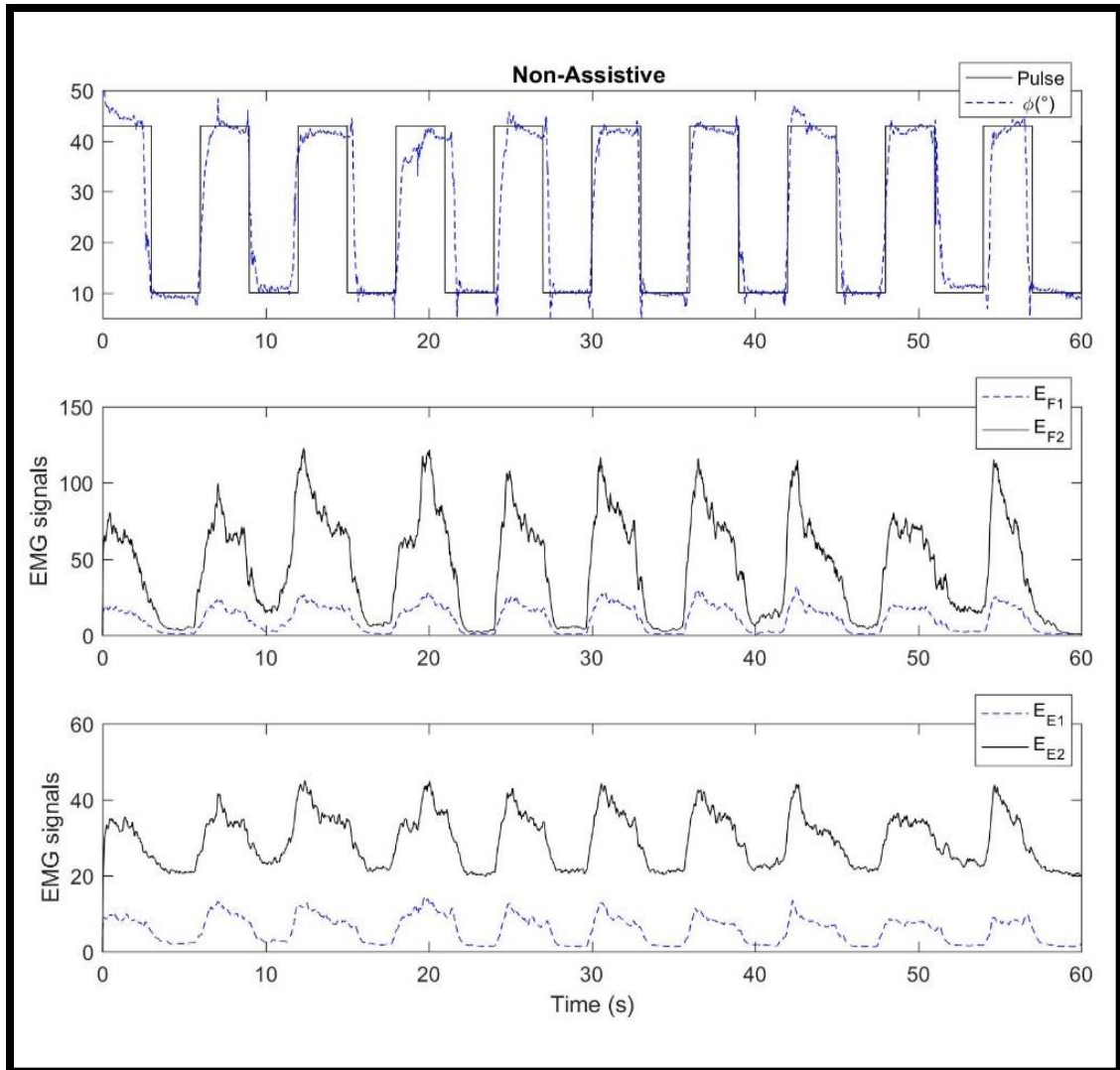


Figure 68. Boa Exoskeleton “Non-Assistive” tests on subject 3.

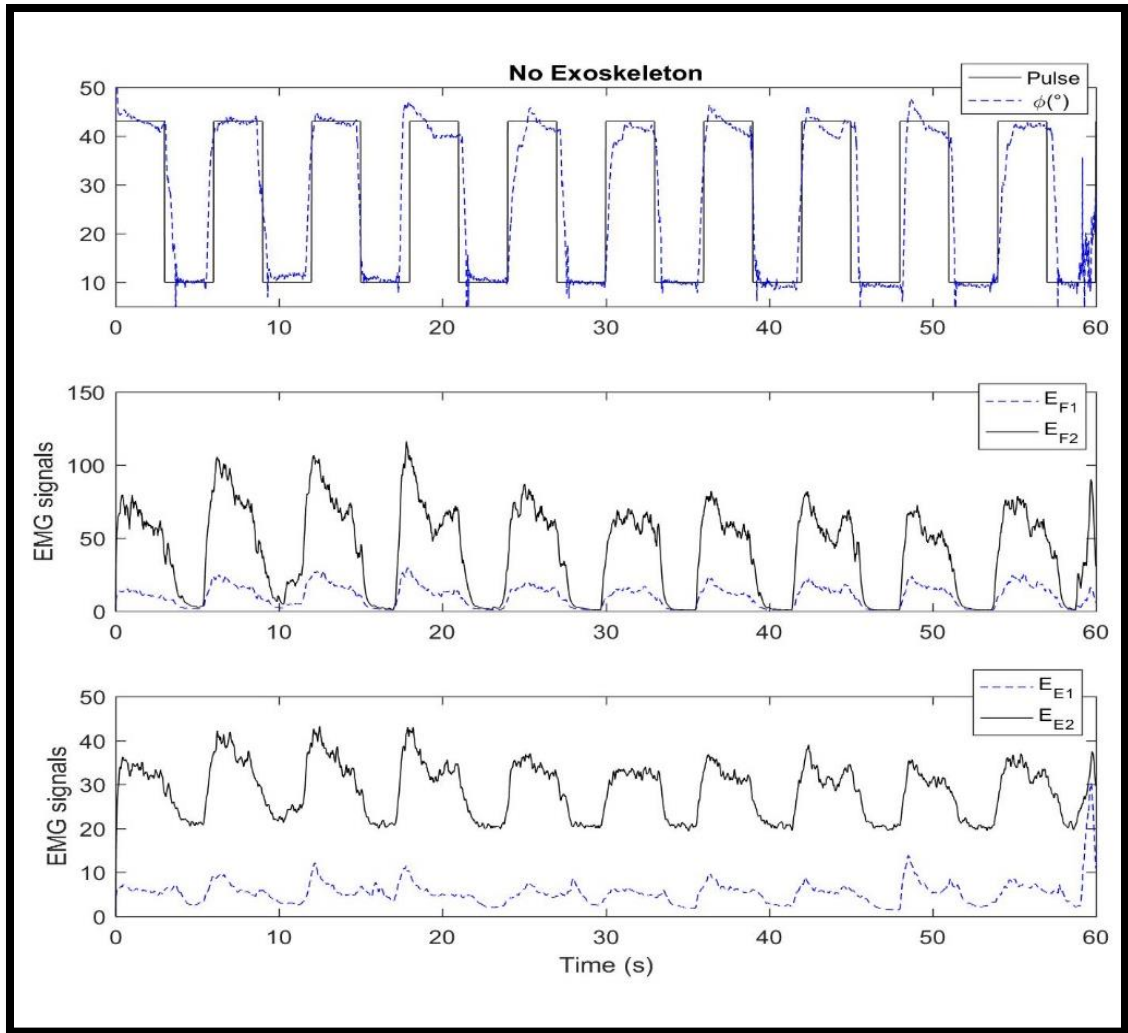


Figure 69. Boa Exoskeleton “No Exoskeleton” tests on subject 3.

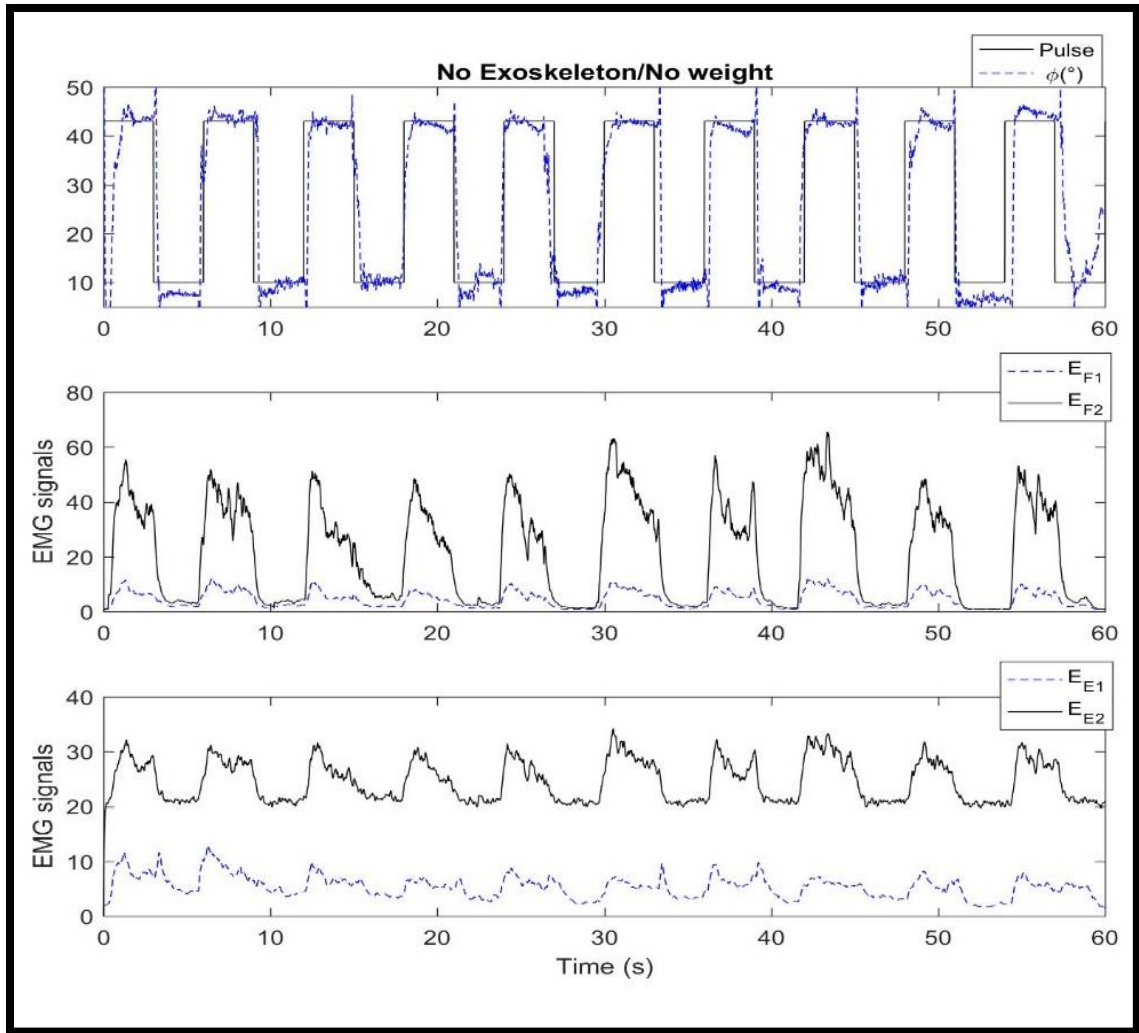


Figure 70. Boa Exoskeleton “No Exoskeleton/ No Weight” tests on subject 3.

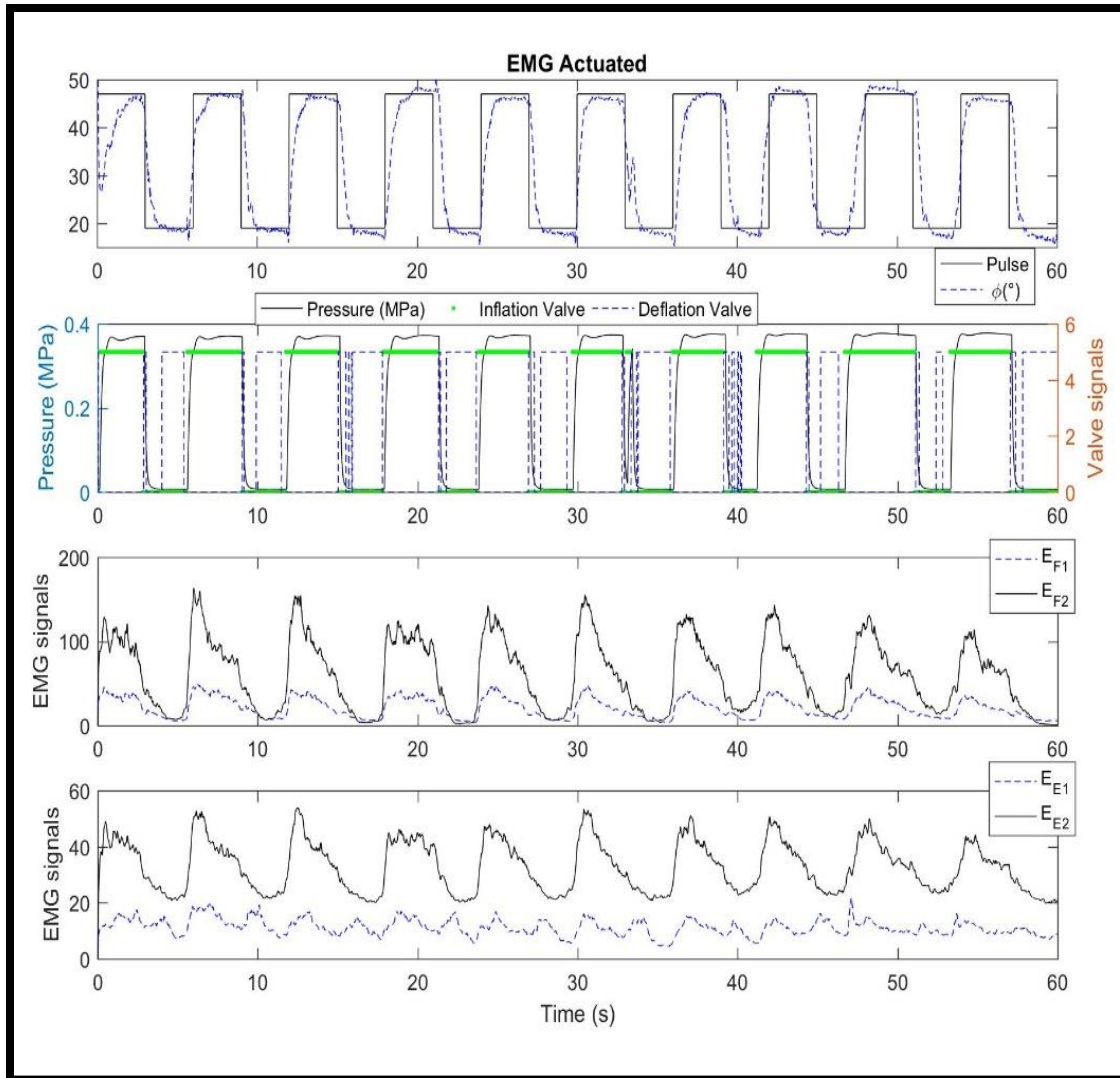


Figure 71. Boa Exoskeleton "EMG Actuated" tests on subject 4.

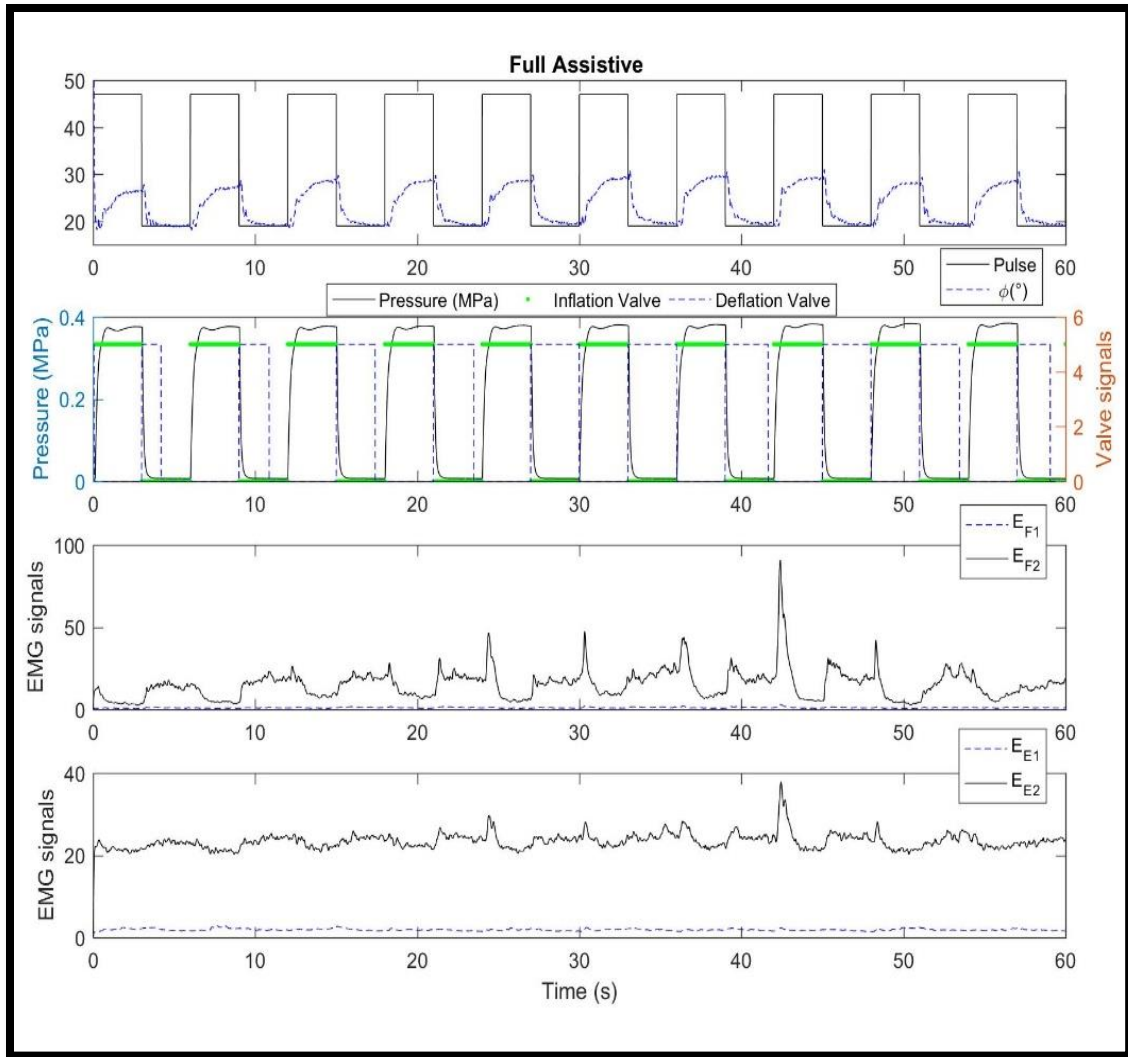


Figure 72. Boa Exoskeleton “Full Assistive” tests on subject 4.

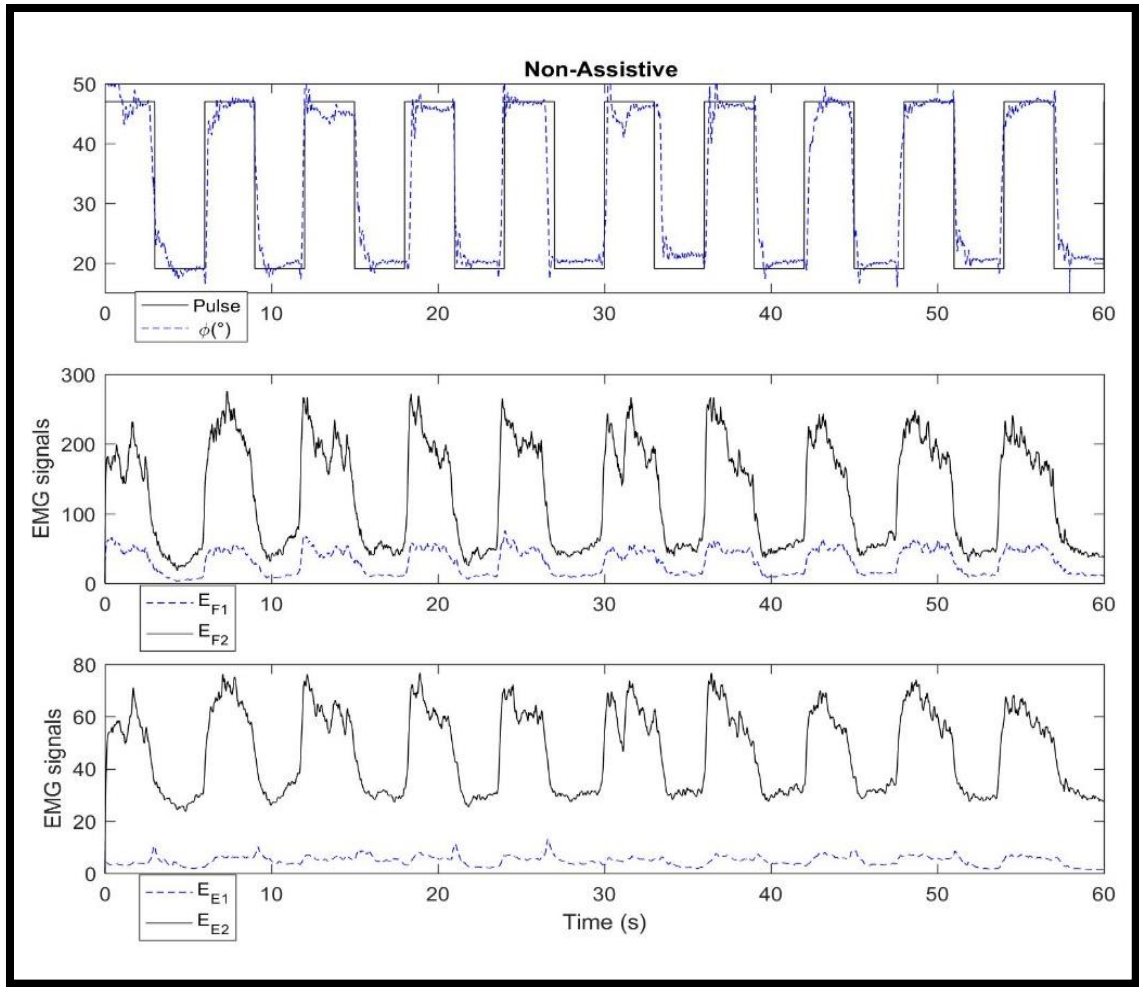


Figure 73. Boa Exoskeleton “Non-Assistive” tests on subject 4.

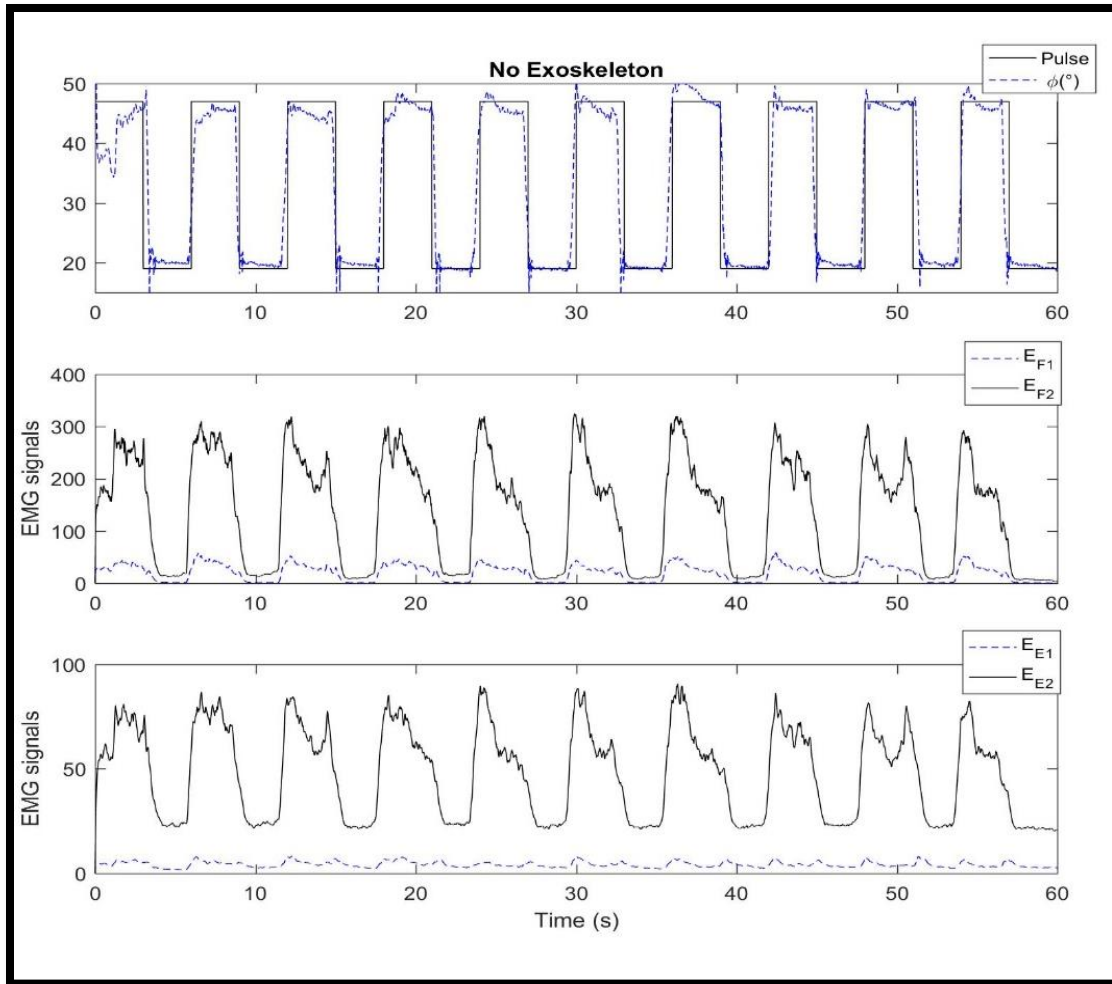


Figure 74. Boa Exoskeleton “No Exoskeleton” tests on subject 4.

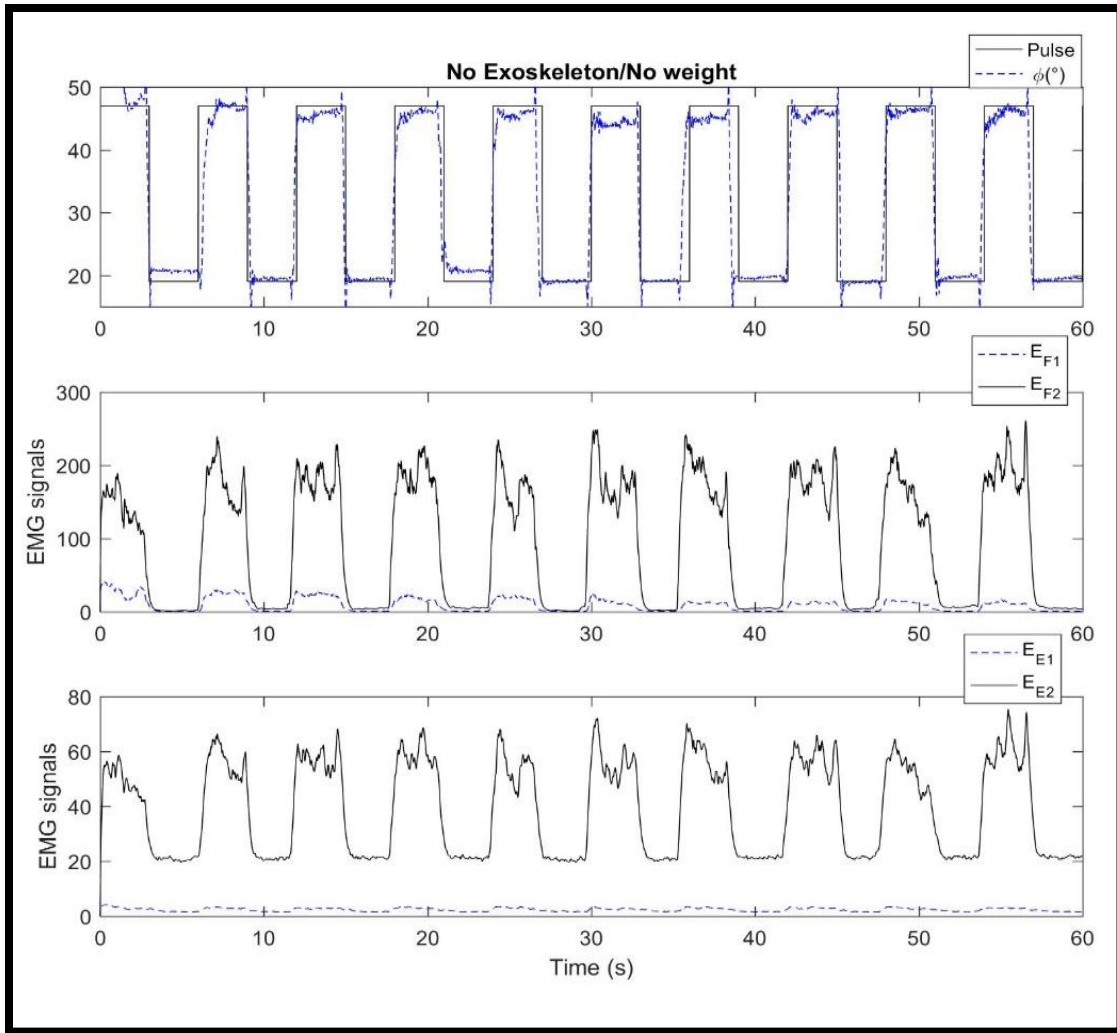


Figure 75. Boa Exoskeleton “No Exoskeleton/ No Weight” tests on subject 4.

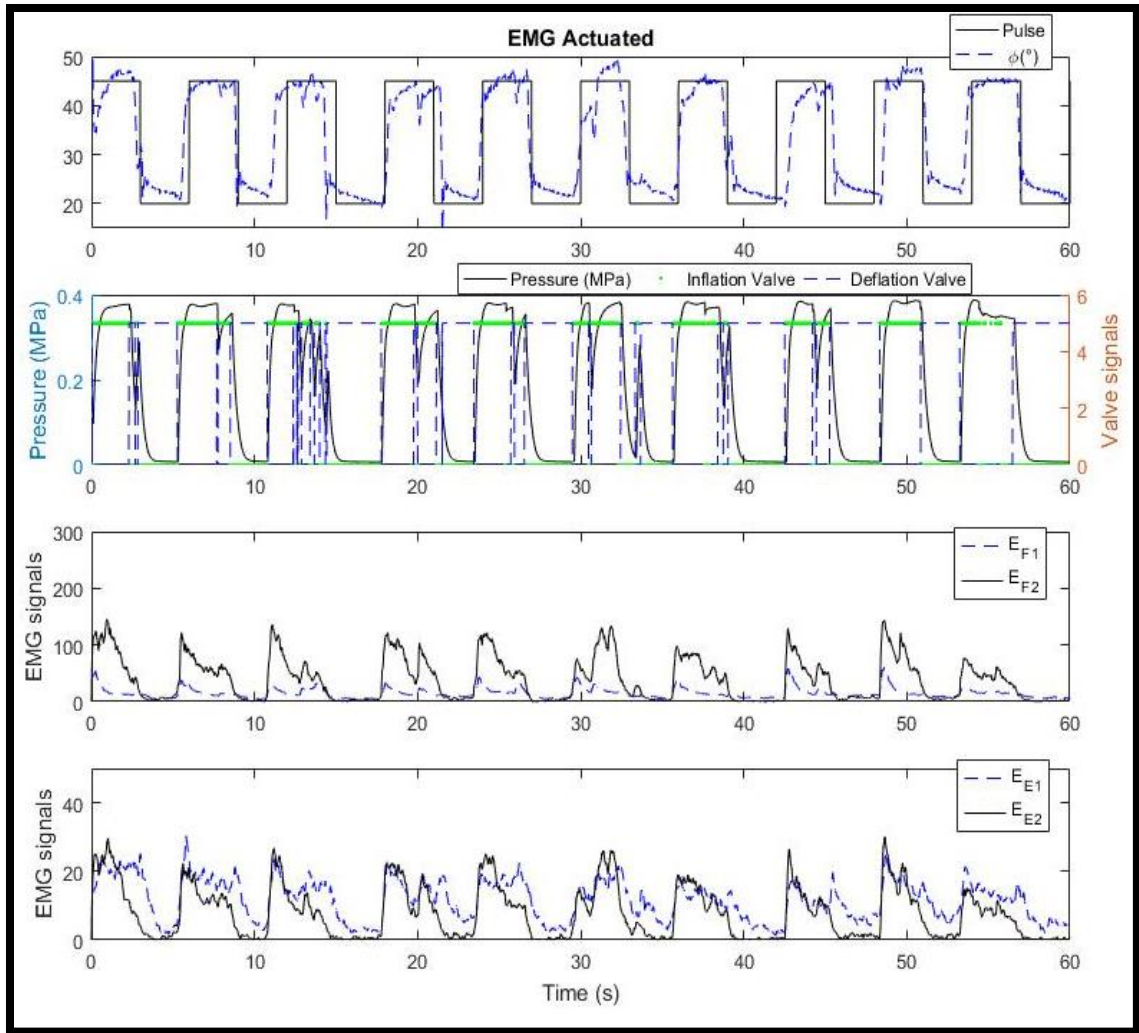


Figure 76. Boa Exoskeleton "EMG Actuated" tests on subject 5.

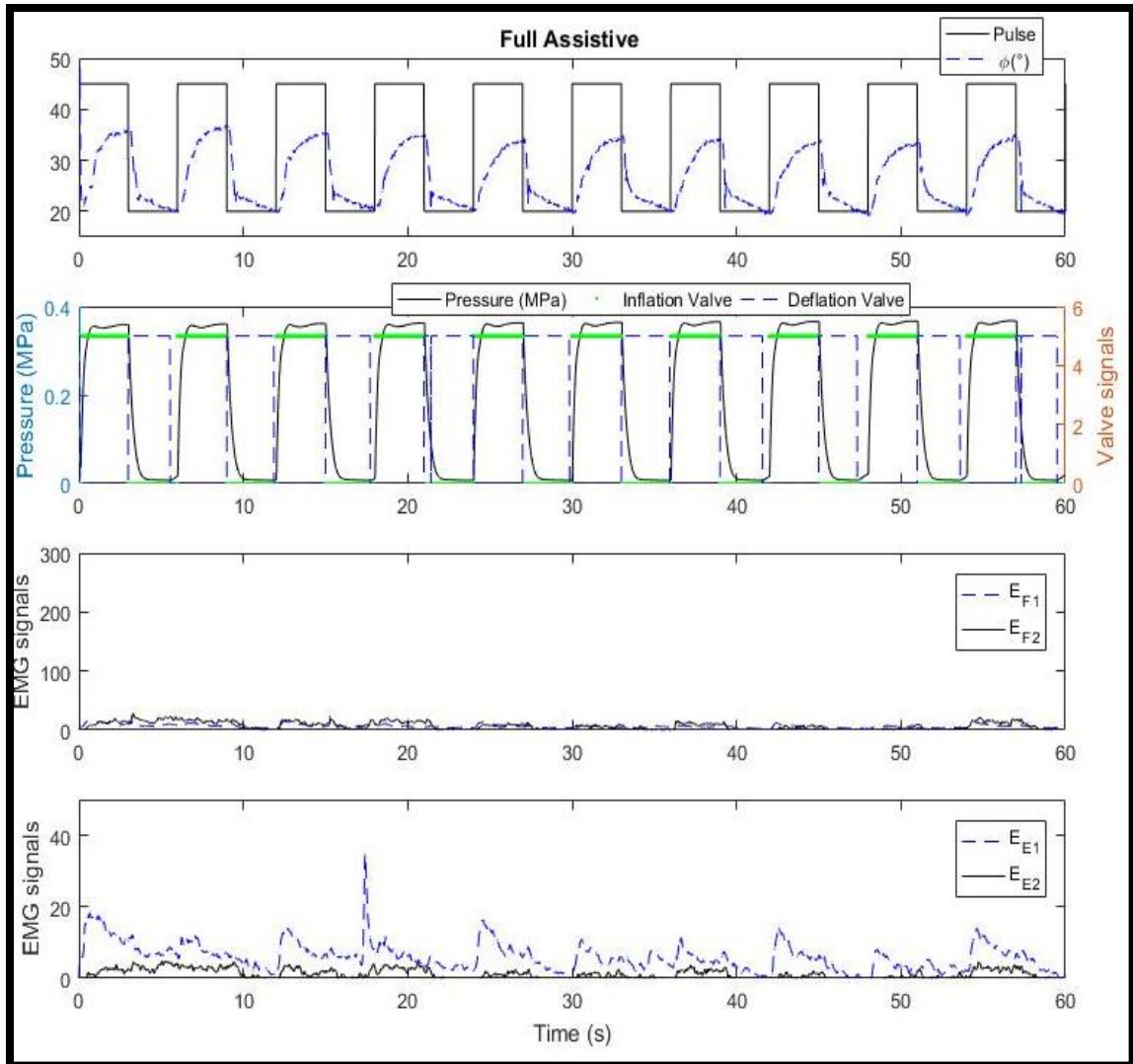


Figure 77. Boa Exoskeleton "Full Assistive" tests on subject 5.

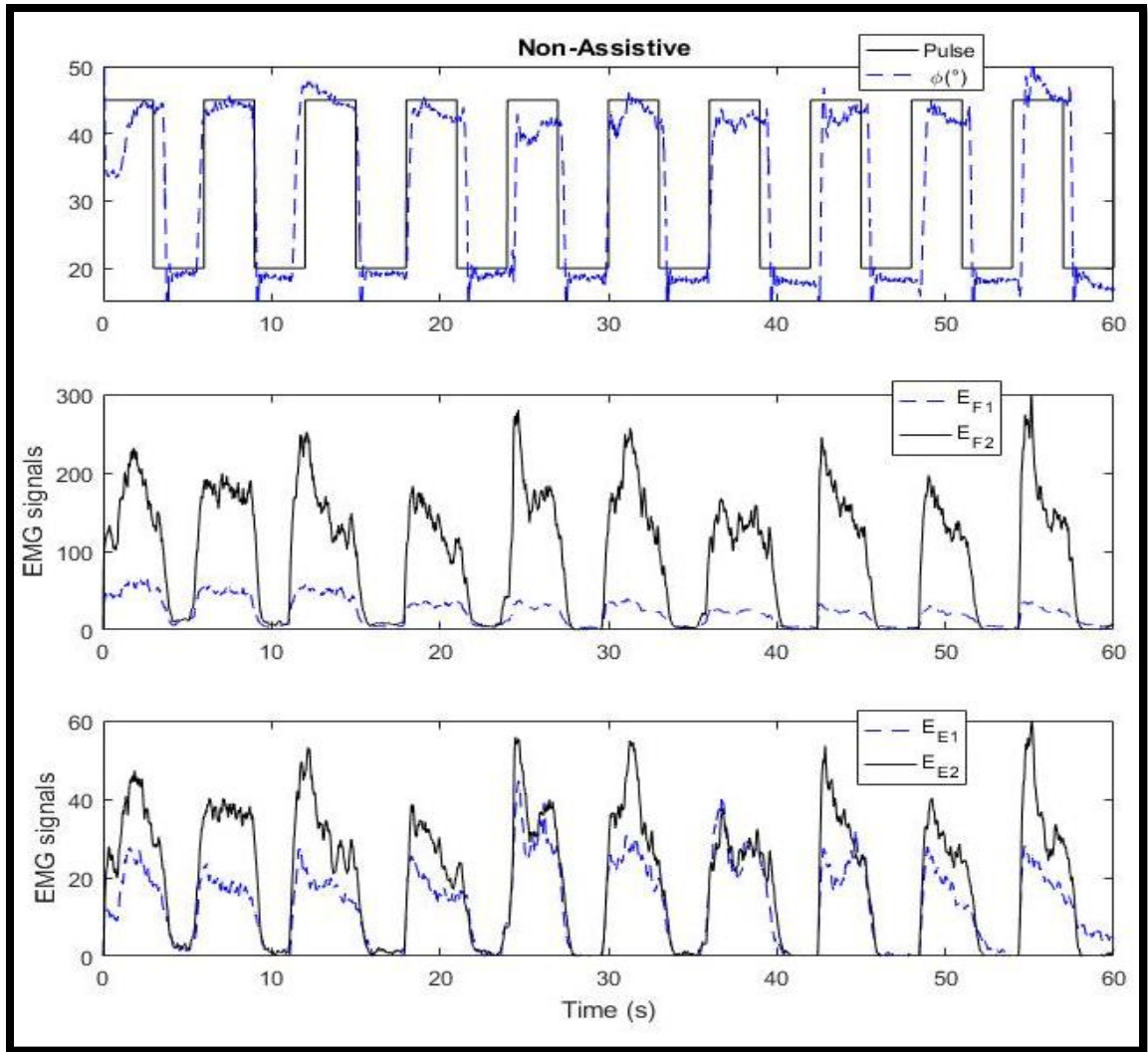


Figure 78. Boa Exoskeleton “Non-Assistive” tests on subject 5.

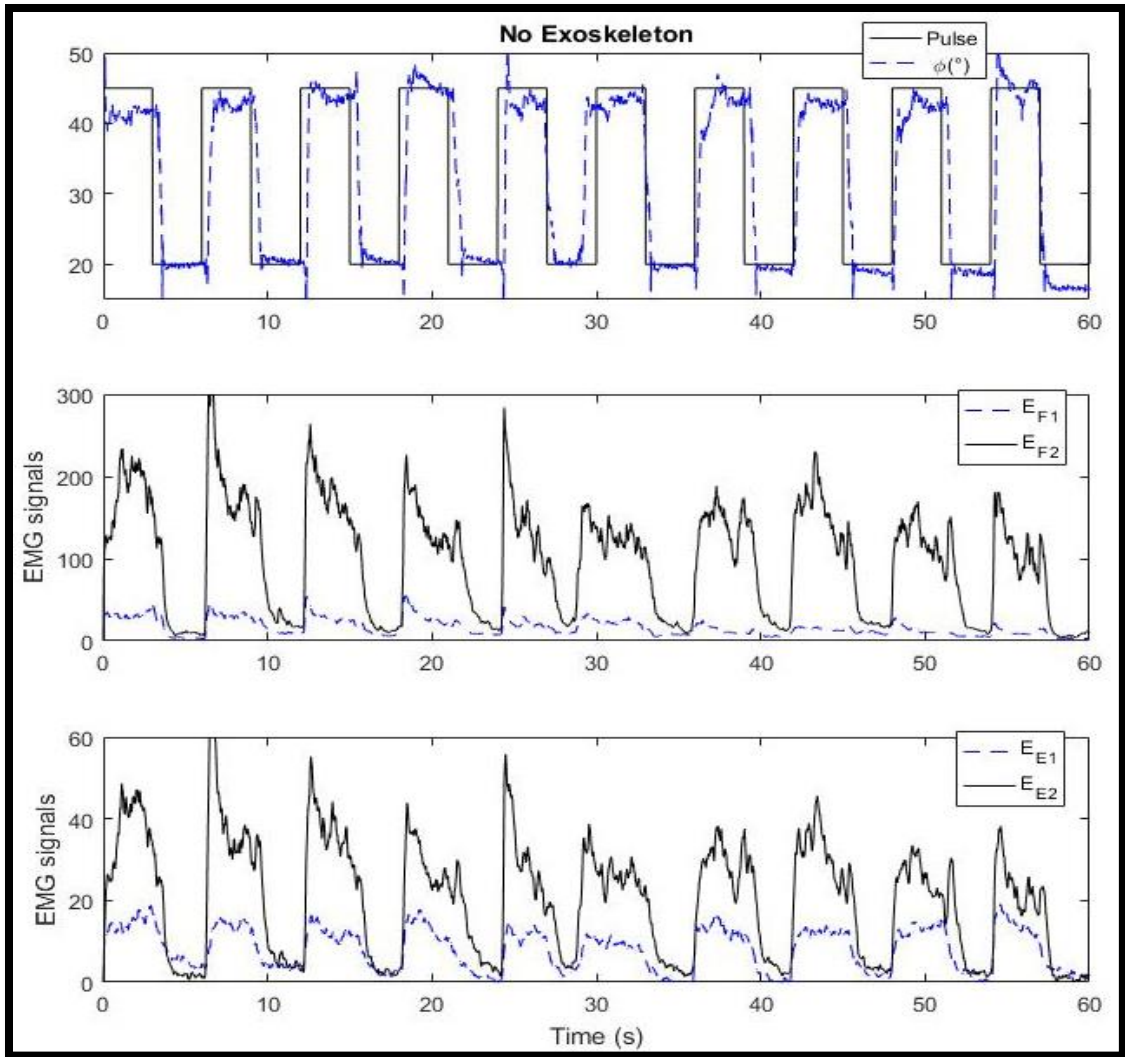


Figure 79. Boa Exoskeleton “No Exoskeleton” tests on subject 5.

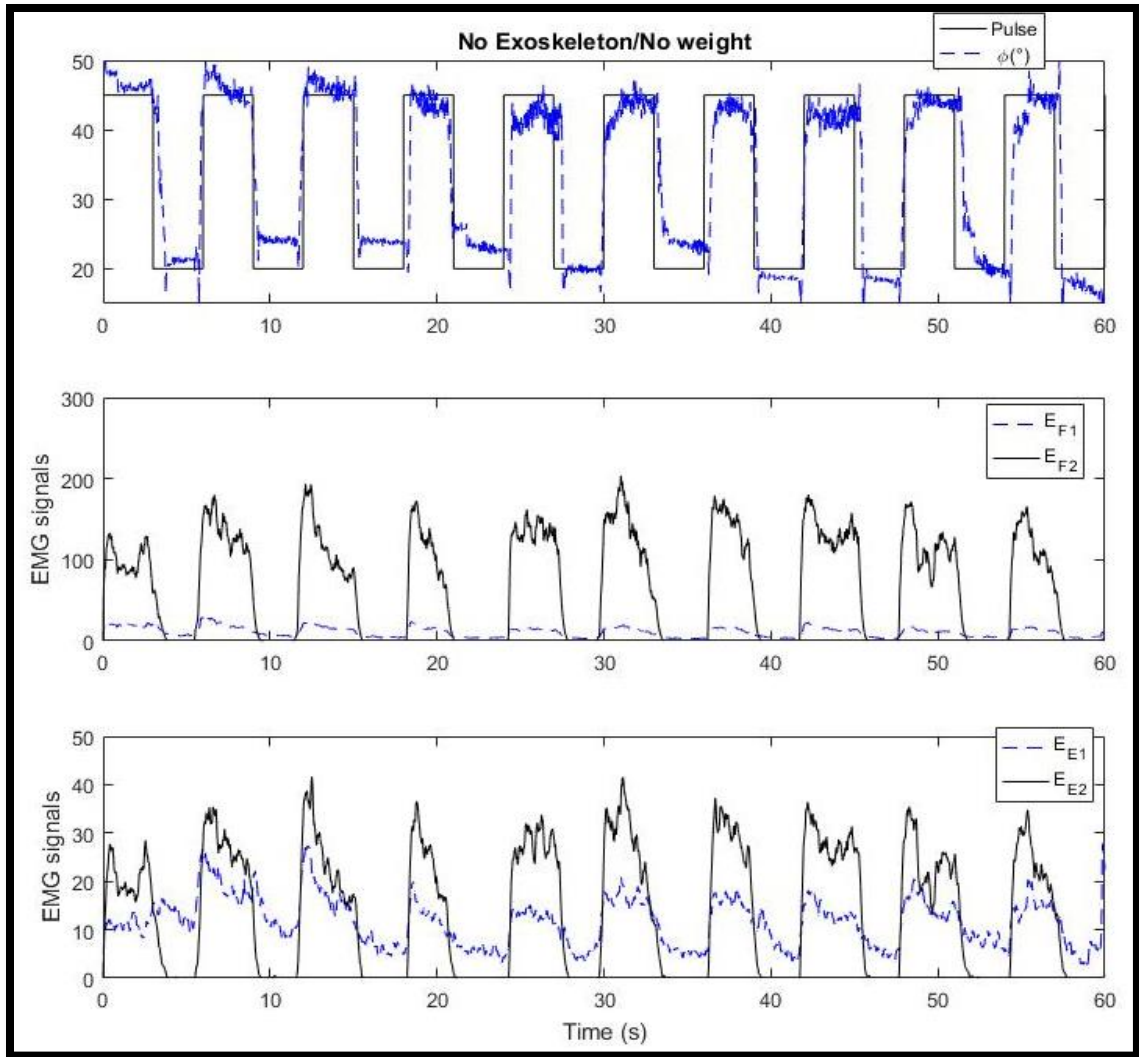


Figure 80. Boa Exoskeleton “No Exoskeleton/ No Weight” tests on subject 5.

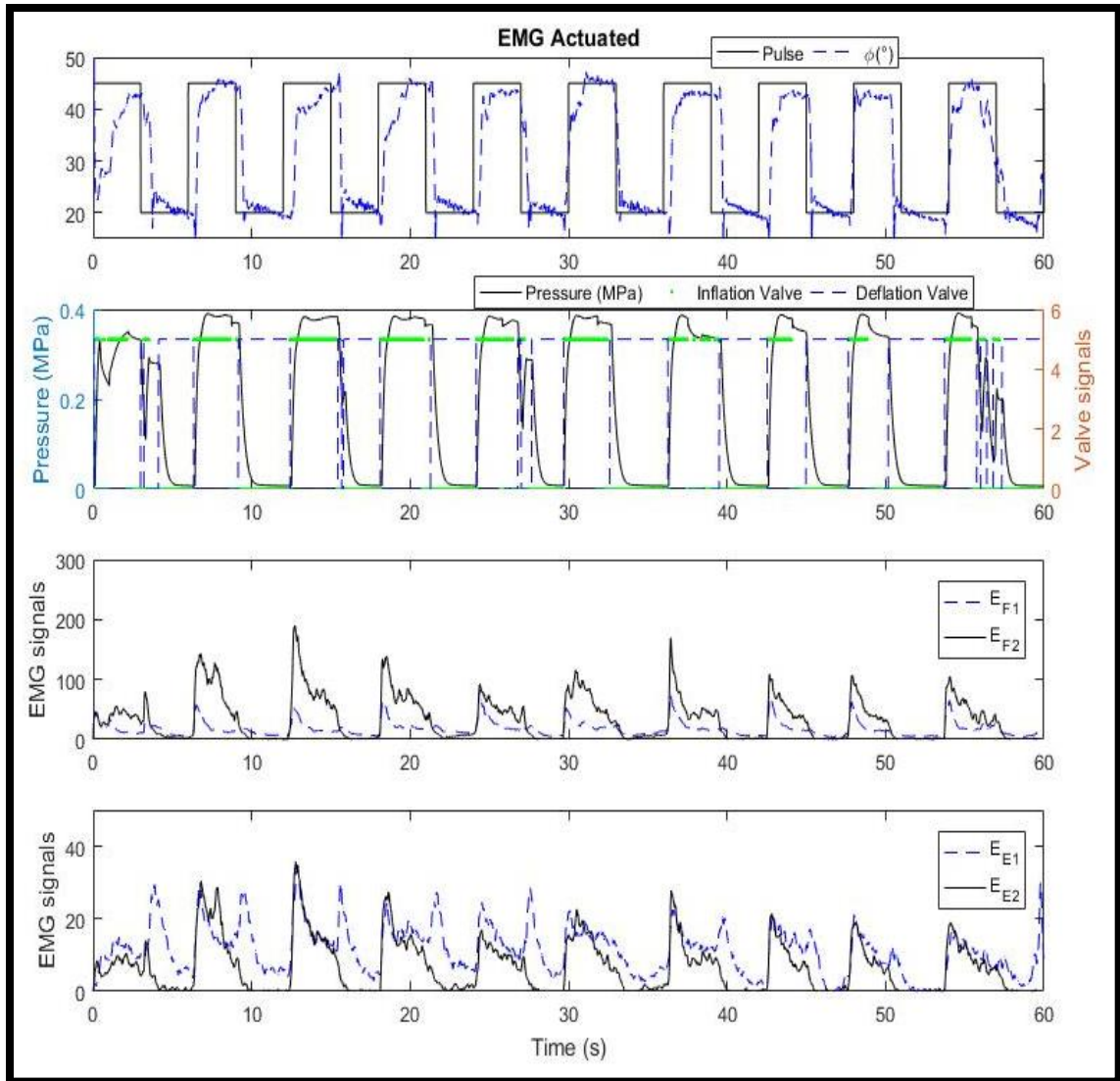


Figure 81. Boa Exoskeleton "EMG Actuated" tests on subject 6.

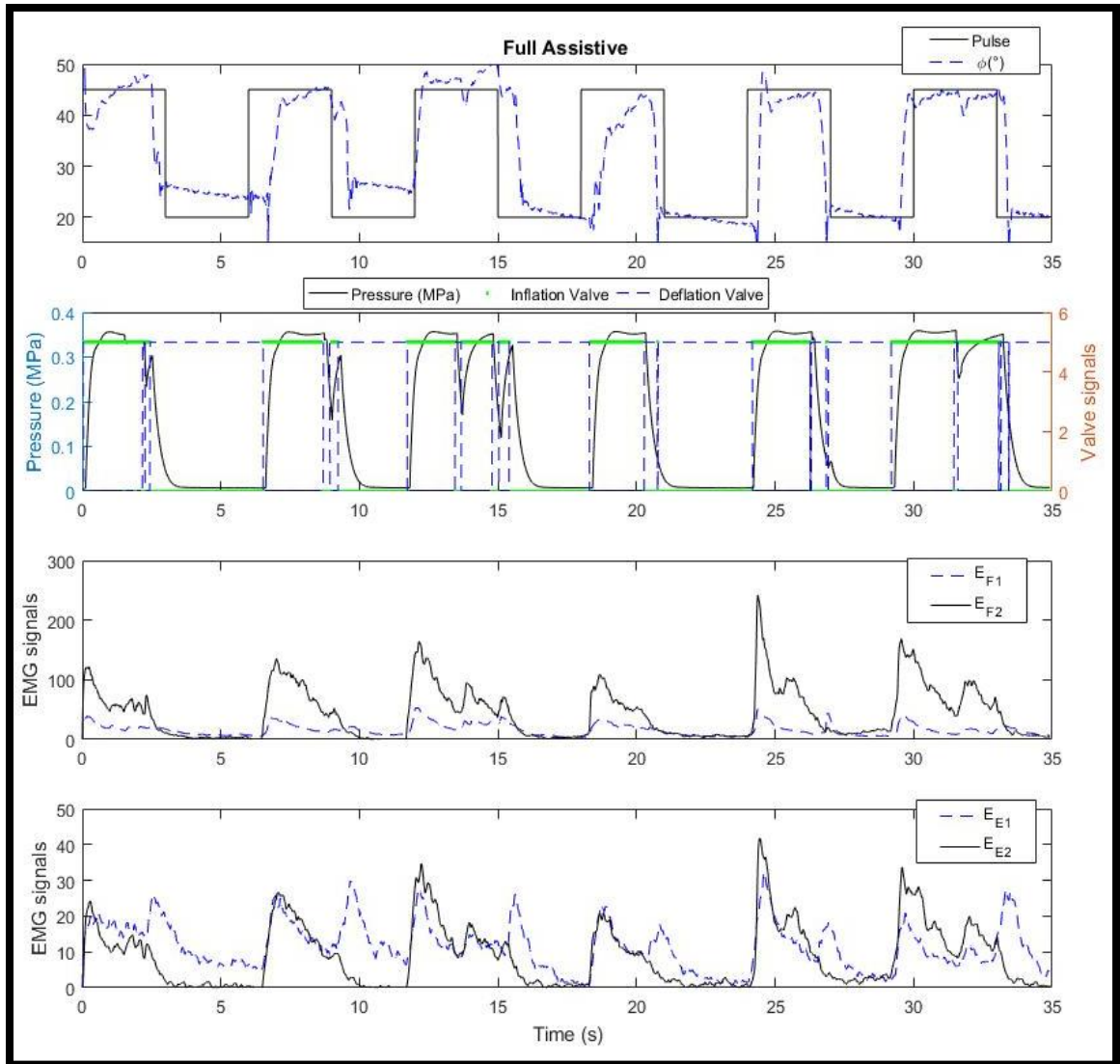


Figure 82. Boa Exoskeleton “Full Assistive” tests on subject 6.

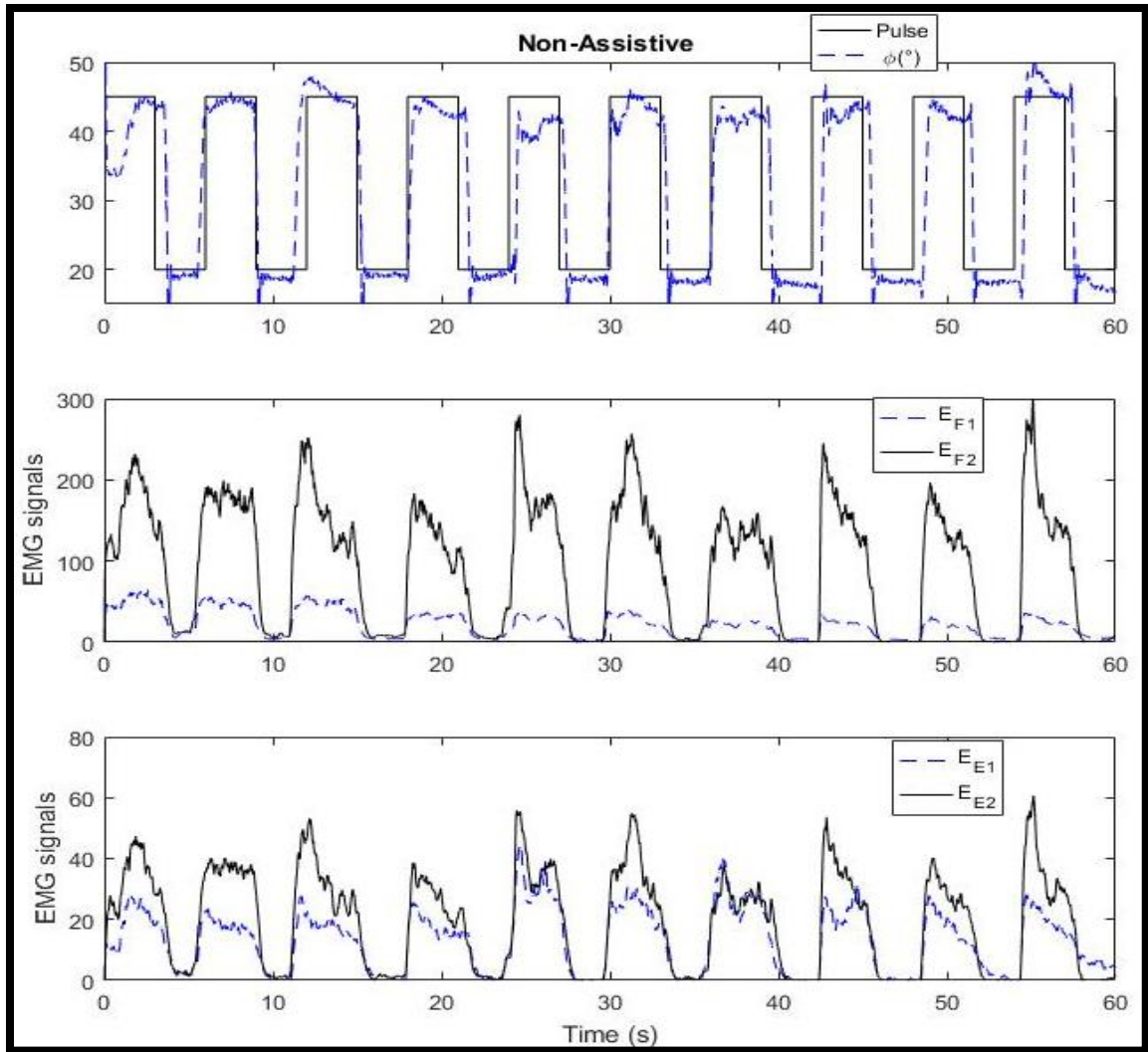


Figure 83. Boa Exoskeleton “Non-Assistive” tests on subject 6.

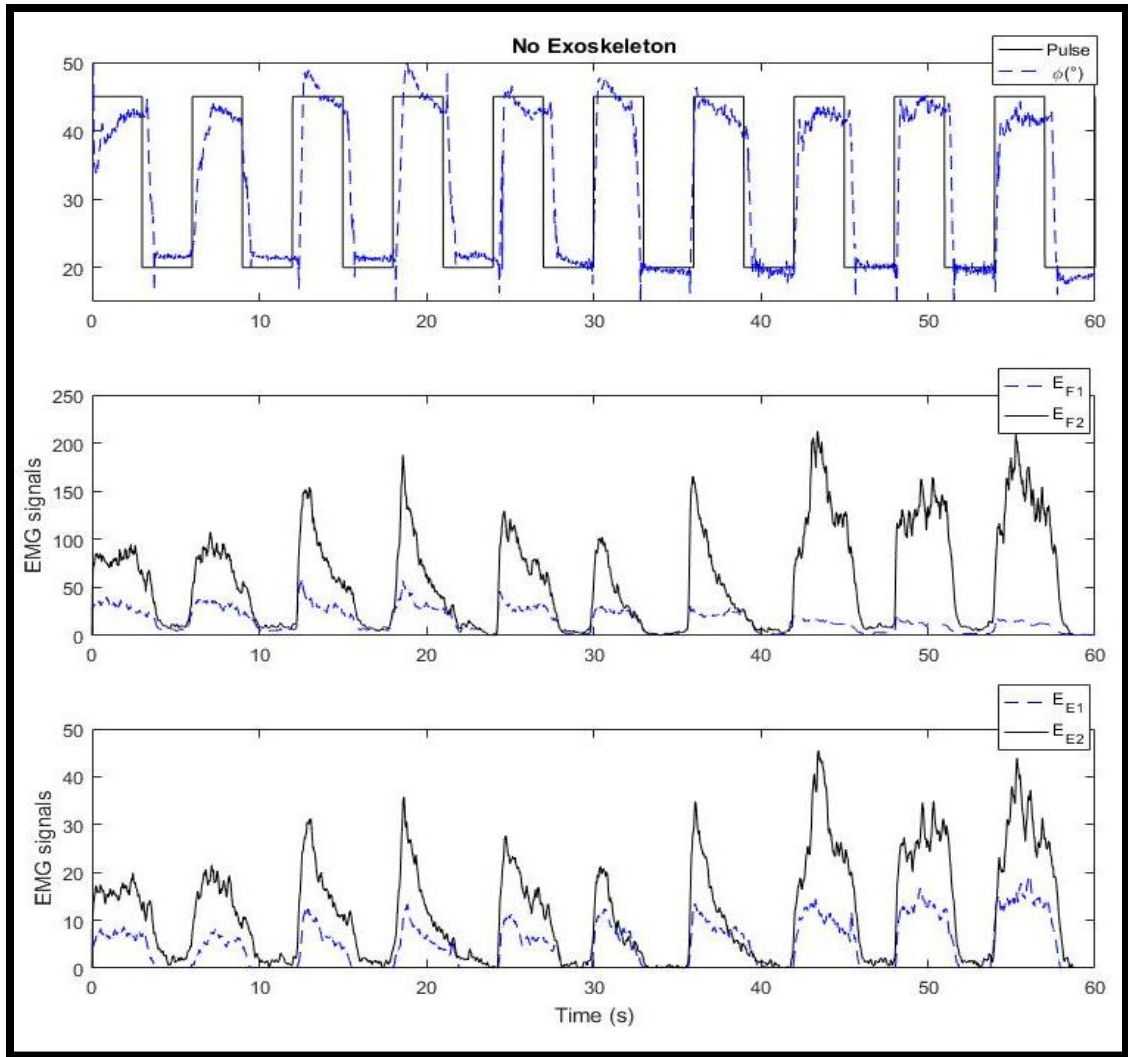


Figure 84. Boa Exoskeleton “No Exoskeleton” tests on subject 6.

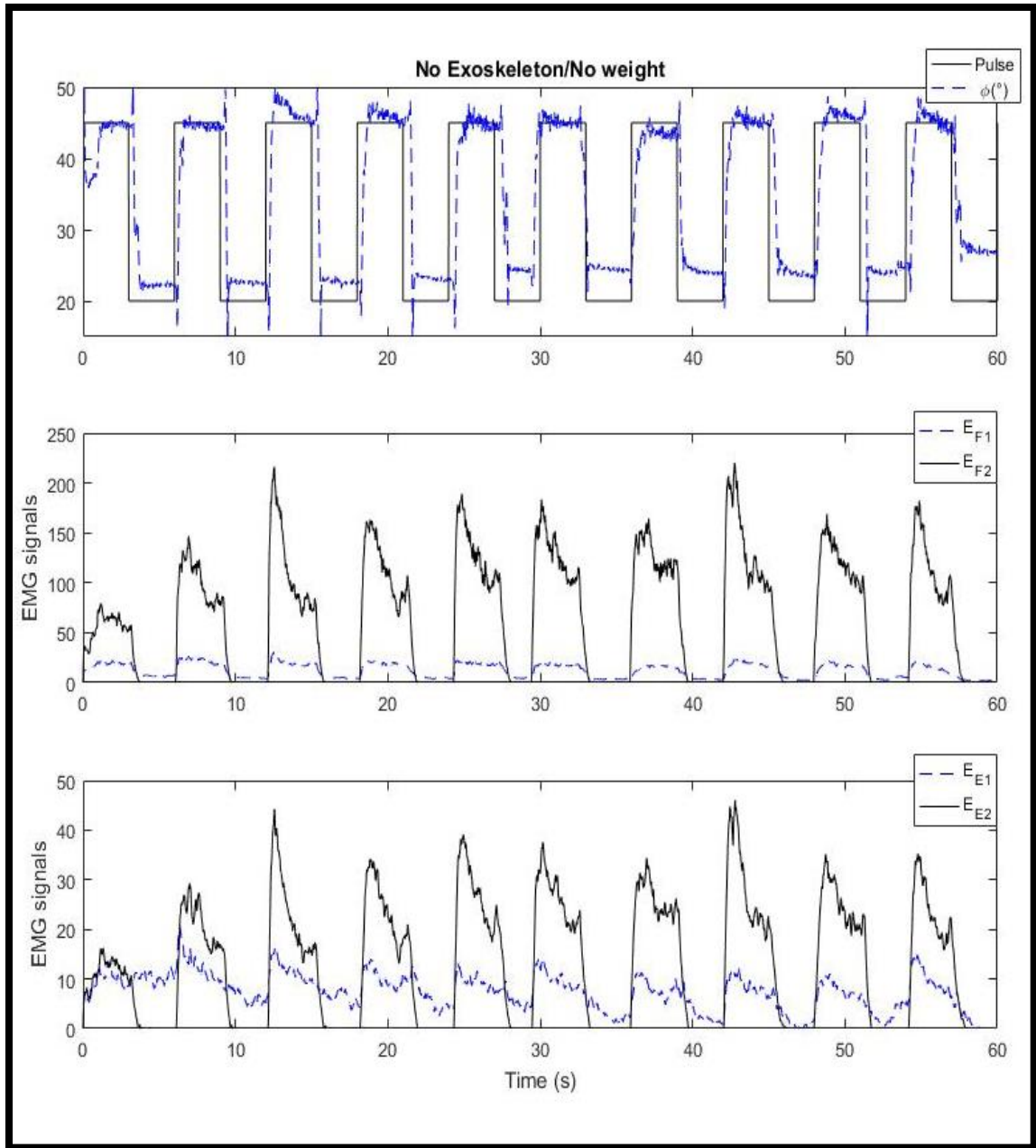


Figure 85. Boa Exoskeleton “No Exoskeleton/ No Weight” tests on subject 6.

10 REFERENCES

- [1] D. Rus and M. T. Tolley, “Design, fabrication and control of soft robots,” *Nature*, vol. 521, no. 7553, pp. 467–475, 2015.
- [2] N. G. Tsagarakis, M. Laffranchi, B. Vanderborght, and D. G. Caldwell, “A compact soft actuator unit for small scale human friendly robots,” *2009 IEEE Int. Conf. Robot. Autom.*, pp. 4356–4362, 2009.
- [3] S. Kim, C. Laschi, and B. Trimmer, “Soft robotics: A bioinspired evolution in robotics,” *Trends Biotechnol.*, vol. 31, no. 5, pp. 287–294, 2013.
- [4] K. C. Galloway *et al.*, “Soft Robotic Grippers for Biological Sampling on Deep Reefs,” *Soft Robot.*, vol. 3, no. 1, pp. 23–33, 2016.
- [5] F. Iida and C. Laschi, “Soft robotics: Challenges and perspectives,” *Procedia Comput. Sci.*, vol. 7, pp. 99–102, 2011.
- [6] R. V. Martinez, C. R. Fish, X. Chen, and G. M. Whitesides, “Elastomeric origami: Programmable paper-elastomer composites as pneumatic actuators,” *Adv. Funct. Mater.*, vol. 22, no. 7, pp. 1376–1384, 2012.
- [7] N. Tsagarakis and D. G. Caldwell, “Improved modelling and assessment of pneumatic muscle actuators,” *Proc. 2000 ICRA. Millenn. Conf. IEEE Int. Conf. Robot. Autom. Symp. Proc. (Cat. No.00CH37065)*, vol. 4, pp. 3641–3646, 2000.
- [8] K. Suzumori, S. Endo, T. Kanda, N. Kato, and H. Suzuki, “A bending pneumatic rubber actuator realizing soft-bodied manta swimming robot,” *Proc. - IEEE Int. Conf. Robot. Autom.*, no. April, pp. 4975–4980, 2007.

- [9] F. Ilievski, A. D. Mazzeo, R. F. Shepherd, X. Chen, and G. M. Whitesides, “Soft robotics for chemists,” *Angew. Chemie - Int. Ed.*, vol. 50, no. 8, pp. 1890–1895, 2011.
- [10] B. Mosadegh *et al.*, “Pneumatic networks for soft robotics that actuate rapidly,” *Adv. Funct. Mater.*, vol. 24, no. 15, pp. 2163–2170, 2014.
- [11] P. Polygerinos *et al.*, “Modeling of Soft Fiber-Reinforced Bending Actuators,” *IEEE Trans. Robot.*, vol. 31, no. 3, pp. 778–789, 2015.
- [12] F. Connolly, C. J. Walsh, and K. Bertoldi, “Automatic design of fiber-reinforced soft actuators for trajectory matching,” *Proc. Natl. Acad. Sci.*, vol. 114, no. 1, pp. 51–56, 2017.
- [13] J. Rosen, J. C. Perry, N. Manning, S. Burns, and B. Hannaford, “The human arm kinematics and dynamics during daily activities - Toward a 7 DOF upper limb powered exoskeleton,” *2005 Int. Conf. Adv. Robot. ICAR '05, Proc.*, vol. 2005, pp. 532–539, 2005.
- [14] I. N. A. Mohd Nordin, M. R. Muhammad Razif, A. M. Faudzi, E. Natarajan, K. Iwata, and K. Suzumori, “3-D finite-element analysis of fiber-reinforced soft bending actuator for finger flexion,” in *2013 IEEE/ASME International Conference on Advanced Intelligent Mechatronics: Mechatronics for Human Wellbeing, AIM 2013*, 2013, pp. 128–133.
- [15] P. Polygerinos, Z. Wang, K. C. Galloway, R. J. Wood, and C. J. Walsh, “Soft robotic glove for combined assistance and at-home rehabilitation,” *Rob. Auton. Syst.*, vol. 73, pp. 135–143, 2015.

- [16] C. D. Takahashi, L. Der-Yeghiaian, V. Le, R. R. Motiwala, and S. C. Cramer, "Robot-based hand motor therapy after stroke," *Brain*, vol. 131, no. 2, pp. 425–437, 2008.
- [17] H. Woldag, K. Stupka, and H. Hummelsheim, "Repetitive training of complex hand and arm movements with shaping is beneficial for motor improvement in patients after stroke," *J. Rehabil. Med.*, vol. 42, no. 6, pp. 582–587, 2010.
- [18] Y. Mao and S. K. Agrawal, "Design of a cable-driven arm exoskeleton (CAREX) for neural rehabilitation," *IEEE Trans. Robot.*, vol. 28, no. 4, pp. 922–931, 2012.
- [19] P. Polygerinos, K. C. Galloway, E. Savage, M. Herman, K. O'Donnell, and C. J. Walsh, "Soft robotic glove for hand rehabilitation and task specific training," *Proc. - IEEE Int. Conf. Robot. Autom.*, vol. 2015–June, no. June, pp. 2913–2919, 2015.
- [20] H. K. Yap, B. W. K. Ang, J. H. Lim, J. C. H. Goh, and C. H. Yeow, "A fabric-regulated soft robotic glove with user intent detection using EMG and RFID for hand assistive application," *Proc. - IEEE Int. Conf. Robot. Autom.*, vol. 2016–June, pp. 3537–3542, 2016.
- [21] K. Kiguchi, T. Tanaka, and T. Fukuda, "Neuro-fuzzy control of a robotic exoskeleton with EMG signals," *IEEE Trans. Fuzzy Syst.*, vol. 12, no. 4, pp. 481–490, 2004.
- [22] C. J. Nycz, M. A. Delph, and G. S. Fischer, "Modeling and design of a tendon actuated soft robotic exoskeleton for hemiparetic upper limb rehabilitation," *Proc. Annu. Int. Conf. IEEE Eng. Med. Biol. Soc. EMBS*, vol. 2015–Novem, pp. 3889–3892, 2015.

- [23] H. K. Yap, J. H. Lim, F. Nasrallah, J. C. H. Goh, and R. C. H. Yeow, "A soft exoskeleton for hand assistive and rehabilitation application using pneumatic actuators with variable stiffness," *Proc. - IEEE Int. Conf. Robot. Autom.*, vol. 2015–June, no. June, pp. 4967–4972, 2015.
- [24] "soft robotics toolkit." [Online]. Available: <https://softroboticstoolkit.com/>.
- [25] M. A. Abd *et al.*, "Impacts of Soft Robotic Actuator Geometry on End Effector Force and Displacement," in *Florida Conference on Recent Advances in Robotics*, 2017, vol. 30, pp. 94–99.
- [26] J. Bishop-Moser, G. Krishnan, C. Kim, and S. Kota, "Design of soft robotic actuators using fluid-filled fiber-reinforced elastomeric enclosures in parallel combinations," *IEEE Int. Conf. Intell. Robot. Syst.*, pp. 4264–4269, 2012.
- [27] F. Connolly, P. Polygerinos, C. J. Walsh, and K. Bertoldi, "Mechanical Programming of Soft Actuators by Varying Fiber Angle," *Soft Robot.*, vol. 2, no. 1, pp. 26–32, 2015.
- [28] "Ultimaker 3D Printer." [Online]. Available: <https://ultimaker.com/>.
- [29] "Smooth On." [Online]. Available: <https://www.smooth-on.com/page/durometer-shore-hardness-scale/>.
- [30] E. Rocon, J. M. Belda-Lois, A. F. Ruiz, M. Manto, J. C. Moreno, and J. L. Pons, "Design and validation of a rehabilitation robotic exoskeleton for tremor assessment and suppression," *IEEE Trans. Neural Syst. Rehabil. Eng.*, vol. 15, no. 1, pp. 367–378, 2007.